A

Dissertation Report

On

FABRICATION & TRIBOLOGICAL STUDY OF COPPER BASED SINTERED COMPOSITES

For partial fulfillment of the degree of

MASTER OF ENGINEERING (PRODUCTION ENGINEERING)

Submitted by:

NALIN SOMANI

Roll Number: 801482016

Under the guidance of:

DR. VINEET SRIVASTAVA
Assistant Professor, MED
Thapar University, Patiala

DR. HIRALAL BHOWMICK
Assistant Professor, MED
Thapar University, Patiala

MECHANICAL ENGINEERING DEPARTMENT
THAPAR UNIVERSITY, PATIALA-147004, PUNJAB, INDIA
June, 2016

CERTIFICATE

This is to certify that the thesis entitled, **"FABRICATION AND TRIBOLOGICAL STUDY OF COPPER BASED SINTERED COMPOSITES"**, being submitted by **Mr. Nalin Somani** , Registration No. **801482016**, in partial fulfillment of the requirements for the award of degree of Master of Engineering in Production Engineering at **Thapar University, Patiala** under the supervision of **Dr. Vineet Srivastava**, Assistant Professor, Mechanical Engineering Department, and **Dr. Hiralal Bhowmick**, Assistant Professor, Mechanical Engineering Department, Thapar University, Patiala submitted in Mechanical Engineering Department of Thapar University, Patiala during July, 2014 to June, 2016. No part of the matter embodied in this report has been submitted to any other University or institute for award of any degree to the best of my knowledge.

Nalin

Date: 14th July 2016 **Nalin Somani**

It is certified that above statement made by the student is correct to the best of my knowledge and belief.

14/07/2016

DR. VINEET SRIVASTAVA
Assistant Professor, MED
Thapar University, Patiala

14/7/16

DR. HIRALAL BHOWMICK
Assistant Professor, MED
Thapar University, Patiala

Countersigned by

Dr. S.K. Mohapatra
Head, Mechanical Engineering Department
Thapar University, Patiala-147004

Dr. S.S Bhatia
Dean of Academic Affair
Thapar University, Patiala-147004

Dedicated to

My respected parents

Mr. Balkrishna Somani & Mrs. Rekha Somani

Acknowledgement

I would like to thank all the people who contributed in some way to the work described in this thesis. First and foremost, I thank my thesis supervisors **Dr. Vineet Srivastava, Assistant Professor, Mechanical Engineering Department, Thapar University, Patiala and Dr. Hiralal Bhowmick, Assistant Professor, Mechanical Engineering Department, Thapar University, Patiala** for their guidance, support and inspiring suggestion, for the development of thesis at every step. They took keen interest in my report and helped me to access facilities of Mechanical Engineering Department laboratories.

I am thankful to Mr. Narinder Singh for assisting and guiding me in laboratory work. I am thankful to MED faculty for support and guidance during the course of my thesis work.

I would also like to thank **Dr. S.K. Mohapatra, Head & Senior Professor, Mechanical Engineering Department, Thapar University, Patiala** for permitting me to access facilities of Mechanical Engineering Department laboratories.

A special thanks to my friends Navjot Singh Gill, Priyanka Kothari, Swati Sharma, PhD scholar Mr. Arminder Singh Walia and Mr. Harpreet Singh (Thapar University), Pankaj Singla, Ranjit Singh and Prakhar Jain for their help and support during thesis work.

Last but not least, I wish to express my deep sense of gratitude to my family, for supporting and encouraging me at every step of my work, which has given me the courage, confidence and zeal for hard work.

Nalin

Nalin Somani

Roll No. 801482016

ABSTRACT

Metal matrix composite using copper as a base material is gaining huge attention in multiple applications because of their good electrical, thermal and mechanical properties. A composite of Cu-SiC with different combinations were fabricated by using powder metallurgy technique. Compositions ranging from 100% copper to 80% copper-20%SiC with nickel and graphite as a binder and wetting agent were sintered and fabricated. Pin-On-Disc machine was used to examine the tribological properties of the composites under the different loads and sliding speed. The addition of the SiC as a reinforcement in Cu-SiC composite increases the wear resistance capacity and reduces the coefficient of friction. ANOVA was used to understand the significance of process variables which were affecting wear rate and the coefficient of friction. Normal load and the sliding distance are found to be most significant process parameters which were affecting the wear rate as well as coefficient of friction. Empirical statistical models have been developed for predicting the value of wear rate and coefficient of friction by using the regression equations. Obtained results were compared with the experimental results and they were found in good agreement with experiments.

Scanning electron microscope (SEM) and Optical microscopes were used to interpret the morphology of worn surface and to comprehend the wear mechanism.

Keywords: Powder metallurgy; wear rate; coefficient of friction; Taguchi method; ANOVA.

CONTENTS

LIST OF FIGURES

LIST OF TABLES

NOMENCLATURE

SiC	Silicon Carbide
TiC	Titanium Carbide
C	Carbon
Cu	Copper
MgO	Magnesium oxide
SiO_2	Silicon Oxide
WC	Tungsten Carbide
ZrB_2	Zirconium dibromide
P/M	Powder Metallurgy
EDM	Electric Discharge Machining
UEDM	Ultrasonic Assisted Electric Discharge Machining
MMC	Metal Matrix Composite
WR	Wear Rate
C.O.F.	Coefficient Of Friction
SEM	Scanning Electron Microscope
SS	Sliding Speed
SD	Sliding Distance
L	Load
WT	Weight
DOE	Design Of Experiment
DF	Degree of Freedom
ANOVA	Analysis Of Variance
SS	Sum Of Square
MS	Mean Sum Of Square
N	Total number of experiments
α	Level of confidence interval

CHAPTER 1
INTRODUCTION

In the recent timings many advancements has been taken place in various technological fields which are demanding the development and the use of the new materials which can resist on high loads at very high temperatures and, having good wear and corrosive resistance capacity and also should have high electrical and thermal conductivity.

1.1 CERAMICS

Ceramic materials are made from the compounds of metal and the non metal and are are inorganic in nature. Advanced structural ceramics like Titanium carbide (TiC), Silicon Carbide (SiC), Silicon Nitride (Si_3N_4), Graphite (C), Alumina (Al_2O_3) and many more are the attractive materials which are finding many applications in different fields ranging from aero engines to manufacturing to dental restoration.

1.1.1 Classification and application of Ceramics

Ceramics are classified as follows:

- **Silicate Ceramics:** Having porous structure with amorphous glass phase. The main components of the silicate ceramics are: SiO_2 & littlie quantities of the : Al_2O_3 ,MgO and the ZrO_2.
- **Oxide Ceramics:** These are different from silicate ceramics. They do not have glass phase and they contains the elements like Al_2O_3, MgO, and the ZrO_2.
- **Non oxide Ceramics:** They cannot be use for practical in case of dental use because they are having high sintering temperature, having opacity and also having the anesthetic color.
- **Glass Ceramics:** These are produced by the nucleation and because of the growth of the crystals in the glass so they are partially crystallized.
- **Refractories:** These are used as firebricks for the furnaces and also for the ovens. Because they are having high Silicon content they don't shows any sign of fusion at high temperatures.
- **Abrasives:** These are having wide range of applications in lapping, grinding, blasting of materials, in advanced manufacturing processes, and also used in cutting and polishing.

The abrasives which are mostly used are like silicon carbide, diamond, cubic boron nitride, alumina etc.

- **Cements:** These are finding many applications in concrete roads, flyovers, roofs, walls and dams etc.

On the other hand, broadly there are two main categories of the ceramics which are traditional and advanced.

The traditional ceramics which were made by the humans are pottery objects which were made from the clay either by itself or by mixing with the other materials such as silica, hardened and then were sintered in the fire. For the traditional ceramics the powders were usually mixed with the water to increase the binding strength of the particles so that proper shape of the material can be achieved. After shaping the green parts were fired (sintered) to increase the hardness of the parts.

Advanced ceramics like Titanium Carbide (TiC), Zirconium Dibromide (ZrB_2), SiC, WC and SiN are appealing for many kinds of the advanced applications because they have the properties like high hardness and strength, having low density, high wear resistance capacity, and also shows high resistance to chemical degradation. The potential applications of advanced structural ceramics are given in Table 1.

Table1.1: Applications of advanced structural ceramics [1]

Aerospace • Bearings • Combustors • Fuel Valves • Turbine engine components	Defense • Armor • Rocket Nozzles • Submarine Shaft Seals • Engine Combustor Section
Automotive • Advanced Reciprocating Engines • Turbines • Turbocharger Rotors • Valves and Valve seats • Piston Rings • Fuel injector components	Bioceramics and Others • Artificial teeths, Bones • Heart Valves • Flow control Valves • Multi layer Capacitors • Semiconductors Packages etc.

Due to the addition of the materials which are hard and refractive, conductive ceramics like titanium nitride (TiN), titanium carbide (TiC), titanium diboride (TiB_2) and titanium carbonitride (TiCN) in particulate form to silicon nitride (Si_3N_4), zirconium oxide (ZrO_2) and

aluminium oxide (Al_2O_3) are being used as an approach to make ceramics which are having sufficient conductivity. Recently an aluminium oxide (Al_2O_3) based ceramic has been developed by adding titanium carbide (TiC) particles to aluminium oxide (Al_2O_3) powder and silicon carbide (SiC) particles to manufacture an EDM (electro discharge machining) tool Al_2O_3-SiCw-TiC.

Table1.2Various properties of some ceramics at room temperature [1]

Ceramic	Young Modulus E (Gpa)	Vickers Hardness H_v (Gpa)	Fracture Toughness (Mpa $(m)^{0.5}$)	Density (g/cc)	Thermal Conductivity(W/m-k)
Al_2O_3	356-362	13.3-17.4	3.8	3.9	26-35
Hot pressed SiC	430-450	26.9	3-4	3.10	150-200
TiC	414	35.6	6	4.93	34
Al_2O_3 + 25 wt % SiC	404-405	21	8.7	3.70	35
Al_2O_3-SiC-TiC	409-410	19-32	9-10	3.85	63

1.2 COMPOSITES

Composite materials are formed from two or more composing materials which are having different physical as well as chemical properties that, when mixed, yields a material which is having different properties from the individual ones. The individual components which were used to produce the composite, remains separate within the final structure. In recent years, composites are the growing interests amongst the researchers. The scientific definition of a composite material is that it contains more than one constituent having wide range of differences in their mechanical & physical properties that when mixed, fabricates a composite which is having the properties dissimilar from the individual constituent. Some properties of the composite materials which are considered as the best are: resistance capacity at high temperatures, showing very low deformations under the action of the forces, good wear resistance, and high conductivity and also having very good abrasion resistance. Significant

improvements in the mechanical properties have been achieved by using silicon carbide (SiC), titanium carbide (TiC) particles into aluminum oxide ($Al_2O_{3)}$ for the single phase alumina ceramic. So that recent evolution in composites is not only focused on the enhancement of properties, but also on the possibilities for substitute methods of the manufacturing.

Metal matrix composite (MMC), in which hard particles used as ceramics are circulate in a ductile matrix, shows superior properties like high modulus of elasticity, high strength, high thermal expansion coefficient, high temperature and wear resistance capacity.

Recently, there has been more effort in developing discontinuously reinforced MMC due to relatively low processing cost and their properties with good performance [2].

1.2.1 Application of Copper Matrix Composites

MMC's are now a day's finding wide applications in structural, automobile field, aerospace industries and also in the industries which are dealing in general engineering work. Copper based composites are having inherent properties like high thermal conductivity, high density and also shows good wear and corrosion resistance capacity. That's why copper based composites are being used.

Such materials are finding many applications including [3]:

- Electrodes used for welding.
- High performance switches and electrometers.
- Heat sink used in electronics components.
- Metallic friction materials for the applications of high speed motors and also for actively cooled parts used in gas turbine structures.
- Structural applications where high temperature is required, like brakes and other frictional applications.
- Electrical contacts.
- Resistance welding electrodes.

1.2.2. Fabrication of Composites

Various methods for fabricating [4] MMCs are

- **Liquid Metallurgy**:

  Spray deposition: A continuous fibre substrate is used on which molten metal is being sprayed.

  Stir casting: In the molten metal the discontinuous reinforcement are being stirred, which are then solidify to get the final object.

  Semi-solid powder processing: In this process, mixture of the powder is being heated up to the semi-solid state and then after pressure is being applied to get the desired composite.

- **Powder Metallurgy(P/M)** :

  Metallic powder and discontinuous reinforcements are being mixed followed by bonding using the process of preheating, compaction (possibly via hot isostatic pressing (HIP) or cold isostatic pressing (CIP)) followed by sintering to increase the bonding strength.

- **Foil diffusion bonding :**

  In this technique metal foil layers are being clubbed up by using the fibers and then pressed to get the desired composite.

- **Physical vapour deposition :**

  In this technique the reinforcing agent is being passed from a thick cloud of the vaporised metal, then after it coating is done.

Many methods are used to fabricate Cu matrix composites among of them casting and powder metallurgy methods are normally used. Because of low splitting capacity, low agglomeration, and also due to the good wettability, powder metallurgy (PM) route is generally more preferred to the other methods [4].

1.2.3 Fabrication of MMC via powder metallurgy route [5]

The step involved in composite fabrication by powder metallurgy route is shown in the flowchart (Figure 1.1). The detailed description of the steps is given below.

a) Mixing and Compounding: In first stage different kinds of materials are mixed having different compositions or may have same compositions to make a compound. In the traditional methods clay and silica were mixed and water was added to increase the bonding strength.

b) Compacting: The process is used to bring out the particles closer to each other and to remove the liquid binder. Due to this a dense structure is being achieved and which has the following advantages:

- Increases density and reduces porosity.
- Very less shrinkage occurs during the firing.
- Enhanced surface texture and also the strength.

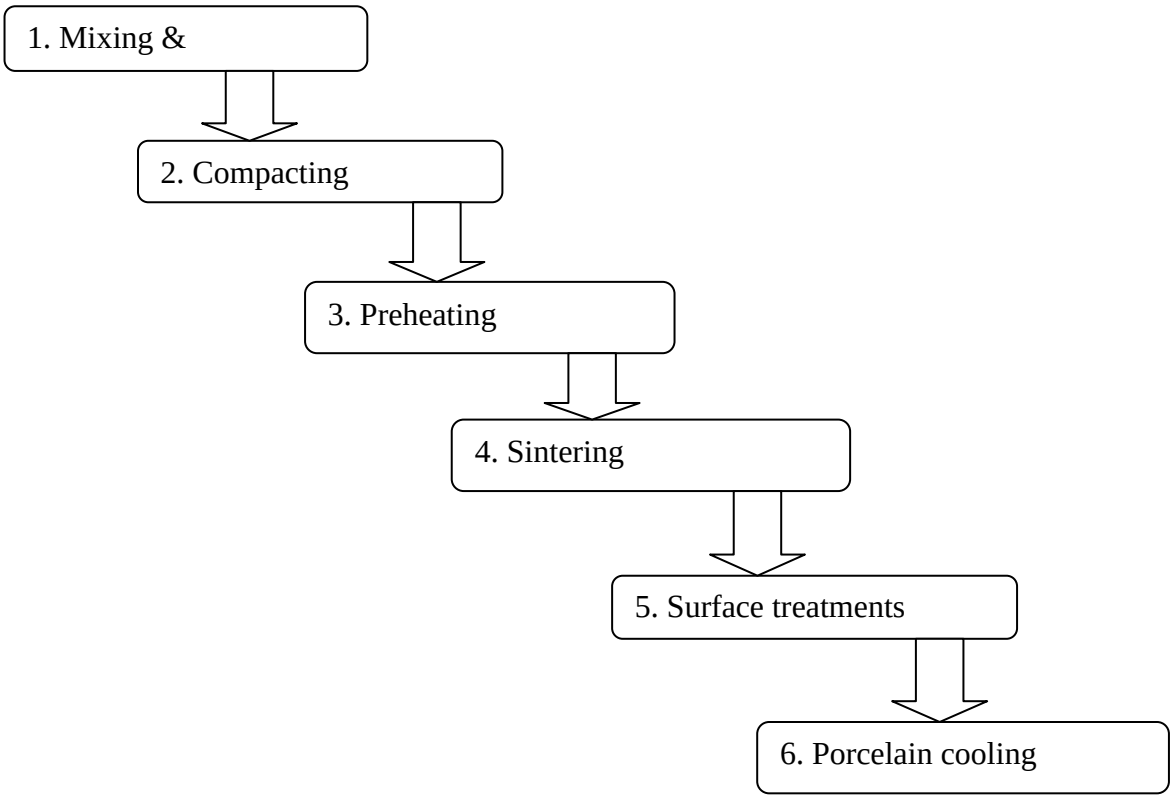

Fig1.1: Flow chart of composite fabrication

c) Pre-heating (Drying): This process is used to removal out of the moisture so that green strength of the part will be increased and porosity will be decreased. This process may be carried out in preheating furnace for the purpose of

- To remove out the excess water so that green strength will be enhanced.
- Prevents sudden production of the steam which could results in fracture of the part.

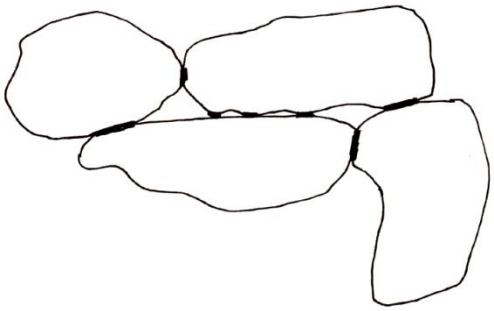

Fig1.2: Ceramic particles held together in the "green state" after all liquid has been dried off

d) Sintering or Firing: This process is carried out to increase the density and to reduce the porosity of the part and also to remove out the air which was entrapped during the compaction. So finally we will get a solid structure. Sintering is performed below the glass transition temperature so that the internal stresses are relieved. Sintering mechanism consist the following steps:

- During the initial firing temperature, the voids which are presented are occupied by furnace atmosphere. As the process of the sintering goes on, the particles start to make bond at their contacting point.
- As the temperature is increased, the voids are completely filled by the furnace atmosphere. The particles get fuses to each other and form a continuous mass, due to which volume gets decreased.

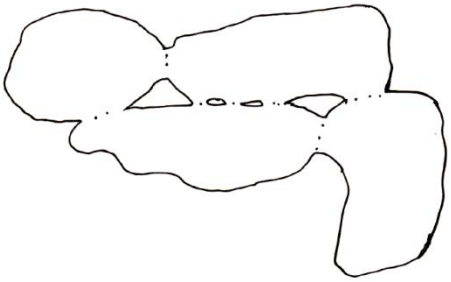

Fig1.3: voids structure during 2nd stage

- With the continuation of the firing, the gaps in between the particle become porosities. The flow rate also increased means the viscosity decreases with the progression of the firing. The result is that the porosity voids will gradually become rounded as firing proceeds.

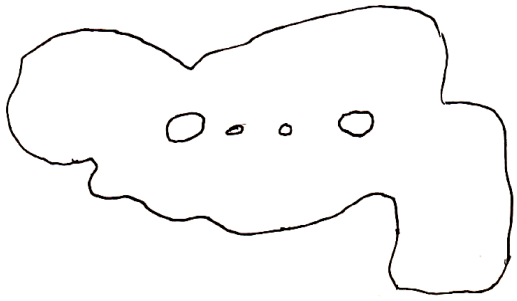

Fig1.4: voids deformation during 3rd stage

- Finally, voids are completely disappeared. So after the sintering process we gets a completely densed structure having no voids.

e) Porcelain surface treatment: After the sintering process some scales are deposited on the part due to which surface roughness of the part increases. To overcome this, many surface treatments can be used such as disc polishing, glazing, blunting, shining.

1.3 FRICTION AND WEAR IN COMPOSITES

There is no mechanism, no machine and no equipment that is not affected by wear and friction problem. Approximately 70% mechanical components during their function are failed due to wear and friction problems. One third of world's energy resources are waste due to friction in one form or the other and then most of these result in wear. So, it is of prime importance to study the wear behavior of materials.

When more than one surface is under different loading conditions having sliding contact to each other, frictional loss and wear out of the parts will be in evident. Wear is the main reason for material squander and friction is the measure cause of heat loss. When the material is removed from one or both of two solid surfaces which are in relative motion (sliding) is called as wear. Sometime wear may be desirable and some time may not be desirable. Operations such as machining and polishing are the examples of desirable wear, while wear takes place in bearings,

gears, seals and cams during perform their function are undesirable because they will reduce the performance of the operation.

Wear takes place either by mechanically abrasion action (where material from soft surface is removed when it is in contact with the harder surface), chemical reaction (depends upon the surface nature of either of the surfaces), or by combination of both processes and is generally increased at very fast rate by the increment of temperature. Accordingly, wear is classified into a number of categories such as Abrasion, Erosion, Adhesion, Surface Fatigue, Corrosion, etc. Appropriate materials have to be selected for composites in such a way that the wear out of the materials will be less and also the frictional coefficient will be less so that performance of the composites which are used for different applications will be increased. So, it is very important to understand the wear behavior of MMCs to prevent the failure of the useful machine components, so that the efficiency and effectiveness of the realistic operations involving these MMCs will be increased.

1.4 MOTIVATION

- Ultrasonic assisted EDM is a hybrid process which utilizes the ultrasonic waves to vibrate the electrode in EDM process. Wear out of the electrode is a major problem in ultrasonic assisted EDM process. The contribution of the tool cost to the total operation cost in UEDM is more than 70%. Due to this reason, the wear of the tool has to be carefully taken into consideration.
- In UEDM process, there are two type of tool wear:
  - Due to the propagation of ions, thermal energy is being generated which increases the temperature and ions imparts forces on the tool and the workpiece which leads to erosion of the material. Due to the erosive effect material is being removed out from the workpiece as well as tool and ultimately it leads to the wear out of the tool.
  - During the process, due to the vibration of the tool, a cyclic force is being set up on the dielectric fluid which generates a resistive force on the tool due to which the tool tip experiences a sudden mechanical compressive force which generates wear and tear on the surface of the tool tip. This result in development of irregular asperities on the tool tip and wear & tear of these asperities.

- It has been reported that replacing copper electrode with composite electrode reduces tool wear in UEDM process. However there is no study reflecting how the mechanical wear explained above is compensated by the new tool tip. On this point, it is important to note that the mechanical wear characteristics can be studied through vibratory and/or sliding wear mechanism. Here, an attempt will be made to study the mechanical wear characteristics of copper based ceramic electrode using dry sliding wear test equipment.

1.5 THESIS ORGANIZATION

The thesis is organized in SIX chapters.

- Chapter 1 presents an introduction to the composites. It presents an overview of the different fabrication processes of composites and its potential applications. This chapter also highlights the motivation for the present research.
- Chapter 2 describes the literature survey in the proposed area of research. Major contributions made in the past covering assessment of electrode wear in UEDM process, fabrication of composites by different modes and tribological study of the composites. The chapter also provides the objectives of present research work.
- Chapter 3 discusses the methodology of fabricating copper based composites with different configurations to be used for the experimentation and also discusses the different instruments used to measure the physical, mechanical and tribological properties of the fabricated composites.
- Chapter 4 describes the observations and findings of experimentations covering mechanical and tribological properties and behavior of the fabricated sintered composites.
- Chapter 5 describes the regression equation correlating mechanical wear and friction with applied normal load, sliding speed and sliding distance. Further the behavior of the responses with respect to the process parameters is also explained.
- Chapter 6 concludes the major findings of the present research work and highlights the directions for future research.

CHAPTER 2
L ITERATURE REVIEW

2.1 INTRODUCTION

As a thermal process EDM is accompanied by high rate of electrode wear and low material removal rate which requires more electrodes for a job. UEDM is one of the approaches developed to enhance material removal rate. But as discussed in the previous chapter, one of the main concerns of UEDM process is the tool life. To improve the tool life, various efforts have been made by different approaches like powder metallurgy, rapid prototyping, electroplating etc. Further there have been efforts to explain the wear behavior of composites. This chapter discusses the past research in the direction of tool wear in UEDM process, different approaches to fabricate electrode tip for EDM and UEDM process and wear study of composites.

2.2 LITERATURE REVIEW

2.2.1 Category 1: Study of tool wear in ultrasonic assisted EDM process

Kremer et al. **[6]** studied the effect of ultrasonic vibrations on the performance in EDM. During their study they observed that the dielectric circulation was accelerated due to the vibration of the electrode, which leads to lesser machining times. They also observed that due to pressure variations in the gap, more discharge was taken place, which leads to more removal of metal from every crater. Effects on other parameters like relative wear, surface roughness and hardness were also observed in their study.

Murti et al. [7] attempted to saw the effect of ultrasonic vibrations on the performance of the work piece and the tool. SEM was used for the analysis of the work piece which shows that most of the particles were having globular shape having solid structure. The particles were in the form of splats, having cracks and dents etc. As the replica of the tool is made on the work material which ensure that the some material is being removed from the tool.

Thoe et al. [8] attempted to make small diameter holes in nickel alloy having coating of ceramics; by using UEDM process. MRR of the workpiece was increased due to the ultrasonic vibrations. Tool wear was also occurred due to hammering action of the tool and it can be improved by using the ceramic tool.

Lin et al. [9] worked on titanium alloy (Ti-6Al-4V) to saw the machining characteristics by using the combination of EDM and the ultrasonic machining (USM). To improve the machining performance; EDM and USM machining mechanisms were integrated. They investigated the effects of the on the MRR, EWR, relative electrode wear ratio and the surface roughness. They concluded from the experimental results that combination EDM/USM process can increase the MRR, surface roughness on the workpiece was slightly increased and also the tool wear was slightly higher.

Jia et al. [10] have developed an EDM machine having ultrasonic vibrations so that holes can be produced in the ceramics. They analyzed that this new technique was highly effective in order to obtain a higher MRR and relatively removal of the material from the tool takes place which propagates the tool wear with increased surface roughness.

Jia et al. [11] carried out an analysis on the mechanisms of USM and EDM, and a combined technology which was having the advantages of both, has been proposed. They observed that, this new technology can be used to machine all the brittle materials with good machining efficiency. After analysis they found that the new technology was having higher efficiency than that of ultrasonic machining, with increased tool wear.

Abdullah and Shabgard [12] dealt with the influence of the Cu tool vibration with ultrasonic frequency on the EDM characteristics of cemented tungsten carbide (WC-Co). During their study they observed that due to ultrasonic vibration of the tool; higher MRR was attained. It was observed that due to the addition of the ultrasonic vibrations; the surface roughness and the TWR was increased.

Shabgard et al. [13] studied the combination of EDM with ultrasonic vibrations, so that the machining efficiency can be improved. Graphite was used as tool electrode and AISIH13 tool steel was used as a workpiece. During their study they observed the effect of machining parameter on the MRR, TWR and also the surface roughness. It was observed that due to ultrasonic vibration; MRR and the surface roughness were increased and also the tool wear was slightly increased.

2.2.2 Enhancement of various properties of copper based MMCs fabricated by different methods

Zaw et al. [14] worked on the compounds of TiSi and ZrB_2 with copper (Cu) for various composition to fabricate the composites either by using liquid phase sintering or by solid-state sintering. A newly composite was formed by this technique and they used it as EDM electrodes. Its performance was compared with the performance of conventional tools which are having materials like copper (Cu) and Graphite (C), for same machining conditions. They observed that ZrB_2-Cu composite have more hardness and the conductivity as compared to the conventional materials like Copper (Cu), Graphite (C).

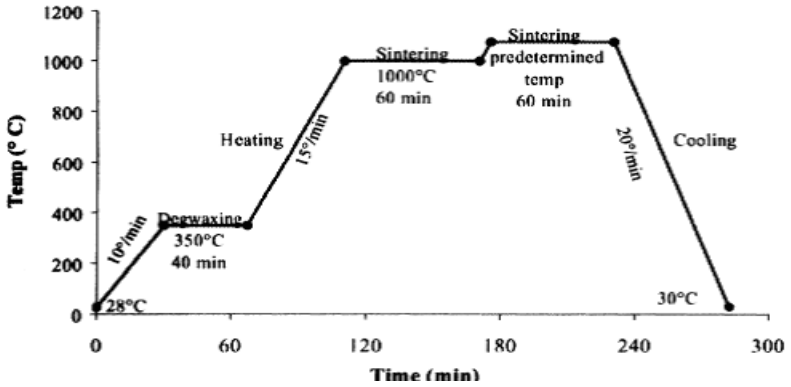

Fig2.1: Sintering cycle of ZrB_2/Cu system

Mohari et al. [15] fabricated the composite by using the materials like copper (Cu), aluminum (Al) and titanium carbide (TiC) using the powder metallurgical route, followed by sintering, to increase the strength of the composite. Properties of these composites were compared with the conventional materials like copper (Cu) and aluminum (Al). After the studies it was observed that due to the addition of the different materials like TiC, Al in the Cu, the hardness and the density of the composite was increased and porosity of the composite was very less as compared to conventional materials.

Samuel and Philip [16] during their study they analyzed the electrical, physical, thermal and mechanical properties of the copper based composite fabricated by powder metallurgy. They used electrolytic copper powder (ECP) with 99.7% purity as basic material. The properties of the fabricated composite were controlled by varying the sintering temperature and compacting pressure. As the compacting pressure as well as sintering temperature was increasing the

conductivity was also increasing. Low pressure fabrication yielded lower mechanical strength, whereas high sintering temperature increased the bond strength. The increase in sintering temperature and also the increase in compacting pressure results in change in electrical, thermal, mechanical and micro structural properties.

Chung et al. [17] worked on copper based composites using TIB_2 and whiskers of silicon carbide (SiC). Composites were made by coated filler method and by mixture method using powder metallurgy route. After the successfully completion of the experiments; the properties of the composites made by two different processes were compared. It was found that for low volume fraction, the composites made by P/M method having superior properties like high hardness, good electrical and thermal conductivity, higher yield strength and also having low thermal expansion. Silicon Carbide (SiC) which were used as whiskers, are one of the highly effectual reinforcement for the purpose of metal matrix composite (MMC).

Samuel and Philip [18] during their investigation found that the powder metallurgy route is preferred over the other methods because of ease of manufacturing and also the ease of control over the properties. It was observed that there was less roughness on the composite material in P/M because of the inert atmosphere during sintering. It was also observed that the mechanical strength was poor and also the relative density was lesser due to low compacting pressure and the sintering temperature.

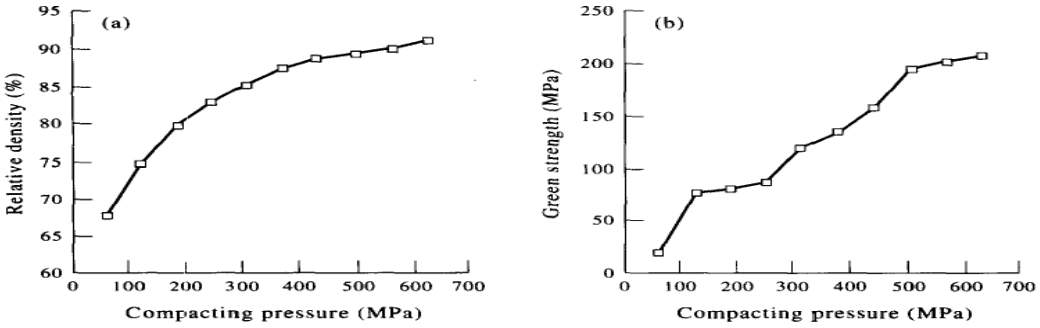

Fig 2.2 (a): Relation b/w relative density & pressure (b): Relation b/w strength & pressure

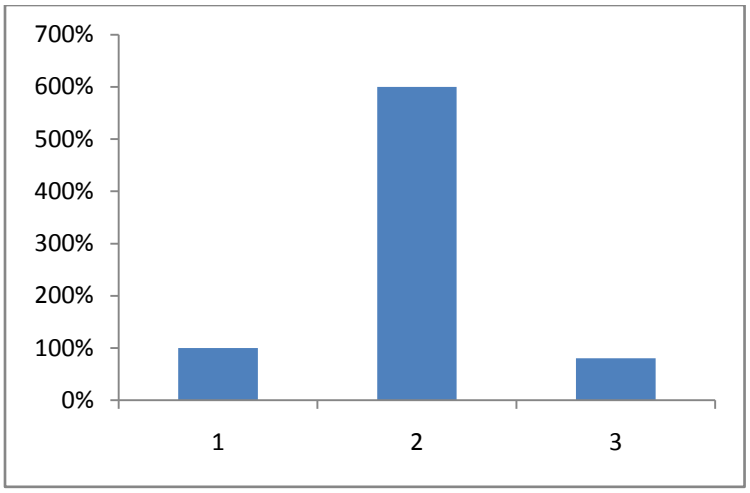

Fig 2.3: Relative (%) increase in electrical, thermal, mechanical properties of the electrodes

Norasetthekul et al. [19] used a conventional method to synthesize ZrB_2-Cu composite, starting from mechanical pressing of polymer-coated ZrB2 powders, and followed by infiltration of copper into the green body in a high-temperature furnace. The way to control the amount of infiltrated copper was to vary the pressure of the press. It was observed that higher the pressure, the lesser the voids between the particles, reducing the amount of copper required to infill the voids. However, it was found that the copper tends to fill the voids incompletely, since its infiltration is mainly due to the flow of molten liquid copper opposing the capillary force inside the voids. However, it was observed that the ZrB_2-Cu composite had the higher hardness and the conductivity than single material like copper (Cu) and also the graphite (C).

Loh et al. [20] fabricated metal matrix composite (MMC) by using powder injection molding. They used copper and silicon carbide as a powder form to made the composite. After the experimentation it was found that the parts made by this technique were defect free and also the addition of titanium carbide microhardness and density were increased. By increasing the sintering temperature the physical and mechanical properties was improved.

Li et al. [21] worked on the electrical discharge machining (EDM) electrodes of sintered copper (Cu) to investigate the effect on the performance of EDM by adding the titanium carbide (TiC). To fabricate the tool they used rapid prototyping technique using selective laser based sintering. Six batches were made of the titanium carbide (TiC) having content varying from 5% to 45%. To fabricate the part, the powders were firstly mixed by using ball mill, than pressing was done, followed by using the technique of sintering with the copper (Cu) and the copper-

tungsten (Cu-W), respectively. A comparison was done with commercial electrode to show the performance of newly formed electrode. Due to the addition of nickel (Ni) densification of TiC-Cu-W system was improved, because nickel (Ni) has property of good solubility in both the tungsten (W) and the copper (Cu). With increasing quantity of titanium carbide (TiC), relative density was firstly increased and thereafter decreased, and also the electrical resistivity of the samples was firstly decreased and after it increased. Due to the addition of titanium carbide (TiC), surface finishing was increasing for electrical discharge machining (EDM) electrodes. In comparison of the parts machined by commercial electrode the surface roughness for most of the specimens was found less. Electrodes having 15% titanium carbide (TiC) has shown the lowest electrical resistivity and highest relative density and EDM performance (i.e. high MRR, low TWR and good surface finishing) was also good.

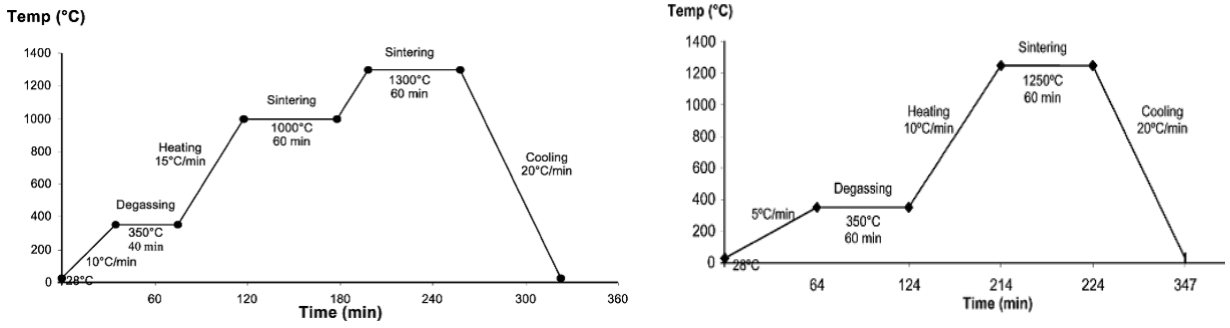

Fig 2.4 Sintering cycle of (a) TiC/Cu ceramic (b): TiC/Cu-W ceramic

Tsai et al. [22] worked on fabrication of composite tools by mixing copper powder having resin with chromium powder. A hot mounting machine was used to form such composites at a pressure of 20MPa and at a temperature of 200°C. After experimentation the results showed that a new layer on surface was formed after sintering due to uncontrolled cooling. After the experimentation it was found that due to the addition of the chromium anti corrosion properties of the composite were increased. The experiment was performed at the appropriate parameters like compacting pressure, proper mixing of the composition and the sintering conditions. Due to addition of the chromium the hardness of the composite was little increased as compared to the copper (Cu) material. So they concluded that chromium is a good material which can increase the corrosion resistance capacity of the material and also having less influence on the hardness of the composite.

Zhao et al. [23] worked on the formation of composite tool for the purpose of machining of conventional materials by using rapid prototyping technique known as selective laser sintering (SLS). A post treatment technique known as Metal Infiltration was used to improve the density as well as mechanical performance of metal prototype made by SLS. A parametric experiment was conducted which shows considerable improvements in mechanical and thermal properties of the composite tool. From the results it was clear that the hardness as well as conductivity of the fabricated tool approaches to that of a general machining tool, and surface roughness of the fabricated tool was acceptable for same machining conditions.

Dimla et al. [24] worked on fabrication of the EDM tool by using laser sintering of rapid prototyping technology. Stereolithography and the laser sintering methods were used to fabricate the electrodes. After the investigation they found that the copper was adhered on both the electrode made by different process which was a major problem due to which electroplating process was not successful and at the inner cavities of the electrodes sufficient amount of copper was not deposited and at outer surface thickness of copper layer was very less. Hence, they concluded that these electrodes can't be used for EDM applications.

Khanra et al. [25] worked on the fabrication of the metal matrix composite MMC by using the ZrB_2 & copper (Cu) to find out an appropriate combination for the composite which is having high conductivity and also having good wear resistance capacity. Different quantities of the copper (Cu) and also the ZrB_2 were taken to form different composites; which were tested for the different machining parameters. For the ZrB_2–40 wt% copper (Cu) composite shows more metal removal rate (MRR) in comparison of generally used Cu tool. They also invested that average surface roughness on the work piece was lesser for composite tool in comparison of copper tool.

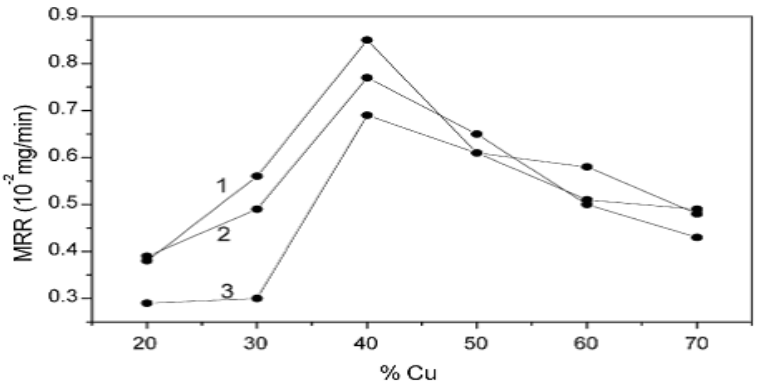

Fig 2.5: Variation of the MRR with increasing wt. % of copper (Cu) at the different runs

Schubert et al. [26] worked on copper based composites by using SiC and diamond as a reinforcement. The composites were fabricated by using powder metallurgy route. Proper control of interfacial interactions was the major challenge for the development of Cu/SiC composite. The bonding strength between the copper and diamond was very for copper diamond composite. By using the molybdenum coating on SiC powders, bonding strength as well as thermal properties was increased. Such kind of composites having applications for heat sink which are used in electronics components due to their high thermal conductivity and high strength.

Mishra and Pathak [27] studied the systematic sintering of the ZrB_2 powder mixed with the carbon (C) between 0 to10 % and the titanium carbide between 0 to 30 %. A similar sintering behavior was observed for all the compositions which were made with Zirconium diboride (ZrB_2) powder. The addition of the carbon(C) propagates the easier densification in between 0 to 4 % and tougher densification in between 4 to 10 %, and the addition of the TiC above the 5 wt.% was found dangerous for sintering of the Zirconium diboride (ZrB_2). Due to the presence of the carbon(C) the size of the grain was not increasing also and a high densified fine grained ZrB_2–C composite may be obtained. Because due to the addition of the carbon more oxygen impurities were removed so the densification was also increased. As the percentage of carbon was increasing, the densification rate was decreasing.

Monzon et al. [28] worked on the fabrication of the new composite by using the rapid prototyping technology. They formed a new copper (Cu) composite by using plastic prototypes. They designed a new tool for copper shells. To saw the performance of the newly formed composite, it was used as an application for tooling purpose of the electro discharge machining and was compared with the copper tools made by conventional method. Results prove that newly fabricated tool shows good behavior as compared to the conventional electrodes.

Celebi et al. [29] worked on how the particle size and its distribution were affecting the properties of silicon carbide (SiC) particle which were reinforced with the copper (Cu) powder. Copper powder was reinforced with silicon carbide (SiC) powder having particle size of 1 and 30 μm and sintered at a temperature of 700°C. SEM studies show that the SiC particles were homogeneously dispersed in the copper (Cu) matrix. Archimedes' principle was used to measure the relative density of composites which was ranging from 91.2% to 95.8% for SiC having

particle size of 1 µm, and having hardness of 110 to 125 HVN, 94.0% to 96.0% for SiC having particle size of 30 µm, and having hardness of 115 to 145 HVN.

2.2.3 Category 3: Tribological Study on copper based MMCs

Tjong et al. [30] they used hot Isostatic pressing (HIP) process to prepare the sample of copper (Cu) reinforced with silicon carbide (SiC). To saw the wear and frictional behavior of copper based composites pin-on disc tribometer was used. The pins were slided against a disc of hardened steel under the dry ambient conditions. The surface of the disc was polished with a abrasive paper of SiC of 240 grit size. After the experiment it was found that soft copper material exhibits very high wear loss. However, the addition of silicon carbide (SiC) particles up to 20 vol.% shows the improvement in the abrasive wear resistance for the applied loads of 15-55N for copper and the wear loss was also less as compared to pure copper (Cu). This phenomenon was happened due to the reinforcing silicon carbide (SiC) particles being effective to minimize the extent of the wear deformation in subsurface region during the sliding conditions.

Badry et al. [31] worked on the composite of Copper (Cu) – graphite (8, 15, 20 wt%) which were fabricated by using the powder metallurgical route. Pin on ring tribometer was used to carry out the experiment. Cylindrical pins having length of 12±1 mm and 7.9 mm in diameter were made by using the discovered materials and were slided against a rotating steel ring of 62HRC. The normal load was varying from 50 to 500 N. During each test of the wear; it was seen that the length of the tested pin was decreasing, and also the frictional force was reducing with sliding distance. Scanning electron microscopy (SEM) was carried out to study the morphological changes in both subsurface and surface for every pin. Results shows that composites made by Cu-graphite have less wear rate and frictional coefficient than those which were made from the pure copper and the wear for both cases was oxidative.

Zhan et al. [32] investigated the wear mechanism and frictional behavior for copper (Cu) matrix composites which were reinforced with the graphite (C) and silicon carbide (SiC) particles. After the experiments it was found that a graphite layer was adhered on the tribo surface which was enhancing the tribological properties like less wear and less frictional coefficient of the hybrid composites at lower normal loads. When graphite content was increased the hardness was decreased and the wear rate was also decreased at high load. A continuous

supply of the graphite to the tribo-surface gives anti-frictional properties for copper reinforced composites.

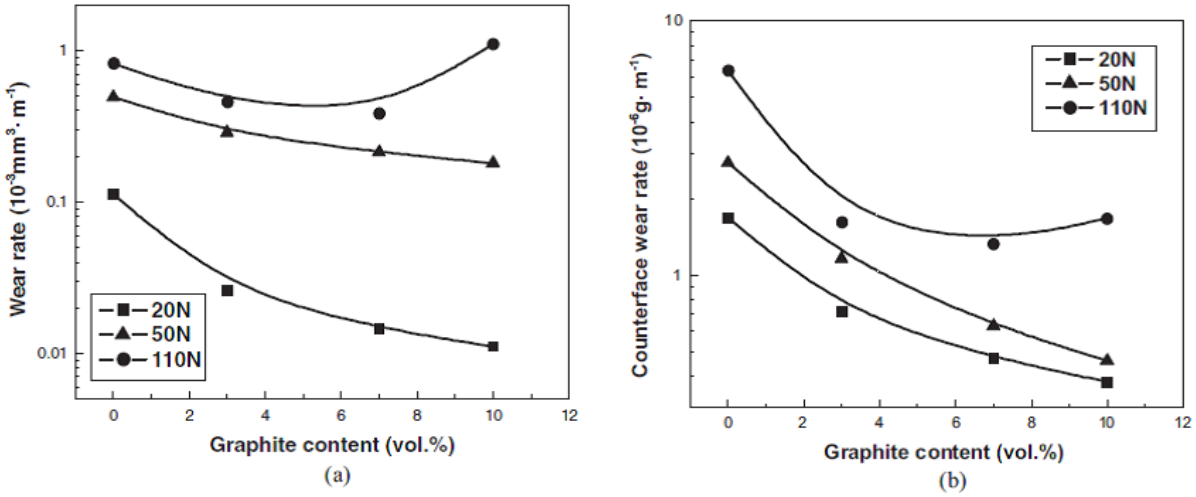

Fig 2.6 Variation of volumetric wear rates for the composites and the counterfaces having graphite fraction at different loads; (a) composites, (b) counterfaces.

K. Rajkumar and S. Aravindan [33] made copper matrix due to their good properties like better thermal and electrical conductivity. By using microwave processing technique they fabricated new series of hybrid composites of copper (Cu)–titanium carbide (TiC) (5–15 vol%) – graphite (5–10 vol%). Pin-on-disc machine was used under different testing parameters to evaluate their tribological properties. They used sliding speed and normal load as their testing parameters. The sliding speed of 1.25–2.51 m/s and normal loads from 12–48 N were used. Graphite layer was formed on the composite which enhances the tribological properties like less amount of material removal from the pin and also the less amount of frictional force was generated which automatically reduces the frictional coefficient. SEM was used to understand the mechanism of wear surface morphology. As the content of titanium carbide (TiC) was increasing; hardness was increasing. As the graphite content was increasing, hardness of the hybrid composites was decreasing.

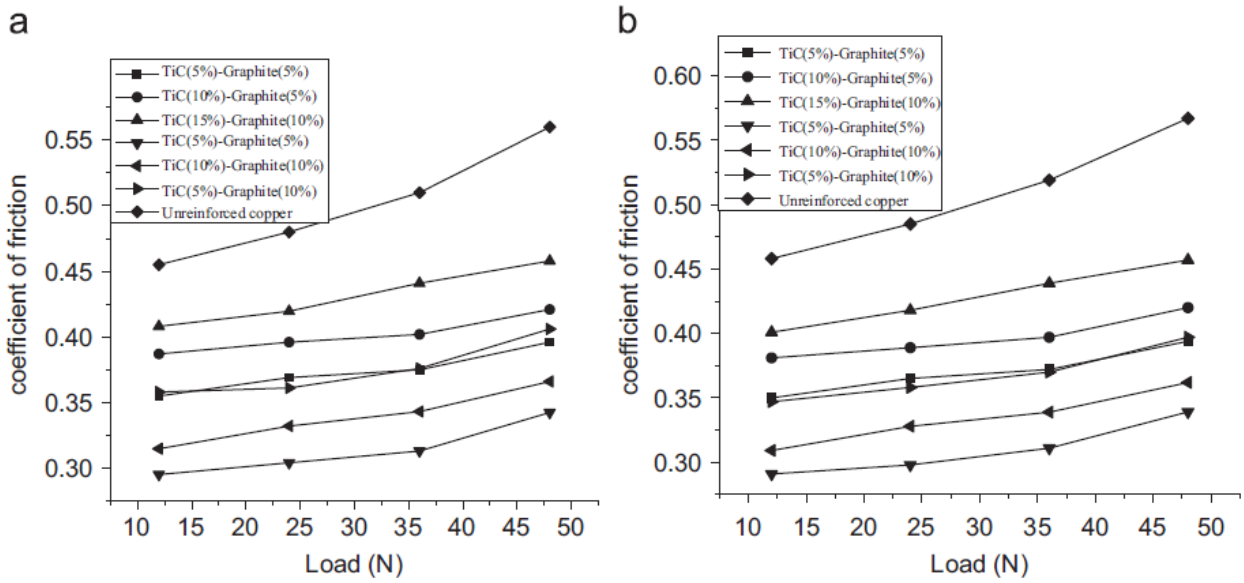

Fig 2.7: Variation of the frictional coefficient (a) at 1.25 m/s (b) at 2.51 m/s.

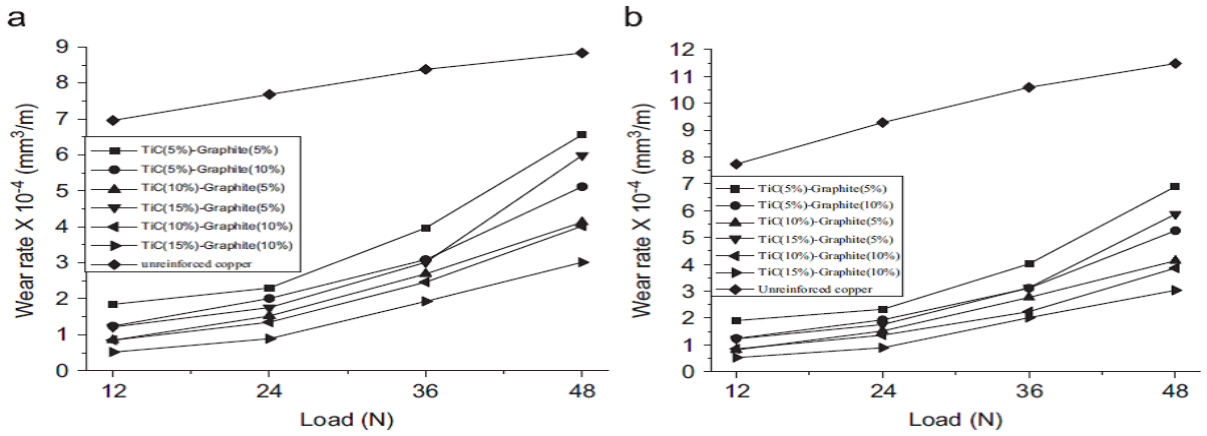

Fig 2.8: Variation of wear rate of composite (a) at 1.25 m/s (b) at 2.51 m/s.

Hong et al. [34] explains the application of the indium doping in the WC particles which were used as a reinforced material for copper based composites. Wear resistance of the composite (Cu-alloy/WCp) was investigated by pin on disc machine, and was compared with the conventional materials. The overall performance of the wear by 38% under the load of 10 N with sliding distance up to 3000 m was improved due to Doped indium. Surface morphology was seen by using the SEM and the result shows that the wear was of abrasive type for (Cu-alloy/WCp).

Huang et al [35] worked on copper-based self lubricated materials having two solid lubricants as graphite (C) and MoS_2 were fabricated by the P/M route using hot pressing technique. A ring on disc machine for wear measurement was used under vacuum and air

conditions to see the effect of MoS_2 and graphite content on frictional coefficient. Tribo-films which were formed on the worn surfaces were characterized by using SEM. The results show that due to the addition of the MoS_2 properties such as hardness, density was increased, while the relative density was showing the opposite trend.

Tiwari et al. [36] worked on the effect of the copper (Cu) addition in the Aluminum (Al) powder under dry sliding conditions. The samples were made by using cold isostatic pressing (CIP) technique on a UTM of 40 ton followed by sintering at 475°C. Copper was varied from 5% to 30% and tribometer was used to evaluate the wear behavior. The applied loads were varied from 10 N to 20 N and the track radius was 25 and 40 mm. The disc was rotated at 1000 rpm. The results show that due to addition of the copper (Cu), wear resistance enhances. With the increasing Cu content the frictional coefficient also shows the increasing trend.

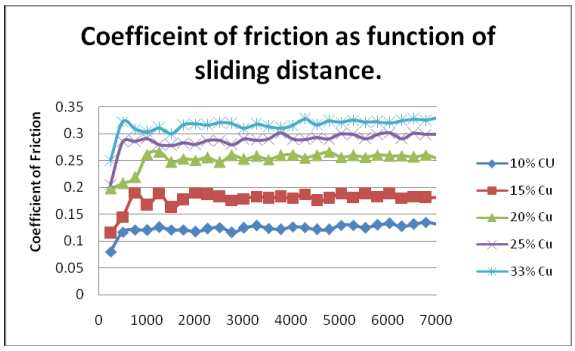

Fig2.9 (a): Friction coefficient v/s sliding distance

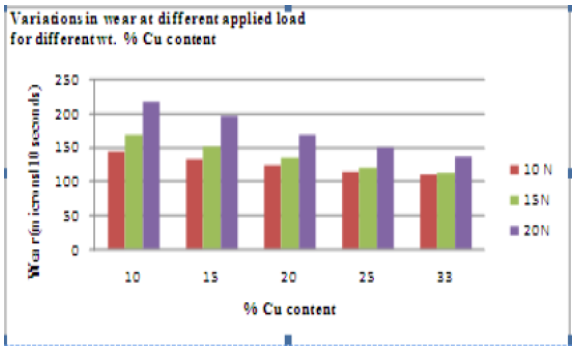

Fig (b): Wear v/s sliding distance

Jin et al. [37] worked on copper matrix composites which were reinforced by the silicon carbide (SiC) particles and Graphite (C) particle. These composites were made by the powder metallurgical route. Archimedes theory was used to measure the density of the composites and the tribometer was used to measure the frictional and wear trend of the materials. The results show that with the increasing content of graphite, hardness of the composites was decreasing, and wear resistance was increasing, and also with the increasing in SiC content the hardness was also increasing. This study extends the applications of copper matrix composites for practical significance.

Reddy et al. [38] worked on the abrasive kind of wear behavior for the copper (Cu) matrix composite which reinforced with the silicon carbide (SiC) and the silica particles. Powder metallurgical route was used to fabricate the samples of Cu-SiC (12%) and Cu-SiO_2 (9%).

Tribometer was used to carry out the experiments. Effect of the load and the sliding distance was studied for Copper (Cu)-silicon carbide (12%) and the Copper-SiO_2 (9%) composites. With increasing in sliding distance wear volume loss was also increasing. Copper (Cu)-silicon carbide (12%) composite shows better abrasion resistance in comparison of the Copper-SiO_2 (9%) composite.

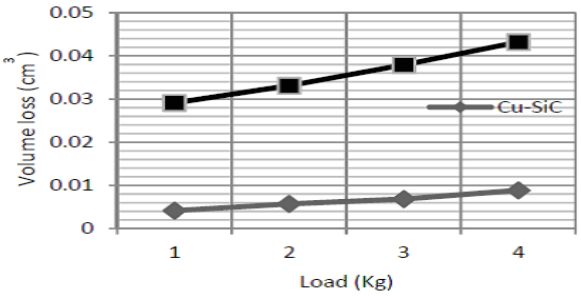

Fig 2.10: Comparison of the volume loss for Copper-(12%vol.) SiC & Copper-(9% vol.) SiO_2

Prabhu et al. [39] worked on copper (Cu) based SiCp composite (20% SiCp by volume) which was made by powder metallurgy route and was investigated for its wear behavior. Particle size of copper powder (≤10µm) and SiCp (25–37µm) were used to make the green compacts at compacting pressure of 438Mpa and sintered at 860°C in the atmosphere of nitrogen. To calculate the wear rate the wear test was done on Pin-On-Disc machine at four loads of (15 N, 25 N, 45 N, and 65 N) and at four sliding speeds (m/s) (0.6, 1.2, 1.8, 2.4).

Shabani et al. [40] worked on Cu and Cu/SiCp composite by using sintering and sinter forging process to prepare the compacts. They investigated the effect of silicon carbide (SiC) particles on the wear and frictional behavior for Copper and the composite of Cu- SiC. After the investigation under dry sliding conditions they found that wear loss was lowest for copper composite having 60 vol% SiC.

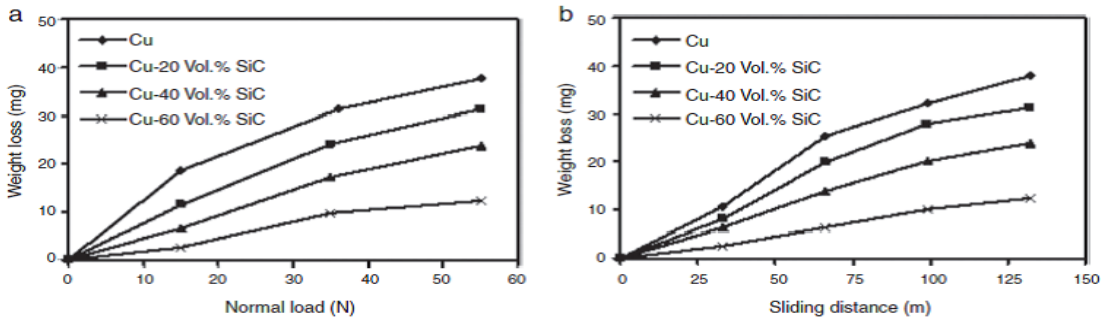

Fig 2.11 (a): normal load v/s weight loss Fig (b): sliding distance v/s weight loss

2.3 SUMMARY OF THE LITERATURE REVIEW

In UEDM process tool wear and surface roughness increases in the range of 5 to 15% [6]. To compensate the mechanical wear which is also observed in the EDM process, researchers developed composite electrodes by mixing metal with ceramics to enhance the mechanical properties of the electrode. It was observed from the literature that researchers have worked on metal matrix composite by using different kind of abrasives as a reinforcement like TiC, SiC, TiSi, ZrB_2, W, Cr etc. in different particle sizes by using different fabrication methods like powder metallurgy, rapid prototyping (selective laser sintering, stereolethography), microwave sintering, Forging, Stir casting, Pressure infiltration etc. for different pressure and temperature conditions.

Composites which are having different percentage of the reinforcements, affects the wear rate as well as coefficient of friction. If the compaction is done at more pressure for more time and the sintering is done above glass transition temperature; void free structure and solid mass will be obtained which will have high density and less porosity. It is also clear from the literature review that addition of reinforcement increases the hardness of the composite which leads to increased wear resistance capacity. By adding more percentage of the reinforcement, wear resistance capacity as well as corrosion resistance capacity will be increased and also the coefficient of friction will be reduced so ultimately the life of the composite will be increased. By increasing the sliding speed and the normal load, wear rate as well as coefficient of friction increases, as the percentage of reinforcement increases, wear rate as well as coefficient of friction decrease even at high speed and at high load.

Scanning electron microscope and optical microscope are used to find out uniform distribution of reinforcement into matrix, surface morphology and grain structure. The overall result revealed that increasing the percentage of reinforced particles improves the hardness, tensile strength, wear resistance capacity of the composites. Particle size also affects the properties of the composite. By increasing the particle sizes, relative density as well as the hardness of the composite increases [28]. Addition of the materials like Chromium, Graphite increases the wear resistance capacity of the composite while due to the addition of the graphite hardness of the composite decreases. Overall it is seen that; by increasing in percentage of reinforcement the wear resistances improve for all the cases.

2.4 RESEARCH GAPS

- It has been found from the literature that the fabrication processes like stir casting doesn't have the capacity of homogeneous dispersion of the particles; rapid prototyping technology having disadvantage of curling and shrinkage of parts, hot iso static pressing has density variation in the final part. Powder metallurgy route doesn't have these kinds of disadvantages and has advantage of volumetric heating during sintering due to which part comes out to be more densed and homogenous. However, very few studies are carried out for the composites fabricated by powder metallurgy route.
- Very few studies has been done on sintered Cu-SiC composite and their wear behavior, which has huge potential applications like EDM electrodes and brakes.
- It has been found that by increasing sintering temperature, densification rate increases and finally a dense part will be obtained. However, to the best of my knowledge, there has been very little work done where sintering is done near glass transition temperature for Cu-SiC composite.

2.5 PROBLEM FORMULATION

It is well known that copper is a good conductor of heat and electricity therefore it is predominately used in ultrasonic assisted EDM applications. It has been observed that surface finishing is poor by copper tools for e.g. in vibratory ultrasonic assisted EDM; the surface finish of the part made from copper electrode tends to be lower. This is mainly due to the tool end getting flattened and deformed due to constant hammering action and subsequent wearing out, as shown in figure 2.12. Hence it was observed that researchers used different abrasives with copper based composites to overcome the above mentioned problem. These composites tool tips can be fabricated by some of the common techniques like sintering, rapid prototyping and tooling, spark plasma sintering etc. However there is very little literature regarding the effect of the sintered abrasive in conjunction with copper on the wear behavior because this property affects the life of tool tip during machining.

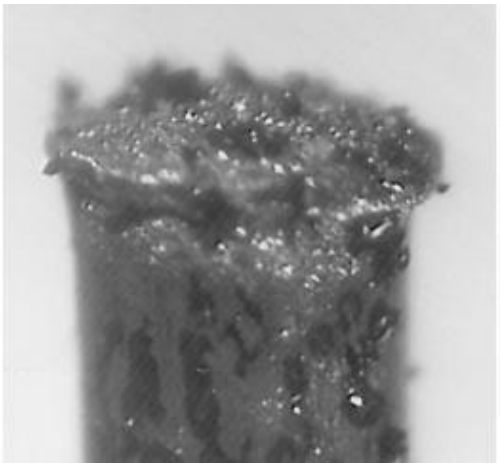

Fig 2.12: Flattening of Copper tool during Vibratory EDM

2.6 RESEARCH OBJECTIVES

Based on literature review and the potential outcome from the study, the following research objectives have been defined:

- Fabrication of the composites by using copper as the base material and using Silicon carbide (SiC) in different compositions.
- Characterization of Physical, Mechanical and Metallurgical properties of the fabricated composites.
- Tribological study of fabricated composites under different loading and sliding conditions.
- Statistical analysis to investigate the significance of the influencing parameters on the tribological behavior of the fabricated composites.

CHAPTER 3
EXPERIMENTAL PROCEDURE & EQUIPMENT

3.1 INTRODUCTION:

This chapter describes the selection of material used to fabricate the composite, the method of fabrication, experimental equipment and facilities used for evaluating the properties of the metal matrix composites and tribological studies, which helped to achieve the objective.

3.2 WORK PLAN:

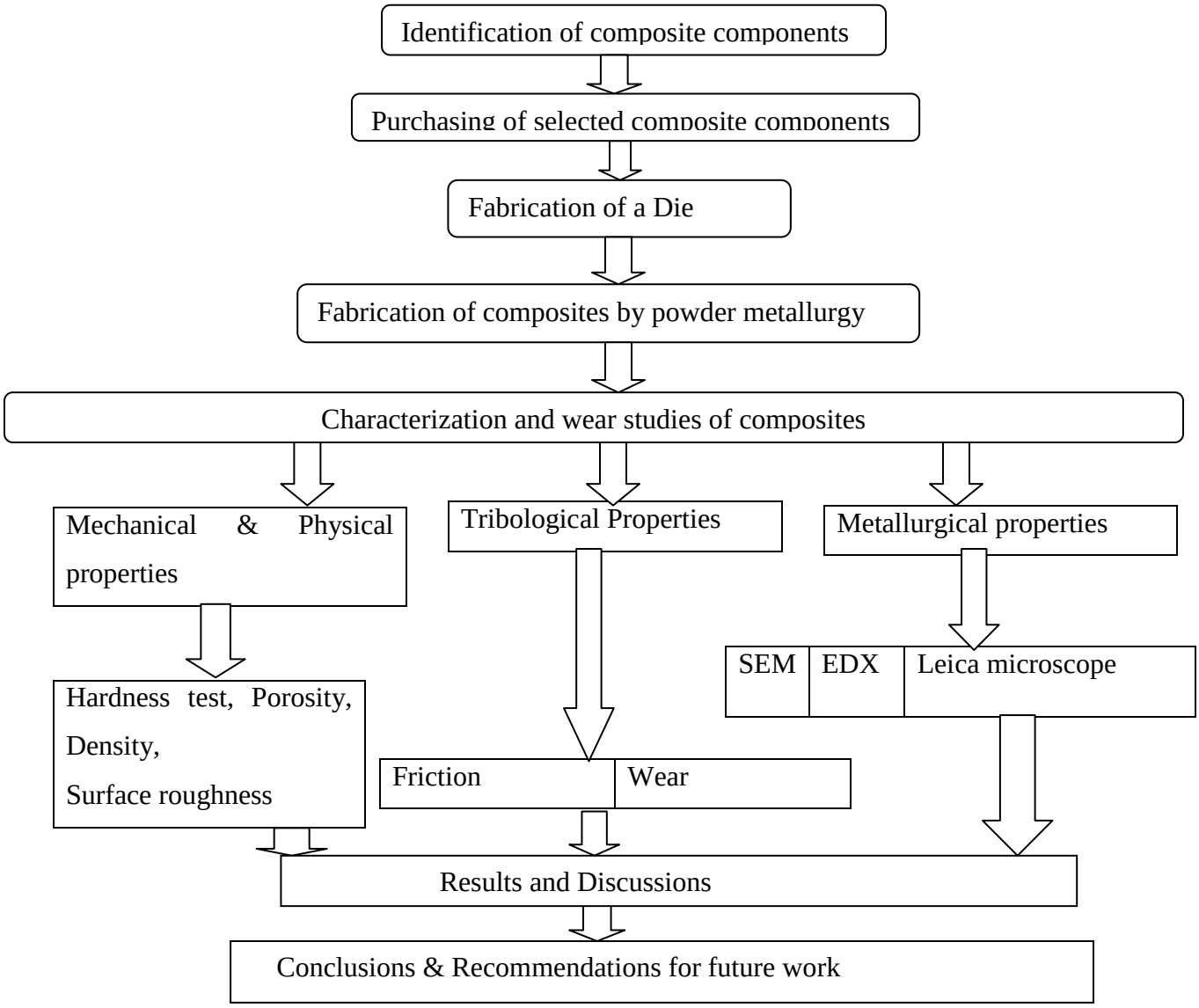

Fig 3.1: Flow chart of methodology of work plan

It includes

- Identification of the composite components for the composite with better mechanical, metallurgical and tribological properties.
- Fabrication of composite using copper as the base material and abrasives of silicon carbide (SiC) in different constituents with nickel and graphite as binder and wetting agent.
- Sample preparations for the different tests and characterization.
- Mechanical, physical and metallurgical characterization of fabricated composites.
- Tribological study of fabricated ceramics under different sliding and loading conditions.
- Optimization study on the material combination to fabricate a suitable wear resistant composite having good metallurgical and mechanical properties.

3.3 MATERIAL SELECTION

Appropriate material has to be selected for the composites in such a way that the composite is having high hardness and also the wear out of the materials will be less and also the frictional coefficient will be less so that performance of the composites which are used for different applications will be increased.

In this stage the suitable materials were selected to carry out the experiment so that the desired objectives can be achieved.

3.3.1 Matrix material

Copper (Cu) was used as a base material due to its high thermal conductivity as well as electrical conductivity, that's why it is used as a constituent of various kind of metal alloys.

3.3.2 Reinforcement

Silicon carbide (SiC) was used as a reinforcement for MMC due to its high hardness and when combined with copper, the strength of the composite will be increased so that the hardness as well as wear resistance capacity of the composite will be increased. Further from the literature it was found that nickel and graphite were the most commonly used ingredients as binder and wetting agent. So the same has been chosen in this study.

3.4 DESIGN AND FABRICATION OF DIE & ITS COMPONENTS

3.4.1 Fabrication of die

For the purpose of compaction a die made of gun metal has been fabricated for the experimentation. It consists of following parts:

Table 3.1 Die Components

Parts	Quantity	Length(mm)	Diameter(mm)
Main Body	1	100	100
Punches	2	50	10
Stoppers	2	10	10
Ejectors	1	10	100
Base	1	20	100

Fig 3.2: Die and its Components

3.5 FABRICATION OF THE COMPOSITES

Samples were prepared by using powder metallurgy technique. Before the fabrication the different combinations of the materials were made.

3.5.1 Different combination of composite materials

Based on the literature survey following composition has been decided to carry the experimental process.

Table 3.2 Different Compositions of Powders

Copper (Cu)	%Cu + % SiC
100	80+20
100	85+15
100	90+10

3.5.2 Fabrication of pallets

To fabricate the pallets firstly the powders were mixed in a blender at 100 rpm for 1 hour so that proper mixing of the powders will take place. Once the mixing was done, mixed powder was compacted on hydraulic press (pr.capacity-600 MPa) for 30 min on the pressure of 250 MPa to achieve the solid structure which was in cylindrical shape.

Fig 3.3: Hydraulic pressure gauge **(**Courtesy: Physics lab, Thapar University, Patiala)

3.5.3 Sintering

This process is carried out to increase the density and to reduce the porosity of the part and also to remove out the air which was entrapped during the compaction. So finally we will get a solid structure. Sintering is performed near the glass transition temperature which is below the melting point temperature so that the internal stresses are relieved. During the sintering process, the particles of the powder diffused and gets bonded due to transportation of the atoms, which results in a dense structure having good mechanical strength.

For the experimentation a temperature controlled sintering furnace (max. capacity 1500°C) was used. This furnace is having a glass tube in which the alumina boat having samples in it is being placed. Then the furnace starts and performs the operations as per the temperature limits which were set prior to the operation.

Fig 3.4: Sintering furnace **(**Courtesy: Magnetic material lab, Thapar University, Patiala)

The temperature was firstly increased to 600°C (heating rate of 3°C/min) for the degassing purpose and then raised to 850°C and stabilized for 60 min to avoid overshooting of the heating temperature and then raised to 950°C and again allowed to stabilized for 60 min so that recovery in physical and mechanical properties can take place. After it it was allowed to cool from 950°C to atm. Temperature with a cooling rate of 5°C/min. The following figure shows the pallets before and after sintering.

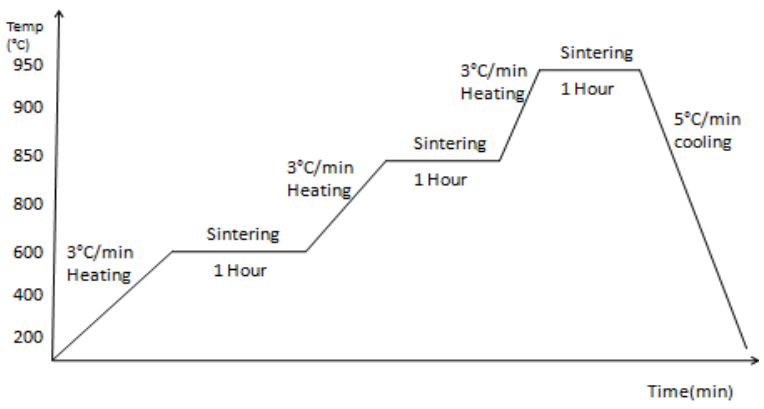

Fig 3.5: Sintering Cycle used for the experimentation

Fig 3.6: Pallets before sintering (a) Cu (100%), (b) Cu(90%)+SiC (10%), (c) Cu(85%)+SiC(15%)

Fig 3.7: Pallets after sintering (a) Cu (100%), (b) Cu(90%)+SiC (10%), (c) Cu(85%)+SiC(15%)

3.6 CHARACTERIZATION OF METALLURGICAL PROPERTIES

Metallographic analysis is a powerful quality tool (Metallurgical microscope, EDX, SEM etc) to investigate the micro structural examination and primary characteristics of a metal matrix composite. These are discussed below:

3.6.1 Metallurgical microscope

Metallurgical microscope shown in Fig 3.8 is an optical microscope which lenses so that the images for the samples can be magnify. The images are captured by normal light-sensitive cameras which helps to generate a micrograph. The Optical microscope is used to observe the internal structure of the metals at different scale and provide a qualitative and quantitative description. In the present study metallurgical microscope is used to analyses the shape, size and dispersion of the reinforcement particles in the matrix alloy. The optical microscope which is used to see the shape, size and dispersion of the particles of the desired sample, the surface of the sample has to be cleaned and etched so that the surface morphology will be clearly visible.

Fig 3.8: Metallurgical Microscope

(Courtesy: Advanced metallurgical lab, Thapar University, Patiala)

Sample preparation: Before examining the structure of hybrid metal matrix composite made by P/M route, samples are well polished with the help of fine grade emery paper, followed by cleaning with acetone and then etched with a Keller etching solution for 20- to 40 seconds. For the copper, nitric acid (50%) and distilled water (50%) and for Cu-SiC, ferric nitrate (50%) and hydrochloric acid (50%) were used as an etchant. After cleaning it (for 30 sec) the optical images of the samples were taken.

3.6.2 Scanning electron microscope (SEM)

Typical image of SEM is shown in Fig 3.9. It is a kind of electron microscope which gives the images of a sample by scanning by using a highly focused beam which is having electrons of high energy. The high energy electron beam is mainly scanned a raster scan pattern, and the beam's position is combined with the detected signal to produce an image. SEM analysis

is considered to be non-destructive because there is no volume loss of the sample during the testing, so the same sample can be used repeatedly.

The SEM used here is a highly accurate and precise instrument for fast characterization and imaging of fine structures and has a magnification range from 5–300,000 X (printed as a 128 mm x 96 mm micrograph). EDX is also associated with the SEM machine and it is used to see the composition of the samples at different spectrum. This facility is available at SAI Labs, Thapar Technology Campus, Patiala.

Fig. 3.9: Scanning electron microscope

(Photo courtesy: SAI Labs, Thapar Technology Campus, Patiala)

Sample preparation: The samples made by powder metallurgical route were used to see the surface morphology, microstructure and composition of the samples. For this purpose the samples were cleaned on the disc polisher machine by using emery papers having grit sizes from 300 to 2000 so that the desired surface is obtained.

3.7 CHARACTERIZATION OF MECHANICAL AND PHYSICAL PROPERTIES

3.7.1 Micro Hardness

Hardness represents the mechanical property of the material. Surface properties of a composite play a main role in wear and friction behavior. Hardness is a quick and very simple method to obtain the mechanical property of the material. The basic principle of the hardness test

is to provide a force through the indenter on a specimen surface and measured the dimensions of the indentation. Micro hardness value was measured by micro vicker hardness tester.

Fig 3.10: Micro hardness tester

Sample preparation: Disc Polisher machine was used to remove out the scales which were deposited on the pallets after the sintering by using different kinds of emery papers having sizes from 100 to 2000 to obtain a clean surface which will be helpful for measuring the hardness values.

Fig 3.11: Disc polishing machine

3.7.2 Density & Porosity

The density of the pallets were measured was using the principle of Archimedes. So the volume of composite sample is determined by using water displacement. The mass of composite

was measured on a highly accurate digital weighing balance with an accuracy of 0.0001g. Rule of mixture [14] was used to calculate the theoretical density of the pallets.

$$\text{Theoretical density} = 100/(w_1/\rho_1 + w_2/\rho_2)$$

Table 3.3 Values of densities of the used powders

S. No.	Material	Density(g/cc)
1	Copper (Cu)	8.79
2	Silicon Carbide (SiC)	4.46

By using the theoretical and the actual densities, porosity for the pallets which are having different compositions can be estimated by using the above formula [14].

$$\text{Porosity (\%)} = 1 - (\text{Measured density}/\ \text{Theoretical density}) * 100$$

3.7.3 Surface Roughness

Once the pallets were sintered, it was observed that some scaling and carbon deposition was there on the pallets. If the surface is rougher then the wear out of the surface will be fast and also it will have higher coefficient of friction which is not desirable. That's why the surface roughness of the parts should be less. A surface roughness meter was used to check the surface roughness of the sintered parts.

Fig 3.12: Surface roughness meter (Courtesy: Machine tool lab,Thapar University, Patiala)

3.8 CHARACTERIZATION OF WEAR AND FRICTION

To characterize the tribological (wear and friction) behavior of the samples a pin-on-disc tribometer (DUCOM Make) was used.

3.8.1 Pin-on-Disc Tribometer

The pin-on-disk apparatus (DUCOM make), shown in fig 3.13. This tribometer was used to see the wear characteristics and also the coefficient of friction of the metal matrix composites. A pin which is made up of composite material is rest on a rotating disc under the effect of a dead weight. Influencing parameters such as normal load, sliding velocity, wear track diameter and sliding distance is to be set according to the design of experiment shown in table 4.5 before running the tests.

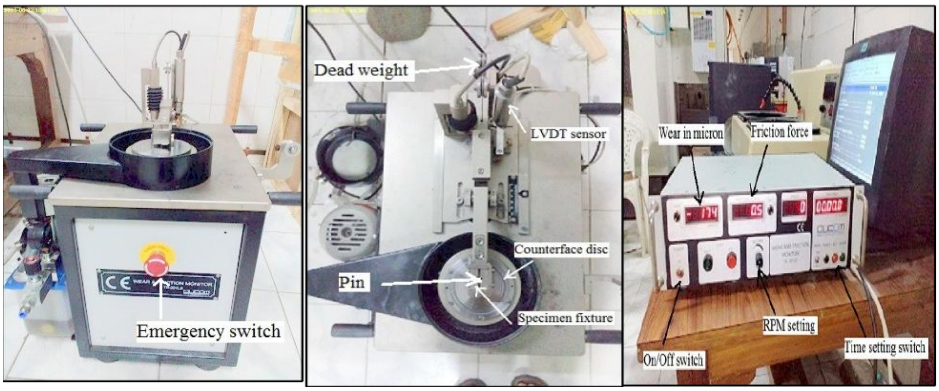

Figure 3.13: Components of pin-on-disk (tribometer) test apparatus

3.8.2 Weighing balance for mass loss calculations

A weighing machine having accuracy of 0.0001gm was used to measure the weight of the samples before and after the wear. The difference between the two readings was weight loss which was helpful to measure the wear rate for the particular samples.

Weight loss= Wt. before wear-Wt. after wear

Wear Rate = Wt. Loss/Density*(Sliding distance)

Fig 3.14: Weighing machine

3.8.3 Sample preparation and experimental procedure for wear tests

The samples fabricated from P/M route were having flat base and for the flat base it is very hard to maintain the exact flat surface so that a proper contact will be there between pin and the disc (Material-EN31, 52HRC). So firstly the hemispherical shape was made on the pins by using CNC milling machine so that a proper contact will be taken place due to which proper wear track will be made on the pins. Once the hemispherical pins were made then after it the pin was hold in the fixture of 10 mm dia. And a proper contact was made between the pin and the disc. Then the desired load was applied on the machine and then machine was started for a particular time of period. Wear and friction behavior with respect to the time was displayed on the wear and friction monitor. A graph was generated on the computer for the wear and the friction with respect to the time. After the completion of specified time, the machine was stopped and again the same process was repeated for the other pins.

3.9 DESIGN OF EXPERIMENTATION FOR FRICTION AND WEAR TESTING RUNS

Wear tests for all the samples were executed on the tribometer as shown in fig 3.13 under the different loading and the sliding conditions. These different parameters under which the wear tests have to be performed were decided by using L9 orthogonal array by using Design of experimentation (D.O.E.). Design of experiment is a systematic method by which a relationship can be find out between the input and output parameters of the process. The following inputs were decided by using the L9 orthogonal array:

Table 3.4: Experimental design using L9 orthogonal array

1	1	1
1	2	2
1	3	3
2	1	2
2	2	3
2	3	1
3	1	3
3	2	1
3	3	2

Parameters to be varied are given below (Table 3.5) and the levels are set based on the pilot study and the desired combination has following pattern (table 3.6).

Table 3.5: Different parameters for wear and frictional study

Load(kgf) 1,2,3	Sliding Speed(m/sec) 0.50,1.00,1.50	Sliding Dist(m) 900,1800,2700

Table 3.6: Desired experiments under different parameters using L9 orthogonal array

	Load	Sliding Speed(m/sec)	Sliding Dist.(m)
Set 1	1kgf	0.50	900
Set 2	1kgf	1.00	1800
Set 3	1kgf	1.50	2700
Set 4	2kgf	1.00	1800
Set 5	2kgf	1.50	2700
Set 6	2kgf	0.50	900
Set 7	3kgf	1.50	2700
Set 8	3kgf	0.50	900
Set 9	3kgf	1.00	1800

CHAPTER 4
RESULTS AND DISCUSSIONS

4.1 INTRODUCTION

This chapter deals with the detailed results and discussion of mechanical, physical, metallurgical and tribological characterizations of the fabricated copper based composites. Also, structure of composites, SEM micrographs of worn surfaces and the optical macrographs analysis results are presented. The effect of various influencing parameters on dry sliding wear and coefficient of friction on copper based composites are presented and analyzed using ANOVA in the subsequent chapter.

4.2 SURFACE ROUGHNESS OF SINTERED COMPOSITES

A digital surface roughness meter was used to measure the surface roughness of the sintered parts. The surface roughness value for different compositions is being shown in the table 4.1.

Table 4.1: Surface roughness values for different compositions

Sample	R_a(μm)	R_z(μm)	R_q(μm)
Cu(100)	0.030	0.20	0.040
Cu(90)-SiC(10)	0.026	0.26	0.023
Cu(85)-SiC(15)	0.029	0.21	0.039
Cu(80)-SiC(20)	0.041	0.39	0.045

4.3 DENSITY AND POROSITY OF COMPOSITES

Actual density of the composites was measured with the help of the Archimedes Principle. Rule of mixture was used to calculate the theoretical density of the pallets. The values shows by these two principles were very near to each other.

$$\text{Theoretical density} = 100/ (w_1/\rho_1 + w_2/\rho_2)$$

Table 4.2 Values of densities of the powders

S. No.	Material	Density(g/cc)
1	Copper (Cu)	8.79
2	Silicon Carbide (SiC)	4.46

Following table shows the values of densities for different compositions.

Table 4.3: Values of density by using different principles

Sample	By using rule of mix.	By Archimedes law
Cu(100)	8.79	8.96
Cu(90)-SiC(10)	8.01	8.30
Cu(85)-SiC(15)	7.64	7.81
Cu(80)-SiC(20)	7.46	7.63

By using the theoretical and the actual densities, porosity for the pallets which are having different compositions can be estimated by using the following formula [14].

Porosity (%) = 1 - (Measured density/ Theoretical density) * 100

Following values were obtained for different samples by using the above formula:

Table 4.4: Values of porosity for different compositions

Sample	Value (%)
Cu(100)	1.9
Cu(90)-SiC(10)	3.48
Cu(85)-SiC(15)	2.28
Cu(80)-SiC(20)	2.24

From the table 4.3 it is obvious that the density of composites is decreasing with the increase in weight % of reinforcement, which is expected. However, if we compare the table 4.3 and 4.4 then we can see that the composites are more porous than the pure metal due to the presence of heterogeneous phases and presence of weak bonding. However, due to the fact that copper can diffuse easily to the interstices between SiC particles at low concentration which lead to higher densification, so the resultant values of porosities are found to be very less in the fabricated composites.

4.4 HARDNESS OF COMPOSITES

Hardness of the composites was measured by the Vickers micro hardness testing machine. The hardness of the Copper and its composites corresponding to different weight percentage of the reinforcement (silicon carbide) particles are shown in Figure. 4.1 and Table 4.3. As it is well known fact and is seen from the Figure 4.1, the hardness of the composites was improved with the increase in weight percent of SiC (Silicon carbide). The enhancement in

hardness of the composite is due to the uniform dispersion of hard SiC reinforcement particles as well as the good bonding to matrix alloy in the composites.

For each sample micro hardness of the pallets was measured under load 300gm and dwell time of 20sec. The data plotted are the average values of the five readings. For composites, the interface of matrix and reinforcements are selected to extract the hardness values. The uniformly distribution of reinforcement improve mechanical properties of composite.

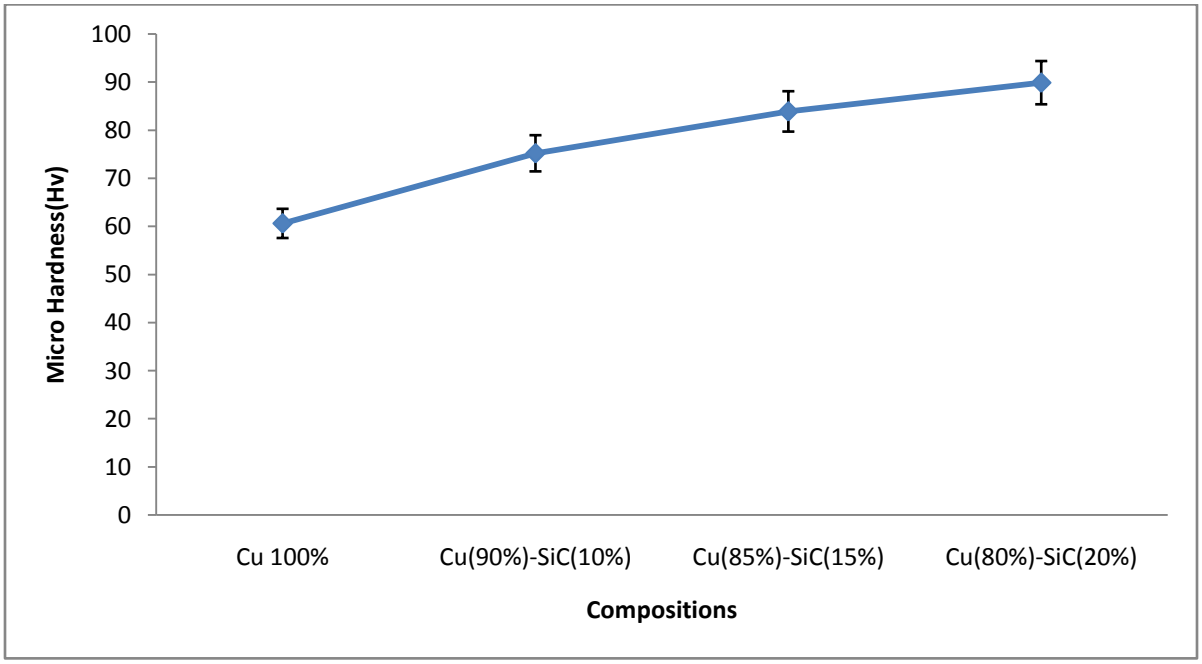

Fig. 4.1: Variation of hardness for different compositions

4.5 MICROSTRUCTURE ANALYSIS

The SEM micrographs of Copper powder and Copper (90%)–SiC (10%) was taken to see the distributions of the powders before sintering and are shown in figure 4.2 (a)-(b). Micrographs revealed the tetrahedral structured silicon carbide particles and dendrite like structured copper particles. EDX was also done to see the composition of powders and a typical micrograph of Copper (90%)–SiC (10%) pallet before sintering.

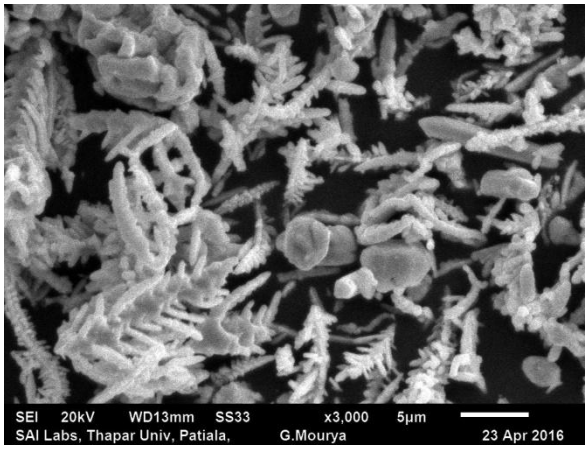

Fig 4.2 microstructure of (a) Copper powder (b) Copper-SiC powder

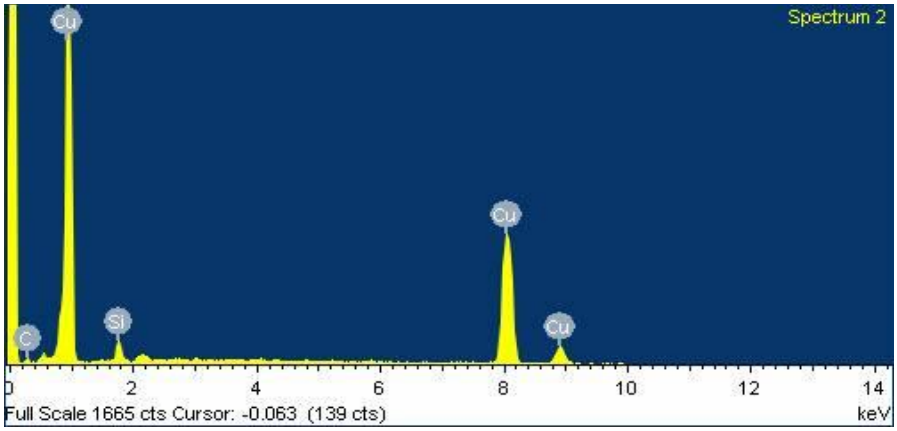

(c) EDX on Cu (90%) /SiC (10%) pallet before sintering

Table 4.5 EDX data for Cu (90%) and SiC (10%)

Element	C	Si	Cu
Weight (%)	9.30	8.08	82.62

All the samples were fabricated using powder metallurgy route followed by the sintering. After the sintering SEM micrographs of the samples were taken to see the structure of the composites. These silicon carbide particles are uniformly distributed throughout copper matrix phase. From the micrographs it is clear that there were no cracks which shows that the volumetric heating was homogeneous, which is the good advantage of powder metallurgy route. These images are shown in figure 4.3 (a)-(d).

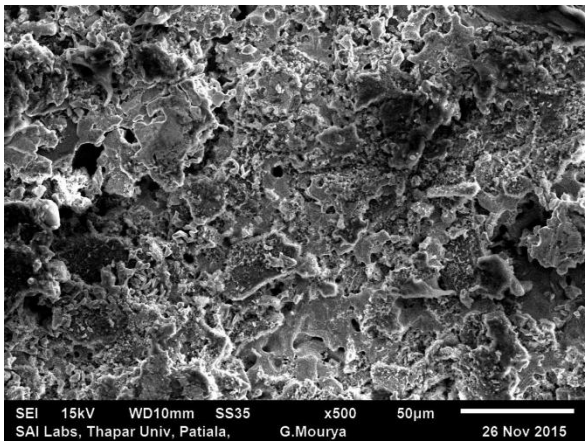

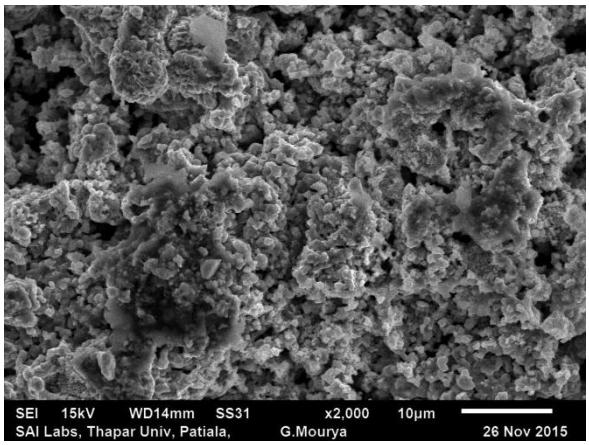

Fig. 4.3: Microstructure of sintered (a) Copper (b) Copper (90%)-SiC (10%)

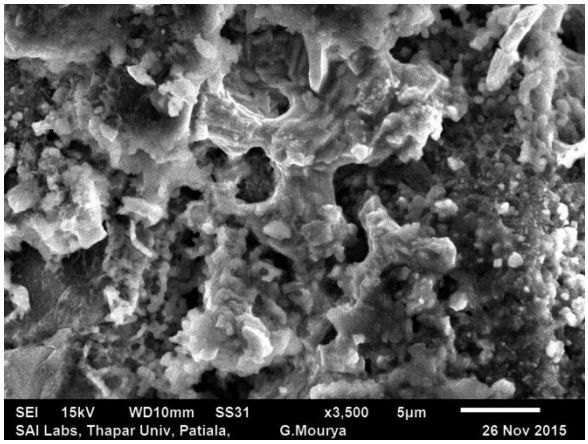

(c) Copper (85%)-SiC (15%)

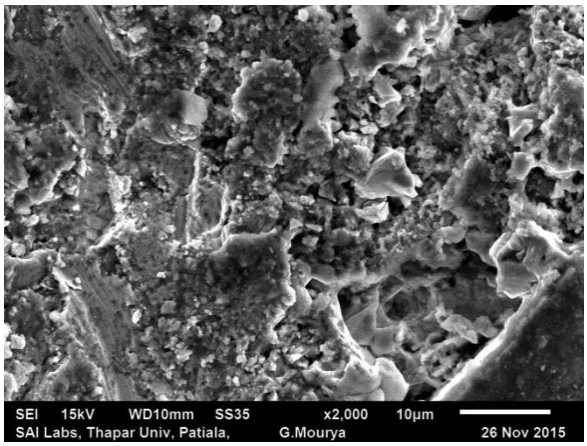

(d) Copper (80%)-SiC (20%)

4.6 WEAR STUDY

Wear tests for all the samples were performed on the pin-on-disc machine under different loading and sliding conditions. Copper and Cu-SiC composites were selected as the samples. L9 orthogonal array was used to carry out the experiment which is shown in following table.

Table 4.6: Experimental design using L9 orthogonal array

1	1	1
1	2	2
1	3	3
2	1	2
2	2	3
2	3	1
3	1	3
3	2	1
3	3	2

Different levels were decided for each of the parameters to carry out the experiments. Load, Sliding speed and Sliding distance were used as parameters to be varied. Different levels for these parameters which are selected from the pilot study are shown in the following table.

Table 4.7: Levels of the parameters for the experiments

S. No	Parameter	Level 1	Level 2	Level 3
1	Load (kgf)	1	2	3
2	Sliding Speed(m/sec)	0.50	1.00	1.50
3	Sliding Distance(m)	900	1800	2700

So the desired combination has following pattern:

Table 4.8: Experiments using L9 orthogonal array

Sets	Load	Sliding Speed(m/sec)	Sliding Dist.(m)
Set 1	1kgf	0.50	900
Set 2	1kgf	1.00	1800
Set 3	1kgf	1.50	2700
Set 4	2kgf	1.00	1800
Set 5	2kgf	1.50	2700
Set 6	2kgf	0.50	900
Set 7	3kgf	1.50	2700
Set 8	3kgf	0.50	900
Set 9	3kgf	1.00	1800

4.6.1 Wear rate

To calculate the wear rate for all the combinations weight before and after the wear was measured for the samples. A highly précised weighing balance having least count of 0.001 mg was used to measure the weight loss before and after the wear out of the samples. Then velocity was found by using the give formula:

Velocity = (Π*D*N)/60 m/sec

Then after it sliding distance was found by using the formula:

Sliding Distance = Velocity*Time

Once all the parameters were known then wear rate was calculated by using the given formula:

Wear rate (mm^3/m) = Wt. Loss/ (Density*Sliding distance)

Table 4.9: Combination of parameters for set 1

Load	**Speed**	**Track Dia.**	**Sliding speed**
1kgf	**240 rpm**	**40mm**	**0.50m/sec**

Sample 1: **Pure Copper**

Wt. before wear = 3.430 gm

Wt. after wear = 3.424 gm

Wt. loss = 0.006 gm

Density = 8.79g/cc

Time = 30min = 1800 sec

Wear Track Dia. = 40 mm & N=240 rpm

Velocity = (3.14*D*N)/60 m/sec = 0.51 m/sec

Sliding Distance = V*T = 0.51*1800 = 918 m

Wear Rate = Wt. Loss/ (Density*Sliding distance)

= 0.006/ ($8.79*10^{-3}$*918) = $6.19*10^{-4}$ mm^3/m

For all the samples at different parameters above discussed method was used and based on the calculations following results were obtained:

Table 4.10: Wear rate for all the experiments for different compositions

Sets	Cu (100%)	Cu (90%)-SiC (10%)	Cu (85%)-SiC (15%)	Cu (80%)-SiC (20%)
Set 1	6.19*10^-4	2.68*10^-4	2.12*10^-4	1.45*10^-4
Set 2	6.82*10^-4	2.986*10^-4	2.322*10^-4	1.69*10^-4
Set 3	6.954*10^-4	3.57*10^-4	2.702*10^-4	1.821*10^-4
Set 4	7.69*10^-4	3.18*10^-4	2.60*10^-4	1.76*10^-4
Set 5	7.92*10^-4	3.41*10^-4	2.98*10^-4	1.88*10^-4
Set 6	7.08*10^-4	6.19*10^-4	6.19*10^-4	6.19*10^-4
Set 7	8.10*10^-4	3.69*10^-4	3.12*10^-4	1.93*10^-4
Set 8	7.48*10^-4	3.36*10^-4	2.62*10^-4	1.78*10^-4
Set 9	7.82*10^-4	3.53*10^-4	2.78*10^-4	1.82*10^-4

Based on the above results following graphs has been drawn to see the wear trend for the different compositions at different conditions.

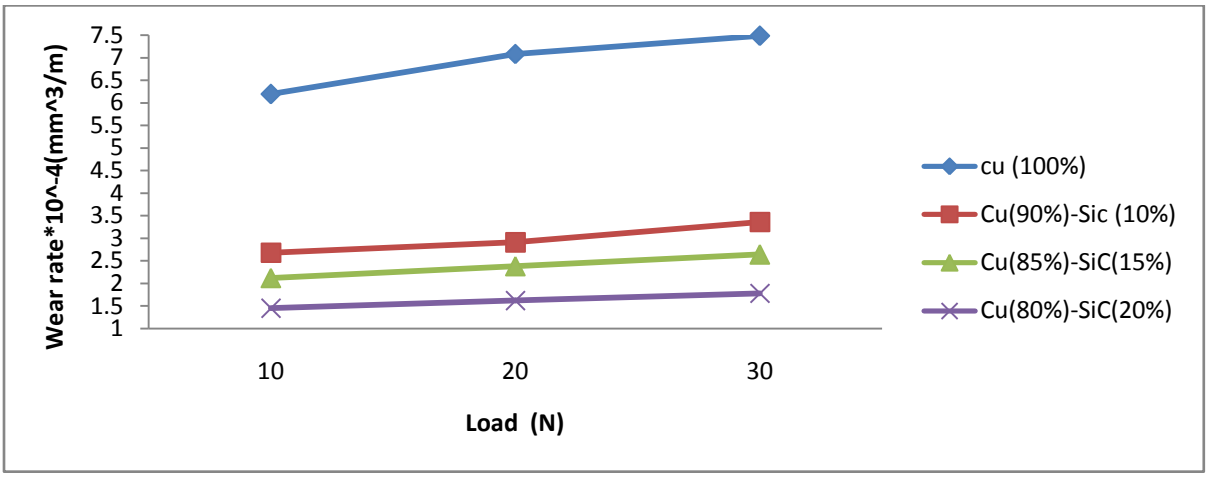

Fig 4.4 (a): Variation of wear rate of composites with normal load at 0.50 m/s

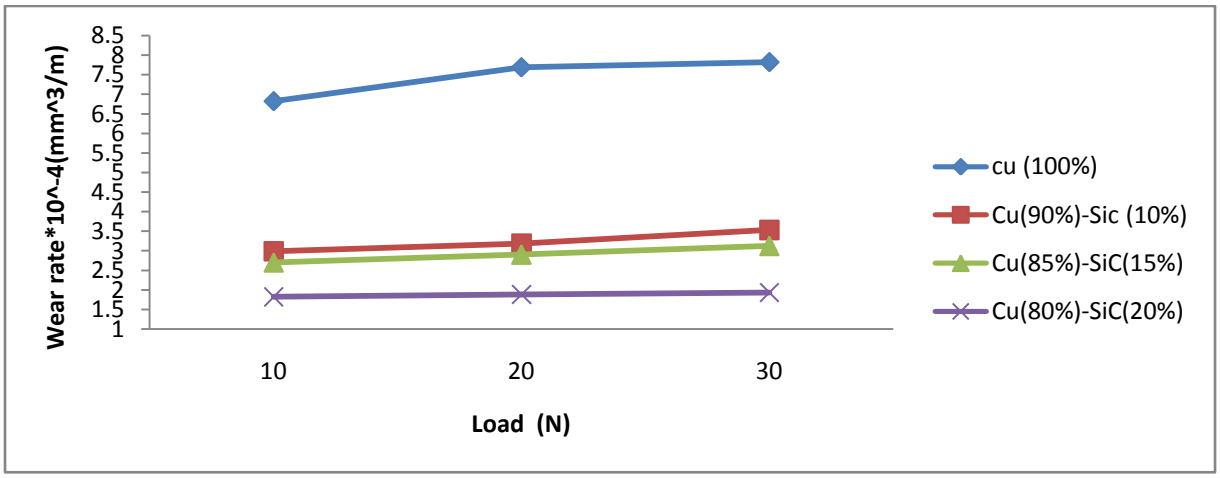

Fig 4.4 (b): Variation of wear rate of composites with normal load at1.00 m/s

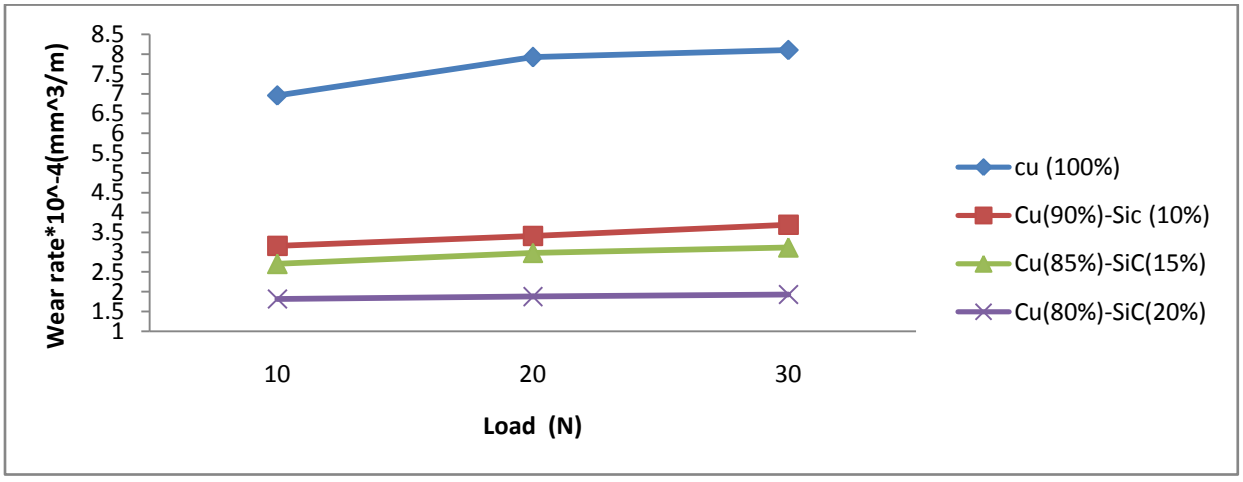

Fig 4.4 (c): Variation of wear rate of composites with normal load at1.50 m/s

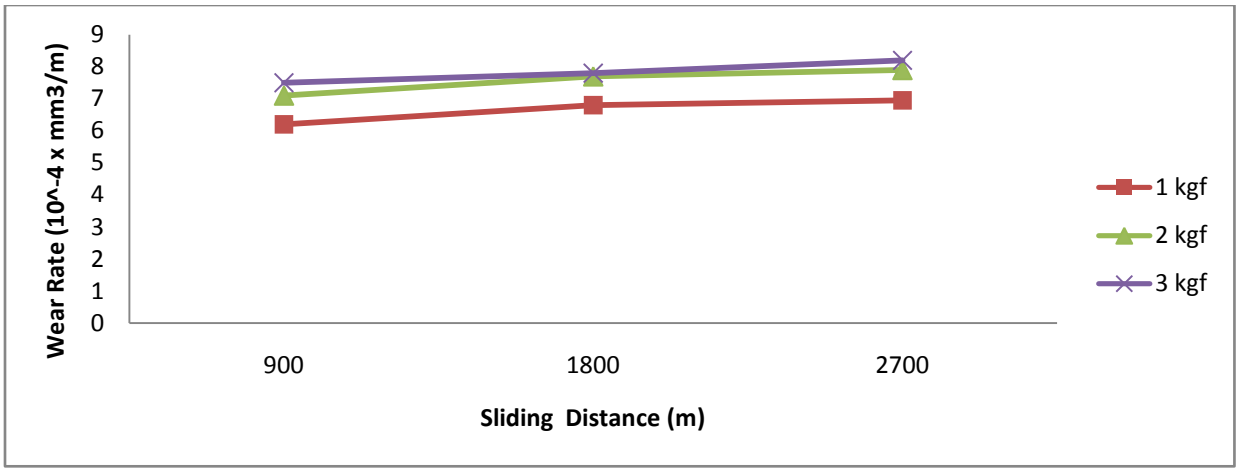

Fig 4.4 (d): Variation of wear rate for pure copper with sliding distance at different loads

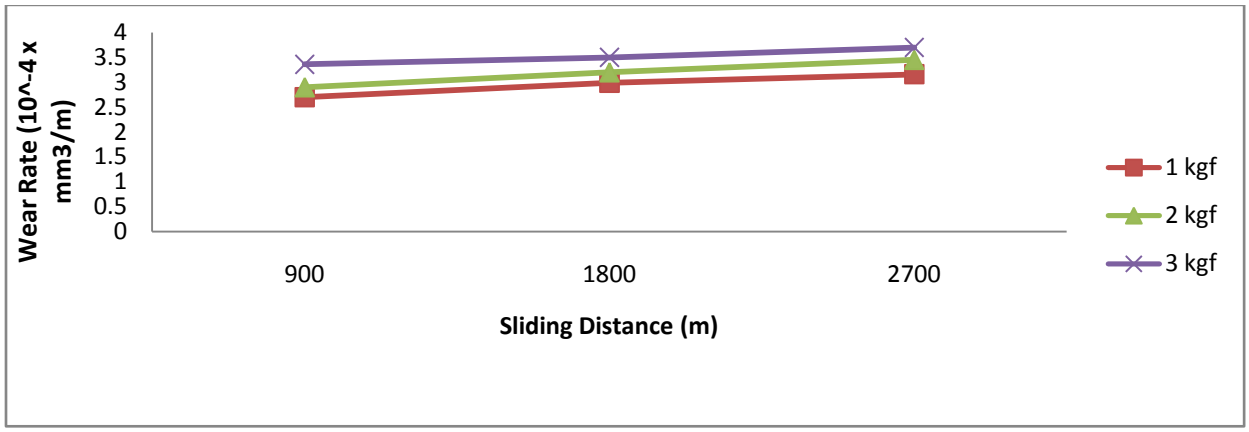

Fig 4.4 (e): Variation of wear rate for 10% SiC-copper composites with sliding distance at different loads

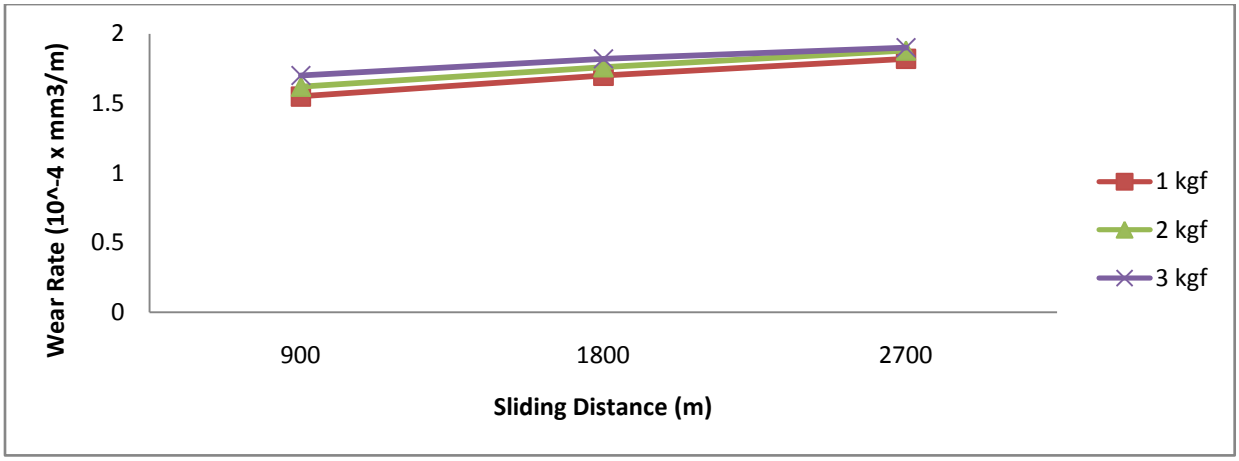

Fig 4.4 (f): Variation of wear rate for 20% SiC-copper composites with sliding distance at different loads

4.6.2 Specific wear rate

The wear rate expressed in mm^3/ (Nm) usually based on Archard's abrasive wear model. This is applicable only in the cases where the wear mechanism is abrasive or predominantly abrasive. As we know in actual contact conditions, there is no single mechanism of wear but a complex combination of several mechanisms simultaneously in play, so, on the prediction of wear, use of specific wear rate should be used very carefully, because it takes into account the contact conditions. In the present study since the operating conditions are changing, we will use wear rate for the comparative study with different composites. Also, use of specific wear rate will be investigating the validity of Archard model in the present contact conditions.

Specific wear rate was obtained by using the following formula:

Specific wear rate=Wear rate/Applied load

For all the samples at different parameters above discussed method was used and based on the calculations following results were obtained:

Table 4.11: Specific Wear rate for all the experiments for different compositions

Sets	Cu (100%)	Cu (90%)-SiC (10%)	Cu (85%)-SiC (15%)	Cu (80%)-SiC (20%)
Set 1	0. 619*10^-4	0.268*10^-4	0.212*10^-4	0.145*10^-4
Set 2	0.682*10^-4	0.2986*10^-4	0.2322*10^-4	0.169*10^-4
Set 3	0.6954*10^-4	0.3157*10^-4	0.2702*10^-4	0.1821*10^-4
Set 4	0.3845*10^-4	0.159*10^-4	0.130*10^-4	0.138*10^-4
Set 5	0.396*10^-4	0.170*10^-4	0.149*10^-4	0.144*10^-4
Set 6	0.354*10^-4	0.145*10^-4	0.144*10^-4	0.131*10^-4
Set 7	0.270*10^-4	0.123*10^-4	0.104*10^-4	0.064*10^-4
Set 8	0.249*10^-4	0.112*10^-4	0.087*10^-4	0.059*10^-4
Set 9	0.260*10^-4	0.118*10^-4	0.093*10^-4	0.061*10^-4

Based on the above results following graphs has been drawn to see the wear trend for the different compositions at different conditions.

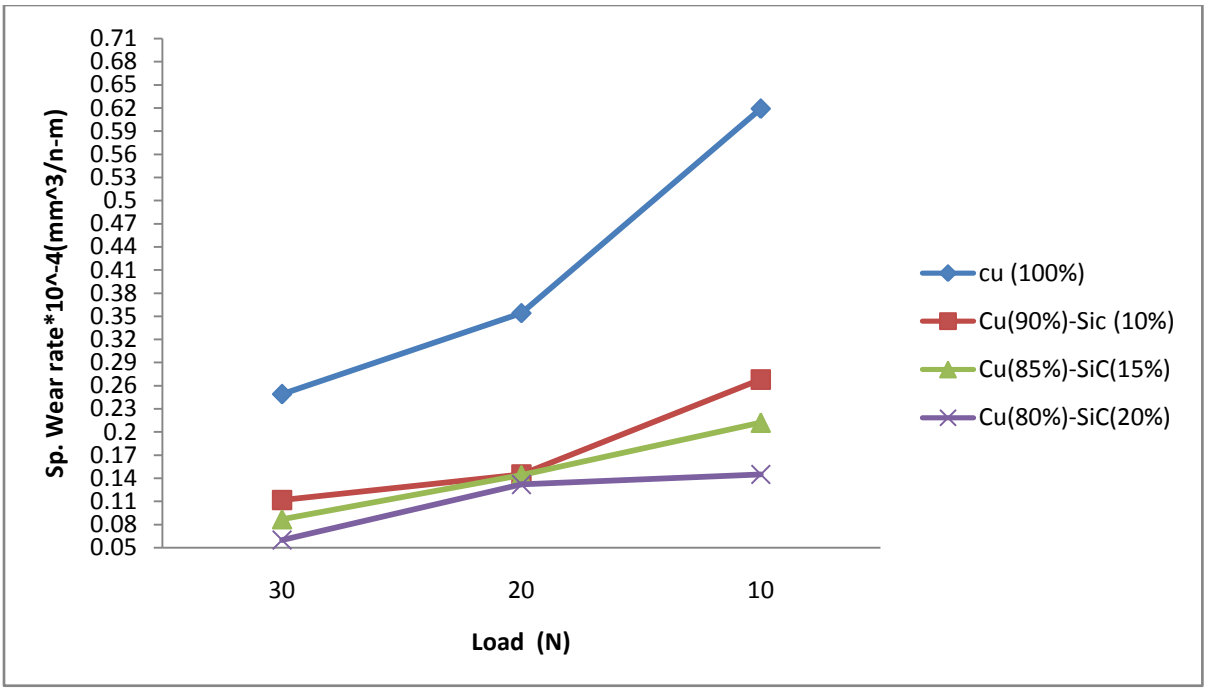

Fig 4.5 (a): Variation of Sp. wear rate of composites with normal load at 0.50 m/s

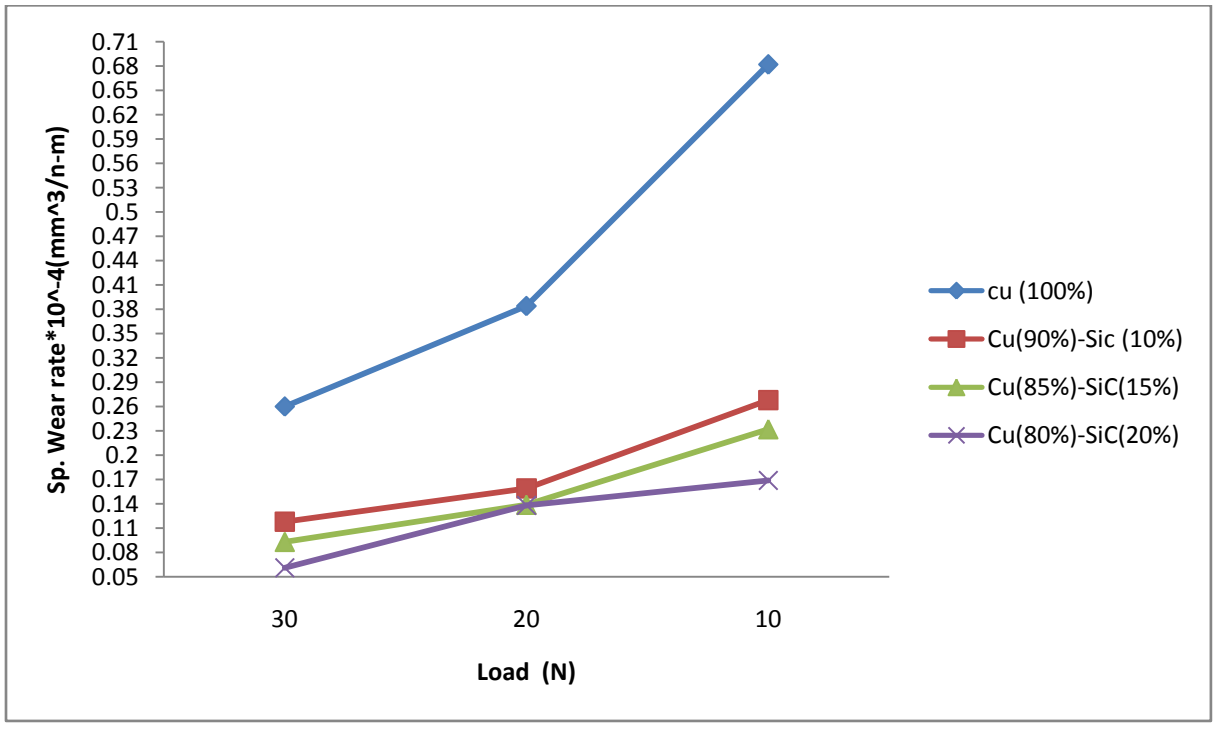

Fig 4.5 (b): Variation of Sp. wear rate of composites with normal load at1.00 m/s

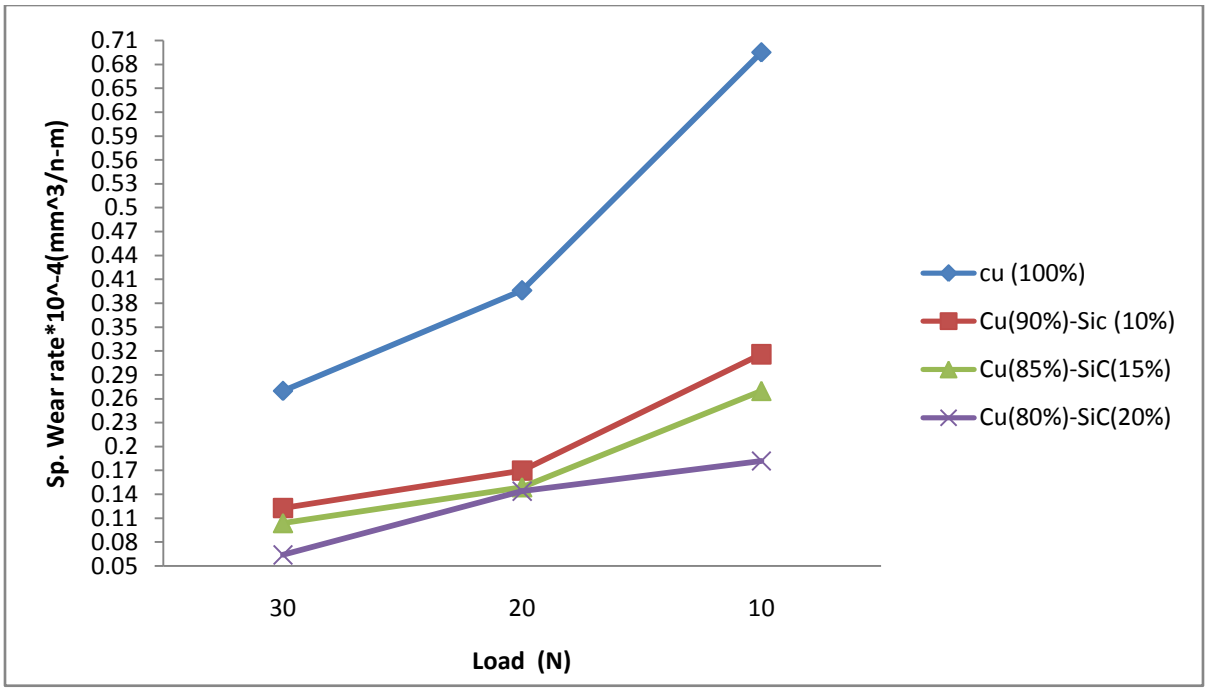

Fig 4.5 (c): Variation of Sp. wear rate of composites with normal load at1.50 m/s

From the above plots (Fig. 4.4 & 4.5), it is clear that predominantly the adhesive wear mechanism rather than abrasive wear mechanism takes place in case of pure copper sample whereas the composite wear mechanism is predominantly abrasive. Influence of various operating parameters on the wear of fabricated composites can be explained as follows.

4.6.2.1 Effect of applied load

The variation for wear rate of the Copper (Cu)–Silicon carbide (SiC) composites with respect to the normal load for the different sliding speeds are shown in fig 4.5 (a-c). From the graphs it is clear that wear rate is insignificantly increasing for all the composites when normal load is increasing. Similar kind of behavior is shown by pure copper also. The trends of the graphs show that there is rapid increment in the wear rate of the pure copper. With the increment in normal loads, considerable plastic deformation for the pure copper has been occurred along with the formation of adhesive junction between the contacting surfaces. It was observed that wear rate was decreasing with increase in volume fraction of silicon carbide (SiC) and Cu (80%)-SiC (20%) composite is least affected by the change in normal load. The linearity in the specific wear rate curve for composites implies the abrasive wear mechanism for all the loading conditions. As the SiC content is increased hardness as well as wear resistance of the Cu-SiC composite is also increased. Subsequently, Cu (100%) shows higher wear rate and the composite

Cu (80%)-SiC (20%) exhibits the lowest wear rate as compared to all of the compositions for all the applied loading conditions.

4.6.2.2 Effect of sliding speed

The sliding speed was varied from 0.5 m/s to 1.5 m/s as per the combinations made by L9 orthogonal array. When the sliding speed was increased from 0.5 to 1.5 m/s, the wear rate shows a marginal increment for all the applied loads for all the composites. The trends of the graphs show that the wear rate is increased more in copper as compared to the other composites. Due to the increased sliding speed, the fracture or pull out of the particles take place from the composite which can abrade the surface of the composite during the sliding conditions [25]. Due to the good bonding strength and also the higher thermal stability of the SiC particles in composites it allows only slight increment in the wear rate.

4.6.2.3 Effect of the reinforcement

The wear rate of the composite was decreased with increase in hardness of the composite. The hardness of the composite increases as the volumetric fraction of the SiC increases. As the SiC volume fraction increases wear resistance capacity of the composite also increases. The increased wear resistance of the composites is due to the presence of hard SiC particles in the Cu-SiC composite. During the sliding, initially there is metal to metal contact due to which the copper metal tends to deform. The harder counter surface abrades the copper. After it the SiC particles are exposed to the worn surface. These hard particles carry the normal load which automatically reduces the load on the copper phase. Due to these harder particles, wear resistance capacity of the composites increases which reduces the surface deformation of the composite.

4.6.2.4 Effect of Sliding Distance

It is clear from the figure 4.4 (d-f) that wear rate gradually increases with the sliding distance. This indicates that the existing wear mechanism prevailed in the particular tribo contacts; do not change significantly with time. This implies that there is no significant tribo layer formation under the contact or there may be the continuous formation and ruptures of oxide layers under sliding.

Also, as mentioned earlier, from the figure 4.4(f) it is evident that for all loading conditions the wear rate for 20% SiC-Cu composite is nearly same, for a particular sliding distance. As sliding distance increase, wear rate is also increased gradually with a lower rate than the other compositions. In case of composites with very low weight percentage of reinforcement

wear rate is significantly influenced by load and sliding distance which may be due to the fact that with sliding time, particles are pulled out of the soft matrix and subsequently the matrix is unable to resist the higher wearing out whereas in case of composites with higher percentage, harder surfaces are exposed uniformly and load bearing capacity as well as the wear resistance of the sample is increased or there is the possibility of forming hard tribolayer of carbides and oxides. This, in turn, is a good indicator of achieving desired wear resistance with the uniformity as well as the optimal formulation of reinforcement in the fabricated composite for the particular application with specified load range.

4.7 WORN SURFACE ANALYSIS

The observed wear behavior and predicted wear mechanism which is explained above can be further validated once the worn surface analysis or fractography of the worn surface is done. These are explained below.

4.7.1 Wear mechanism for pure copper

Scanning electron microscope (SEM) examination of the worn surfaces for the pin of the pure copper is shown in fig 4.6. When the pure copper sample is rubbed against the hardened EN31 steel disc, the asperities of the hard surface of the steel penetrates the pin, due to which high amount of material is being removed out from the pin by ploughing action. Due to the increased metal to metal contact and ploughing action by the asperities of the hard counter surface, the resultant wear rate is higher as compared to the other compositions. However, at higher speed and large sliding distance, oxide layer such as CuO may form as indicated from the table 4.12, which prevents abrasive action on soft surface to some extent (Fig. 4.6 (b)). For all tests under different conditions, fracture width on the worn surfaces was measured and it was more for pure copper as compared to the Cu-SiC composite.

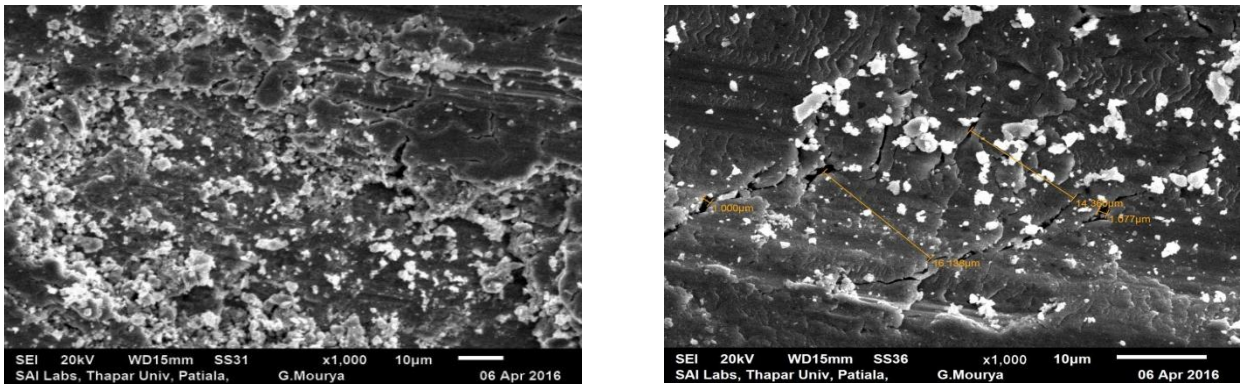

Fig.4.6. Typical worn surface of copper (a) 0.5 and (b) 1.5 m/sec at 10 N.

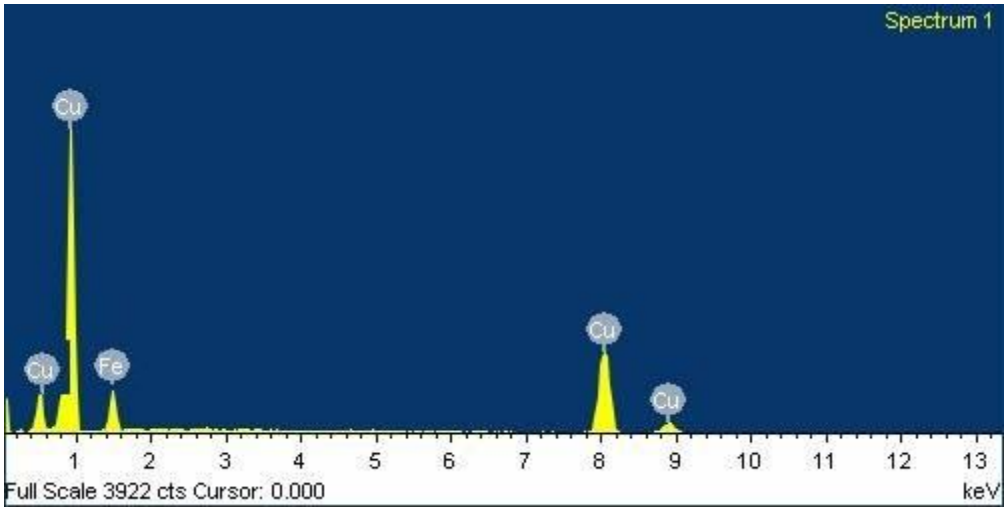

Fig. 4.7 EDX spectra on wear track for pure copper sample

Table 4.12 EDX data on wear track for pure copper sample (1.5 m/sec at 10 N)

Element	Cu	Fe
Wt (%)	85.33	4.67

4.7.2. Wear mechanism at 10 vol% SiC composites

Fig 4.8 shows the typical SEM micrographs for the worn surfaces of the Cu (90%) - SiC (10%) composites tested under the sliding speed of 0.50 m/s. The result shows that for the lower load (10 N), worn surface is smoother than that of the pure copper. The micrographs show irregular grooves due to the extensive plastic deformation of the matrix on the worn surface. Due to the inadequate hardness and bonding of reinforced particles in the matrix, dislodging of the SiC particles are easier from the matrix. Fracture width on the worn surfaces was measured and it is less as compared to the pure copper due to the presence of the harder SiC particles. The size of the grooves and width of fracture increases with increase in load.

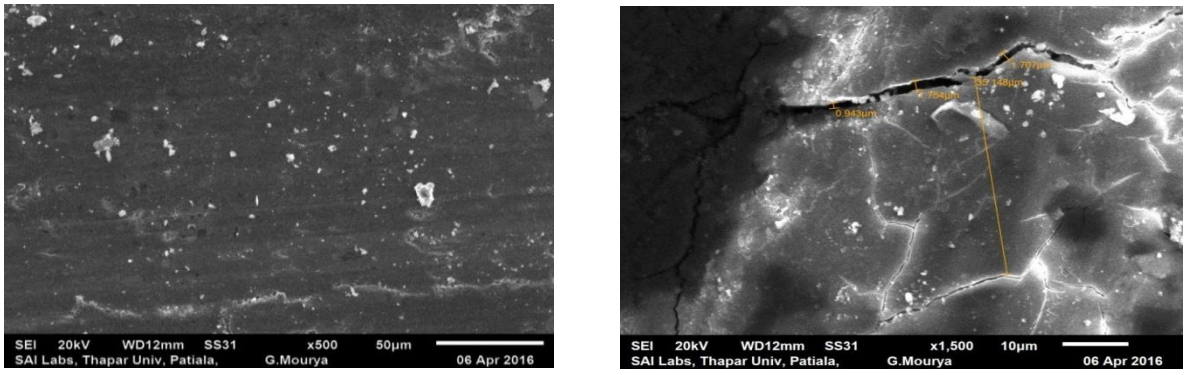

Fig.4.8. Typical worn surface of Cu (90%)-SiC (10%) for 0.5 m/sec at 10 N.

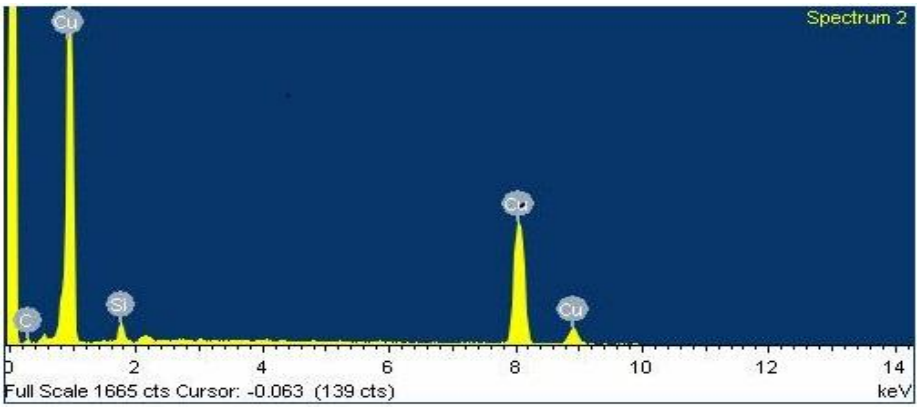

Fig. 4.9 EDX spectra on wear track for Cu (90%)-SiC (10%) sample

EDAX of the worn surface of 10% SiC at 10 N and 0.50 m/s is shown in table 4.13. It is clear from the EDAX results for worn surfaces that it has a low peak of carbon, highest peak of the copper and low peak of the silicon. The higher peak of the copper without any oxide or iron content indicates no tribo layer or transfer film formation. Similar, trend was also observed for higher speed also.

Table 4.13 EDX data for Cu (90%)-SiC (10%)

Element	Cu	Silicon	Carbon
Wt (%)	88.72	7.18	4.10

4.7.3 Wear mechanism at 15 vol% SiC composites

Fig 4.10 shows the SEM micrographs for the worn surfaces of the Cu (85%) - SiC (15%) composites tested under the sliding speed 0.5 m/s and the load of 10 N. The observed wear feature (Fig. 4.10 (a&b)) shows that for the sliding speed of 0.5m/sec, smearing out of reinforced particles and a few smaller cracks are found on the surface. This is due to the fact that the matrix now becomes more wear resistant due to the increase in hardness of the composite. For large sliding distance or high load, gradually hard particles from the composite starts to bear the load, the fracture sizes further reduces and the wear debris particles becomes smaller in size. As evident from the table 4.14, there is also the possibility of formation mechanically mixed layer transferred from the counter surface. Due to the presence of uniformly distributed hard reinforcement particles in the matrix material, the wear resistance is improved for the composite material. The wear process in the composite material is by plastic deformation of the matrix as well as gouging and smearing out of reinforcement particles which in turn may crush to very

minute particles and form mechanically mixed layer (MML) which withstands high stresses and is very effective in reducing the sliding wear.

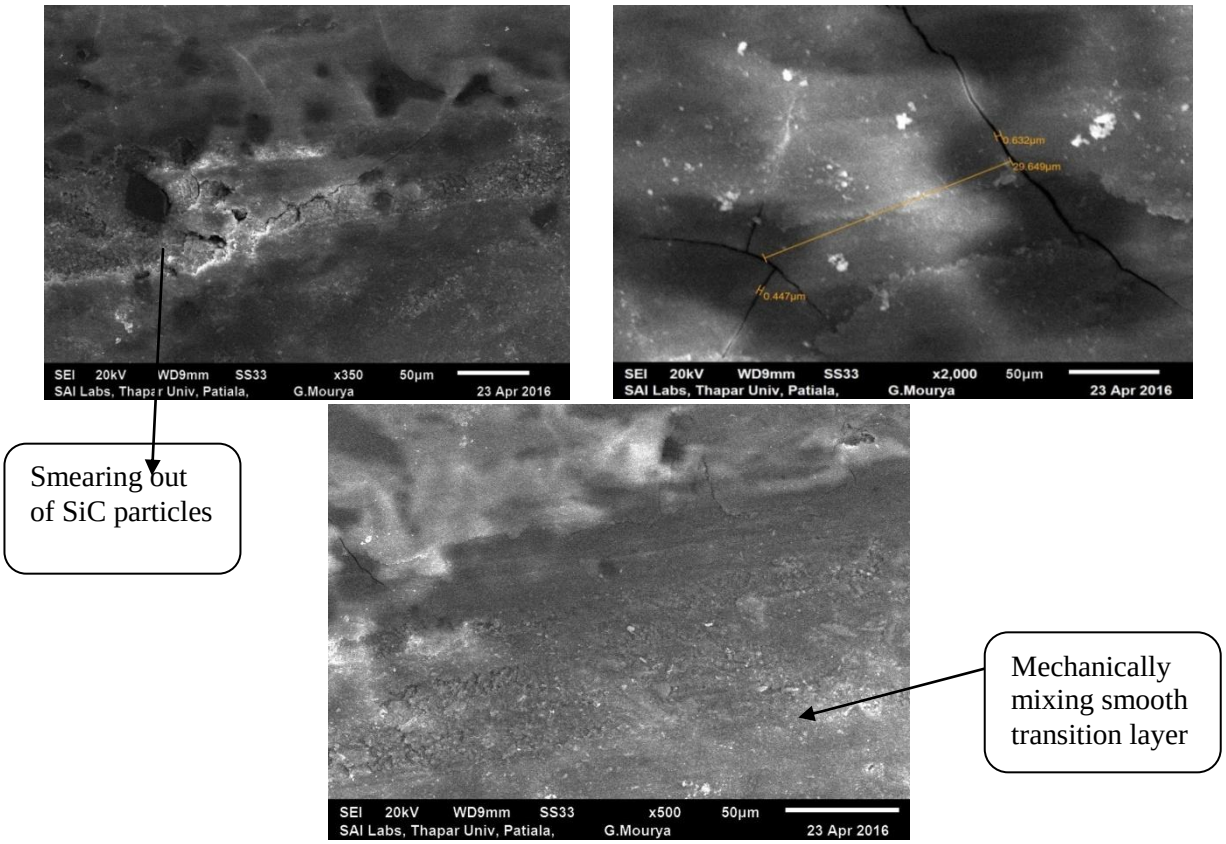

Fig. 4.10 Typical worn surface of Cu (85%)-SiC (15%) (a, b) 0.5 and (c) 1.5 m/sec at 10 N

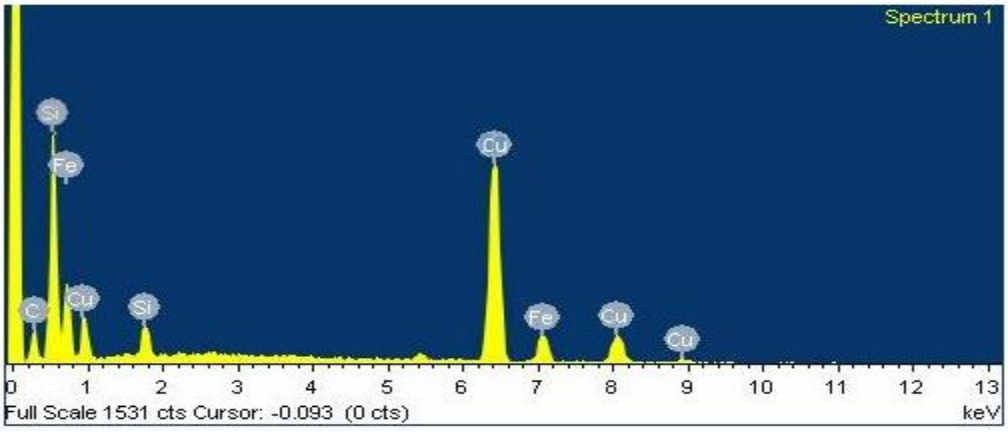

Fig. 4.11 EDX spectra on wear track for Cu (85%)-SiC (15%) sample

Table 4.14 EDX data for Cu (85%)-SiC (15%)

Element	Cu	Silicon	Carbon	Iron
Wt (%)	80.72	12.28	1.10	5.90

4.7.4 Wear mechanism at 20 vol% SiC composites

Fig 4.12 shows the typical SEM micrographs for the worn surfaces of the Cu (80%) - SiC (20%) composites tested under the sliding speed of 0.5 m/s and the load of 10 N respectively. Increased SiC reinforcement in copper matrix has improved the hardness due to which the wear resistance and load bearing capacity also improves. With increased load and sliding speed, hard particles are projected out from the matrix and carry the normal load, which in turn reduces the load and subsequent plastic deformation of copper matrix. Hence these harder particles protect the progressive wear rate of copper matrix to some extent. Also, additionally there may be the possibility of the presence of SiO_2 and CuO in the wear track which further increases the wear resistance. Also, when the contact is established, the harder SiC particles protrude from the softer matrix and will be pulled out. Which in turn induce third body rolling action between the contact surfaces and thereby decrease the coefficient of friction. In other words, there is less ploughing and adhesive components in the steel-composite interactions.

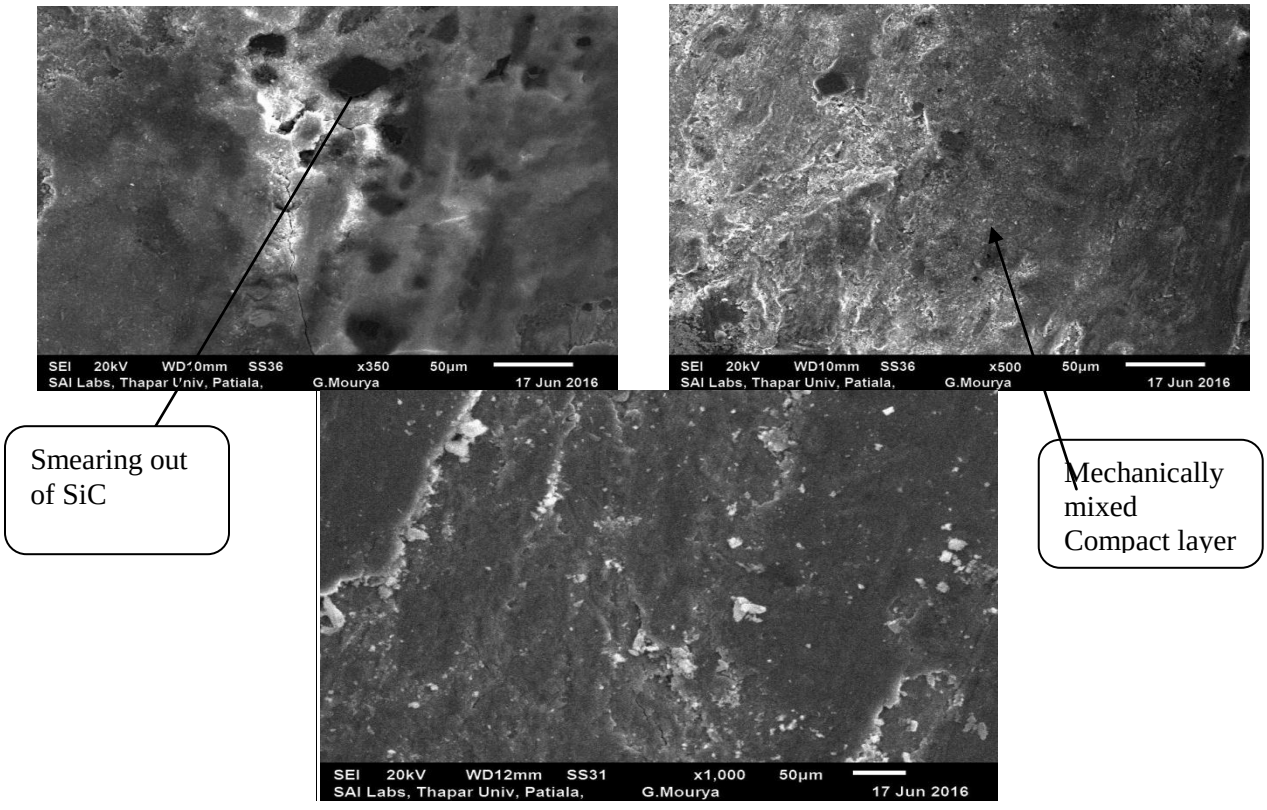

Fig 4.12 Typical worn surface of Cu (80%)-SiC (20%) (a) 0.5 (b) 1.0 and (c) 1.5 m/sec at 10 N

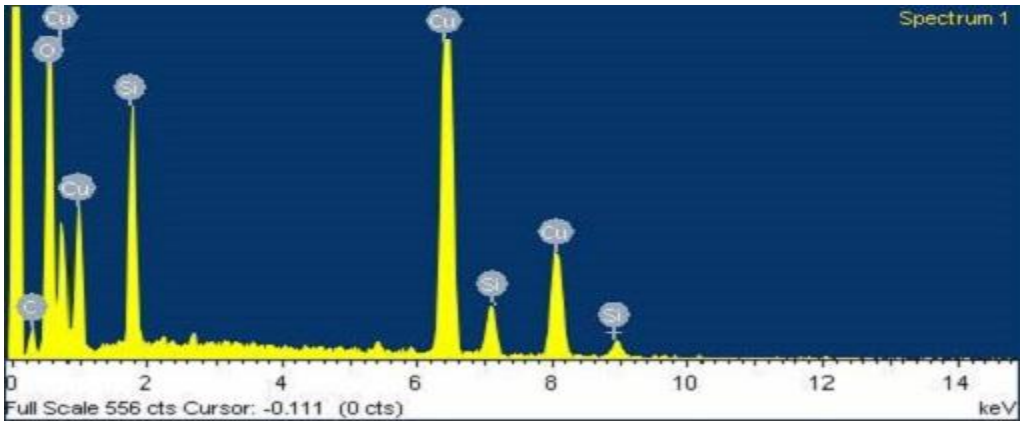

Fig. 4.13 EDX spectra on wear track for Cu (80%)-SiC (20%) sample

Table 4.15 EDX data for Cu (80%)-SiC (20%)

Element	Cu	Silicon	Carbon	Oxygen
Wt (%)	76.60	16.32	2.16	5.92

However, the increased content of hard SiC particles in the composite starts to abrade the counterface in the absence of any steady tribolayer between the contacts, as evident from the Fig 4.14. This limits the percentage of reinforcements in the soft matrix when it is to be used with the metallic surfaces.

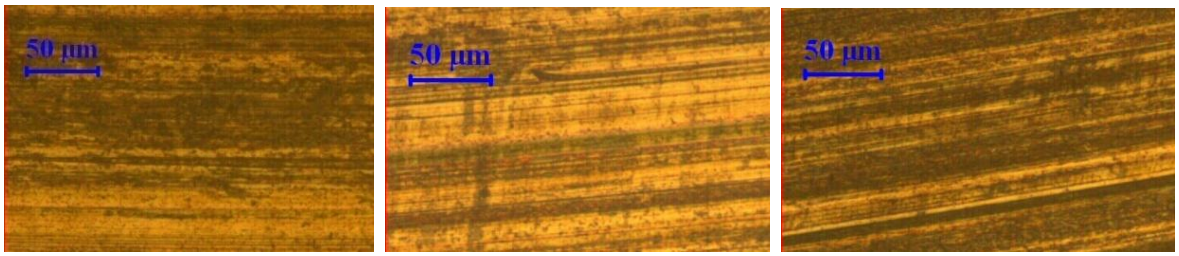

Fig 4.14 .Optical macrographs of the worn surface of disc mated with respective composite pin at 1 m/s with (a) 10% SiC, (b) 15% SiC and (c) 20% SiC

4.8. FRICTIONAL COEFFICIENT

Coefficient of friction was calculated for all the samples by using following formula:

Coefficient of friction= Frictional force/Normal load

E.g. set: 1

Table 4.16: Combination of parameters for set 1

Load 1kgf	**Speed 240 rpm**	**Track Dia 40mm**	**Sliding speed 0.50m/sec**

Sample 1: **Pure Copper**

Coefficient of friction= Frictional force/Normal load

Coefficient Of Friction = 2.4/9.81 = 0.245

For all the samples at different parameters above discussed method was used and based on the calculations following results were obtained:

Table 4.17: Coefficient of friction for all the experiments for different compositions

Sets	Cu (100%)	Cu (90%)-SiC (10%)	Cu (85%)-SiC (15%)	Cu (80%)-SiC (20%)
Set 1	0.245	0.203	0.163	0.142
Set 2	0.275	0.214	0.174	0.153
Set 3	0.285	0.224	0.183	0.160
Set 4	0.290	0.225	0.182	0.159
Set 5	0.298	0.234	0.186	0.166
Set 6	0.265	0.219	0.178	0.151
Set 7	0.308	0.240	0.193	0.168
Set 8	0.272	0.232	0.186	0.160
Set 9	0.295	0.235	0.189	0.165

Based on the above results following graphs has been drawn to see the trend of coefficient of friction for the different compositions at different conditions.

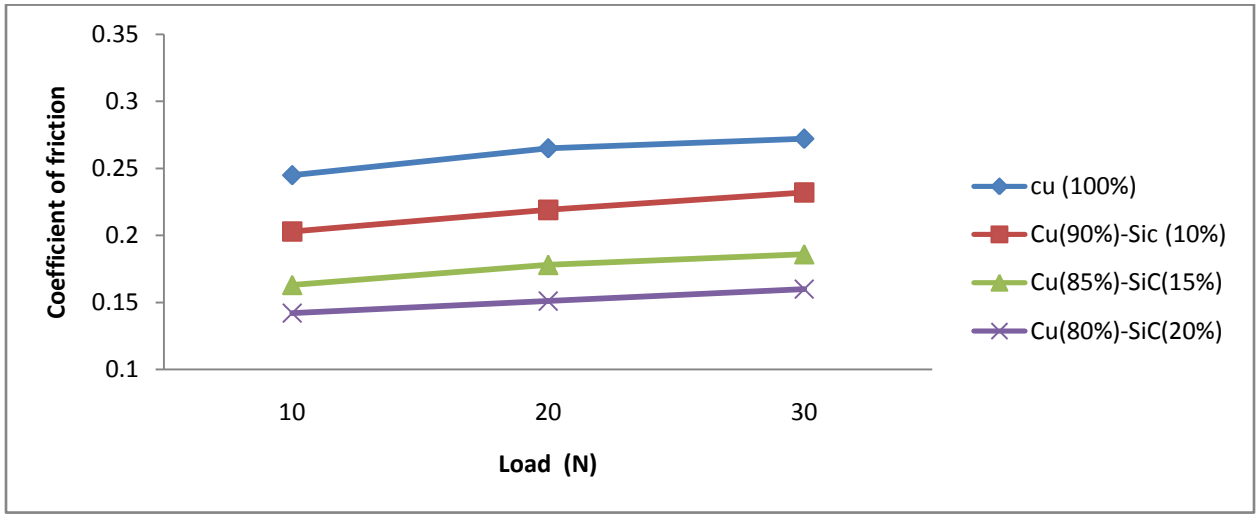

Fig 4.15 (a): Variation of c.o.f of composites with normal load at 0.50 m/s

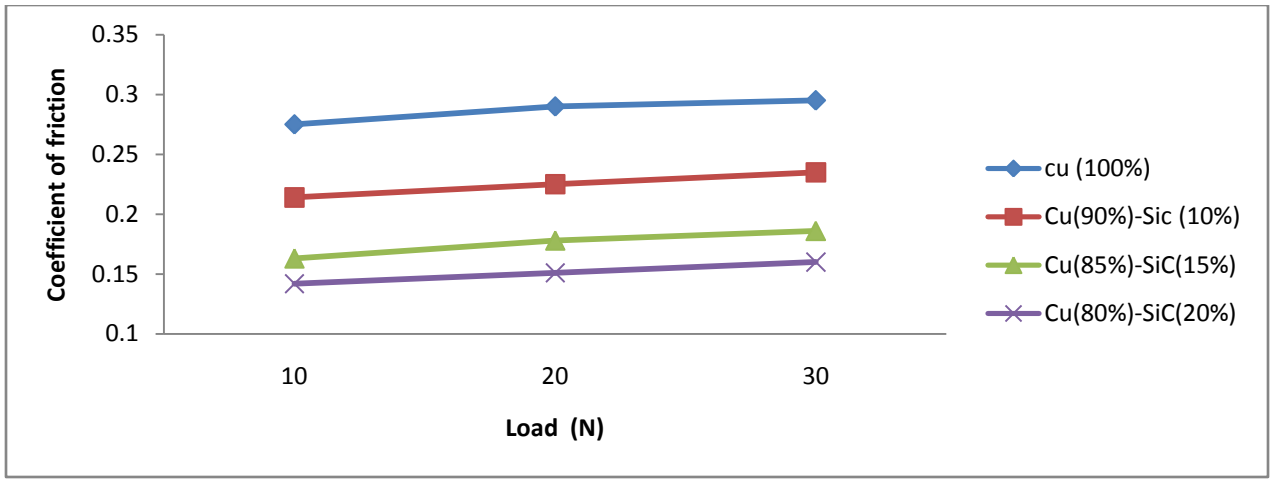

Fig 4.15 (b): Variation of C.o.f of composites with normal load at1.00 m/s

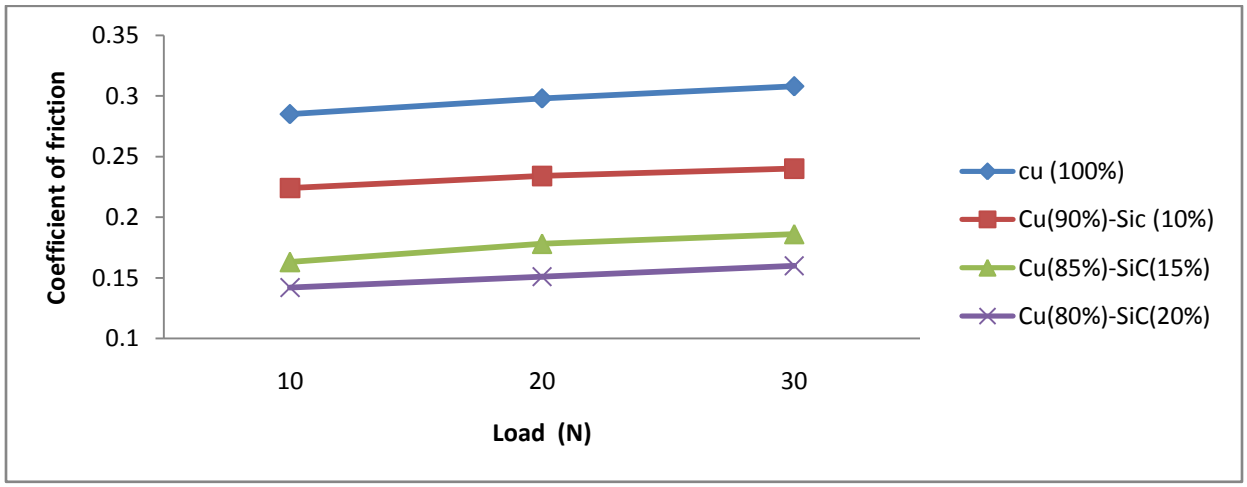

Fig 4.15 (c): Variation of C.o.f of composites with normal load at1.50 m/s

4.8.1. Effect of load

Variation of the frictional coefficient with the normal load for the pure copper and the Cu-SiC composites for the sliding speeds of 0.5, 1.0 and 1.5 m/s are shown in fig 4.15. From the graphs it is clear that as the normal load was increasing, coefficient of friction was also increasing. It was also observed that the Cu-SiC composites exhibit the lower frictional coefficient as compared to the pure copper. Higher frictional coefficient was exhibited by the pure copper for all the different loading conditions. As the normal load was increasing, the severity of the plastic deformation was also increasing. Also, at low load frictional heat is not considerable and if load is higher, then the frictional heating will contribute to increase in friction It increases the exposure of the silicon carbide (SiC) particles and subsequent increase in

interlocking between the counter surfaces. These may be the possible reasons for the increase in frictional coefficient with the increased normal load [26].

4.8.2. Effect of sliding speed and sliding distance

Variation of the frictional coefficient with the normal loads has shown in the figure for the sliding speeds of 0.5, 1.0 and 1.5 m/s. The results reveal that the sliding speed has less effect on the frictional coefficient of the composites. When the sliding speed was increased from 0.5 m/s to 1.0 m/s, so be the sliding distance, only smaller increment for the coefficient of friction was observed and similar kind of behavior was seen when the sliding speed was increased from 1.0 m/s to 1.5 m/s. Friction response in pure copper is significantly affected by sliding speed. However, the trend of the frictional coefficient for the different compositions was remaining same for the different sliding speeds.

4.8.3 Effect of reinforcements

The frictional coefficient decreases as the volumetric fraction of SiC content increases. The coefficient of friction was lowest for the composite having highest content of SiC (20%).This may be due to the smearing out of the silicon carbide particles during the sliding conditions due to which the nature of contact between the surfaces which are in contact to each other during the operations will be changed so that direct contact between the surface and the counter surface will be prevented due to which frictional coefficient will be reduced [25]. Moreover, when the contact is established, the harder SiC particles may protrude from the softer matrix and there is a possibility of pulling out of reinforced particles from softer matrix. Which in turn induce third body rolling action at the contact surface and thereby decrease the coefficient of friction. In other words, there is less ploughing and adhesive components in the steel-composite interactions. That’s why for the composite Cu (80%) - SiC (20%), coefficient of friction is lowest due to higher content of SiC as compared to the other compositions.

4.9 CONCLUSION

In the present chapter, mechanical, metallurgical and wear studies has been performed using fabricated samples with different compositions. Friction and wear behaviors are characterized for different load, sliding speed and sliding distance. The results revealed that both hardness and wear resistance properties as well as physical properties are improved by adequate reinforcement on the metal matrix. It is also observed from the data that applied load, sliding distance and composition play the important role in defining the wear and friction mechanism

under the majority of the tested conditions. It was found that the wear rate and the coefficient of friction decreased as the % of the SiC were increased in the composite. The recorded values of friction and wear at different conditions along with the SEM micrograph and EDX spectra helps us in explaining the underlying wear and friction mechanism and identifying the optimal process parameters. The mechanism of wear observed in the composites was abrasive in nature which is accompanied by ploughing, smearing and wedging action by abrasives. There is also possibility of oxidative wear with plastic deformation in case of pure copper and composites with low concentration of reinforcement. The wear resistance of the composite material is improved due to the presence of hard reinforcement particles in the matrix material. The wear process in the composite material is observed to be combination of plastic deformation of matrix, smearing out of reinforcement particles which may crush to very minute particles and form a mechanically mixed layer (MML) which helps in withstanding high stresses and is very effective in reducing the sliding wear.

CHAPTER 5
STATISTICAL ANALYSIS OF THE TRIBOLOGICAL BEHAVIOR

5.1 DEFINITION

"Design of experiment" (DOE) is an arranged method which helps to identify the relationship between the parameters which influence the process and the response of that process.

5.2 PURPOSE OF EXPERIMENTATION

The purpose of experimentation is to improve the performance characteristics of the response relative to the process variables. The purpose of experimentation is to understand how to analyze the process parameters which affects the performance of the response. The approach based on the use of orthogonal arrays (Taguchi) to conduct small, highly fractional factorial experiments is one methodology to design an experiment, which is most flexible in accommodating a variety of situations and yet easy to execute on a practical basis.

5.3 DEFINITION OF A DESIGNED EXPERIMENT

A designed experiment is the evaluation of two or more process parameters for their ability to affect the response. To accomplish this, the levels of the process parameters are varied in a continuous manner, the results of the particular experimental combinations are observed, and the complete set of results is analyzed to determine the influential process parameters and their preferred levels.

5.4 DESIGN OF EXPERIMENT PROCESS

DOE process uses five different steps which are experiment planning (to decide the objective, factors and methods to be used and also gives information that which factors and which levels lead to improved process performance), designing the experiments (to decide the number of experiments and the manner in which these experiments has to be done), conducting the experiments (experiments are performed as per design considerations), analyzing the results

and in final step the predicted results are confirmed to saw that how close the results are matching to the predicted ones.

So the main advantage of this procedure that it is very less time consuming with respect to the traditional methods which are used to plan the experiments and also the number of experiments are less to optimize the outputs.

The five steps for experimental planning using Taguchi method are presented in the following flow chart [41].

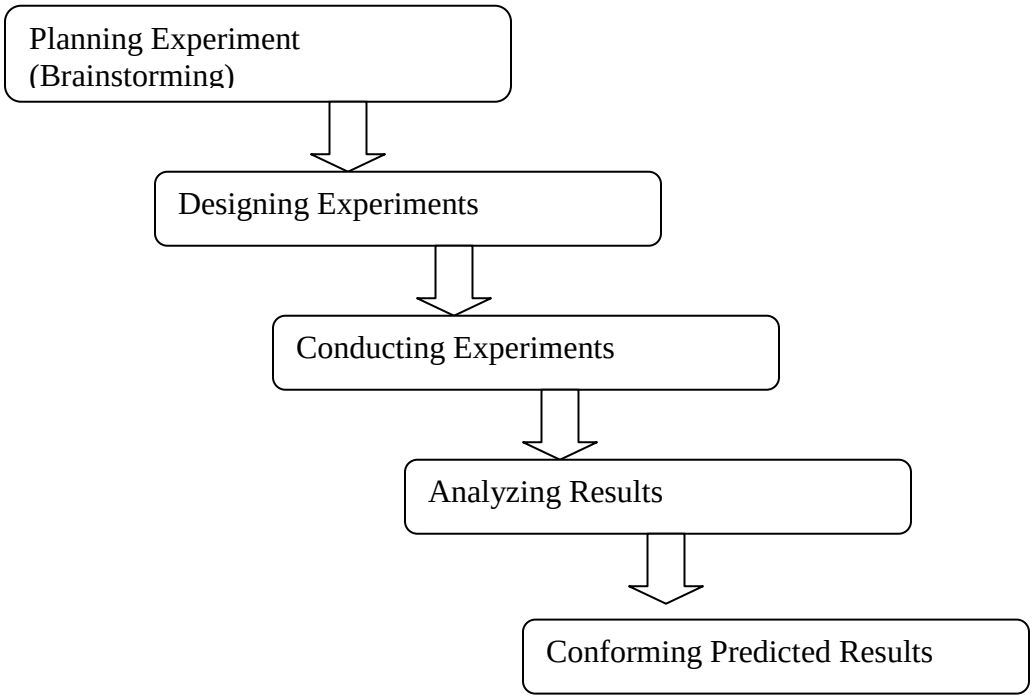

Fig 5.1: Flow chart of major steps using taguchi method

5.5 DETAILS OF WORK MATERIAL

The work material which was used for this study was Copper (Cu) and Silicon carbide (SiC) composite in different constituents. Copper was chosen as a base material due to its good electrical as well as thermal conductivity and SiC was used as a reinforcement, which will enhance the hardness of the composite which leads to less wear rate for the composite. These samples were having cylindrical shape. EN 31 steel disc was used as a counter surface having hardness of 52 HRC.

5.6 SELECTION OF THE PROCESS PARAMETERS

The process parameters for the experimentation are sliding speed, applied load and the sliding distance. The experiments have been conducted keeping these three factors at different

levels. The values were selected based on preliminary experiments and the capabilities of the Tribometer. The range of sliding speed was 0.5 to 1.5 m/sec; applied load was 1kgf to 3kgf and sliding distance was from 900m to 2700m. The control parameters and their levels were already presented in Table 4.7.

5.7 PLANING OF EXPERIMENTS

5.7.1 Experimental design

Pure copper and different combinations of Cu-SiC composites were selected as the specimens for the study based on literature survey & pilot study. Detailed list of combinations of Cu-SiC is presented in table 5.1. L9 orthogonal array was applied for experimentation and analysis of the outcome was performed based on S/N ratio and ANOVA.

Table 5.1 List of different compositions of the samples for experiment

Sample Number	Percentage (%) of Copper (Cu)	Percentage (%) of Silicon Carbide (SiC)
1	100	0
2	90	10
3	85	15
4	80	20

The experimental plan and the complete details for each experiment decided as per L9 orthogonal array for each composition was presented in Table 4.7 and 4.8.

5.7.2 Analysis of variance

In the present study ANOVA is used to carry out the statistical analysis of the experimental results. ANOVA is a kind of computational technique which is used to estimate the relative contribution of each of the factor which is responsible for the responses. The significance of the individual and interaction effects is quantified by comparing the variance between the control factors effects against the variance in the experiment data due to random experimental error. The variation of the data due to random experimental variability and interaction is referred to the variation within the control factors that make up the experiment. This ratio is known as F- ratio and can be formed between the control factors effect variance. The ANOVA process also helps to find out the main effects, interaction effects and also the less

significant and noise. This is useful to decide the factors which are most relevant for specific process or the product robustness.

5.8 FRICTION AND WEAR: EXPERIMENTAL RESULTS

The experimental results for wear and friction which was discussed in the previous chapter is rearranged and shown in the table 5.2 and 5.3, respectively.

Table 5.2: Wear rate for all the experiments for different compositions

Sets	Cu (100%)	Cu (90%)-SiC (10%)	Cu (85%)-SiC (15%)	Cu (80%)-SiC (20%)
Set 1	6.19*10^-4	2.68*10^-4	2.12*10^-4	1.45*10^-4
Set 2	6.82*10^-4	2.986*10^-4	2.322*10^-4	1.69*10^-4
Set 3	6.954*10^-4	3.57*10^-4	2.702*10^-4	1.821*10^-4
Set 4	7.69*10^-4	3.18*10^-4	2.60*10^-4	1.76*10^-4
Set 5	7.92*10^-4	3.41*10^-4	2.98*10^-4	1.88*10^-4
Set 6	7.08*10^-4	6.19*10^-4	6.19*10^-4	6.19*10^-4
Set 7	8.10*10^-4	3.69*10^-4	3.12*10^-4	1.93*10^-4
Set 8	7.48*10^-4	3.36*10^-4	2.62*10^-4	1.78*10^-4
Set 9	7.82*10^-4	3.53*10^-4	2.78*10^-4	1.82*10^-4

Table 5.3: Coefficient of friction for all the experiments for different compositions

Sets	Cu (100%)	Cu (90%)-SiC (10%)	Cu (85%)-SiC (15%)	Cu (80%)-SiC (20%)
Set 1	0.245	0.203	0.163	0.142
Set 2	0.275	0.214	0.174	0.153
Set 3	0.285	0.224	0.183	0.160
Set 4	0.290	0.225	0.182	0.159
Set 5	0.298	0.234	0.186	0.166
Set 6	0.265	0.219	0.178	0.151
Set 7	0.308	0.240	0.193	0.168
Set 8	0.272	0.232	0.186	0.160
Set 9	0.295	0.235	0.189	0.165

5.9 STATISTICAL MODELING

5.9.1 Statistical modeling of Wear rate

A statistical model was made for the wear rate for each composition by correlating the input parameters namely sliding speed, applied load and the sliding distance, based on the analysis of the data presented in table 5.2. It is required to check the fitness of model of the obtained data. It includes the significance test of regression model and also the lack of fit. ANOVA is performed to check the adequacy of the experiment.

5.9.1.1 Pure Copper

Based on the data presented in table 5.2, the statistical model for the wear for pure copper sample is given below in equation (1).

Wear rate = 0.000550 + 0.000057 L - 0.000004 SS + 0.000002 SD…….(1)

The value of *R* is 90.27% that indicates that there is strong correlation between the parameters and the output (wear rate). The F value which is obtained by ANOVA is shown in the table 5.4 for the model is 15.40. The calculated F value is more than the tabulated value of $F_{0.01,\ 3,\ 5}$ that is 3.45 for the significance level of $\alpha = 0.01$. This proves that the statistical model is adequate for the confidence level of 99%.

Table 5.4: ANOVA Table for Copper

Source	DF	Adj SS	Adj MS	F-value	P-value	R	Remarks
Regression	3	0.000000	0.000000	15.40	0.006	0.9027	Model is Adequate 15.40>3.45
L	1	0.000000	0.000000	32.59	0.002		
SS	1	0.000000	0.000000	0.05	0.838		
SD	1	0.000000	0.000000	13.57	0.014		
Error	5	0.000000	0.000000				
Total	8	0.000000					

Table 5.5: Response table for means for Copper

Level	Load	Sliding speed	Sliding distance
1	0.000665	0.000733	0.000692
2	0.000756	0.000741	0.000744
3	0.000780	0.000728	0.000766
Delta	0.000115	0.000012	0.000074

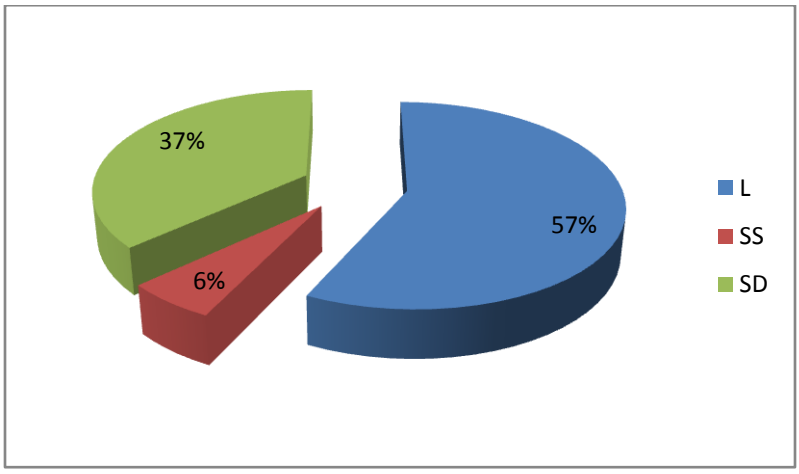

Fig 5.2: Pie chart distribution for each parameter for copper

Pie chart (Fig. 5.2) shows the individual contribution of the input variables in statistical modeling for wear rate. From the table and the graphs it is clear that applied load and the sliding distance are most significant parameters which affects the wear rate and are contributing 57% and 37%, respectively. Sliding speed has 6% contribution also affects the wear rate but not too much as compare to the load and the sliding distance.

Fig 5.3 shows the main effect plots for the pure copper. By using the experimental data, three points are obtained.

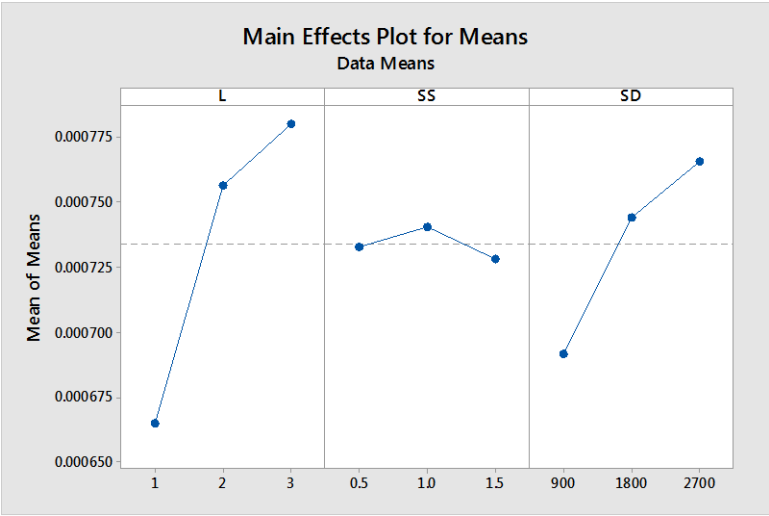

Fig 5.3: Main effect plot for Copper specimen

5.9.1.2 Cu (90%) - SiC (10%) Composite:

Statistical model for the wear for Cu (90%) - SiC (10%) Composite was developed based on the data presented in table 5.2 and is given below as equation (2).

Wear rate=0.000217 + 0.000029 L + 0.000001 SS + 0.000002 SD…….(2)

Table 5.6: ANOVA Table for composite Cu (90%) - SiC (10%)

Source	DF	Adj SS	Adj MS	F-value	P-value	R	Remarks
Regression	3	0.000000	0.000000	65.06	0.000	0.9750	Model is Adequate 65.06>3.45
L	1	0.000000	0.000000	125.60	0.000		
SS	1	0.000000	0.000000	0.09	0.776		
SD	1	0.000000	0.000000	69.50	0.000		
Error	5	0.000000	0.000000				
Total	8	0.000000					

The R value obtained by ANOVA is 97.50% (Table 5.6) which indicates that there is strong correlation between the input parameters and the output (wear rate). The *F* value for the model is 65.06. The calculated F value as shown in table is greater than the value of $F_{0.01,\ 3,\ 5}$ that is 3.45 for the significance level of $\alpha = 0.01$, which prove that the model is statistically adequate for the 99% confidence level.

Table 5.7: Response table for means for Cu (90%) - SiC (10%)

Level	Load	Sliding speed	Sliding distance
1	0.000294	0.000318	0.000298
2	0.000317	0.000325	0.000323
3	0.000333	0.000320	0.000342
Delta	0.000039	0.000014	0.000044

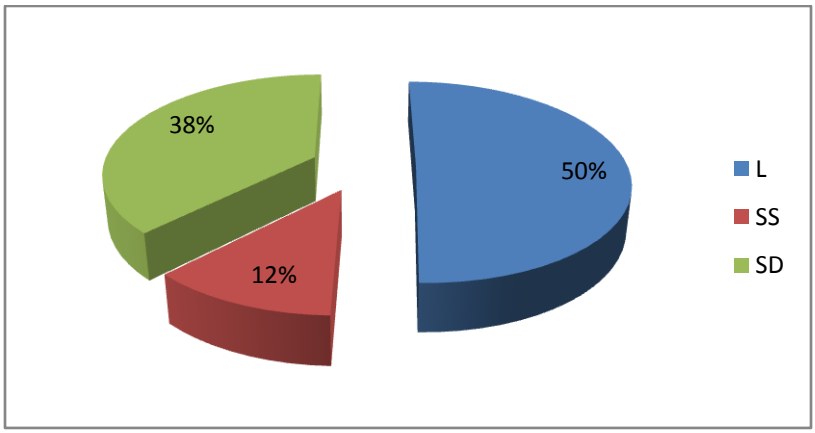

Fig 5.4: Pie chart distribution for each parameter for Cu (90%)-SiC (10%) Composite

Fig 5.4 shows the individual contribution of the input variables in statistical modeling for wear rate. From the table and the graphs it is clear that applied load and the sliding distance are most significant parameters which affects the wear rate and are contributing 50% and 38%, respectively. Sliding speed has 12% contribution to the wear rate. Fig 5.5 shows the main effect plots for the Cu (90%)-SiC (10%) composite. Wear rate is less as compared to the pure copper because of addition of SiC, which enhances the hardness of the composite. It is clear from the plots that by increasing the load wear rate are increasing. As the sliding distance is increased there is an increase in wear rate for the specimen and the sliding speed has very less effect on the wear rate of the specimen.

Fig 5.5: Main effect plots for Cu (90%)-SiC (10%) composite

5.9.1.3 Cu (85%) - SiC (15%) Composite:

A statistical model for the wear for Cu (85%) - SiC (15%) Composite, based on the data presented in table 5.2, is given below as equation (3).

Wear rate = 0.000165 + 0.000023 L + 0.000003 SS + 0.000017 SD…….(3)

Table 5.8 ANOVA Table for composite Cu (85%) - SiC (15%)

Source	DF	Adj SS	Adj MS	F-value	P-value	R	Remarks
Regression	3	0.000000	0.000000	5.14	0.055	0.9730	Model is Adequate 5.14>3.45
L	1	0.000000	0.000000	8.24	0.035		
SS	1	0.000000	0.000000	1.17	0.329		
SD	1	0.000000	0.000000	6.02	0.058		
Error	5	0.000000	0.000000				
Total	8	0.000000					

The value of *R* in this case is 97.30% (table 5.8) which is an indication of strong correlation between the parameters and the output (wear rate). The F value obtained by ANOVA for the model is 5.14. The calculated F value as shown in table is greater than the value of $F_{0.01,\ 3,\ 5}$ which prove that the model is statistically adequate for the 99% confidence level.

Table 5.9: Response table for means for Composite Cu (85%) - SiC (15%)

Level	Load	Sliding speed	Sliding distance
1	0.000238	0.000261	0.000261
2	0.000272	0.000264	0.000257
3	0.000284	0.000278	0.000293
Delta	0.000046	0.000017	0.000032

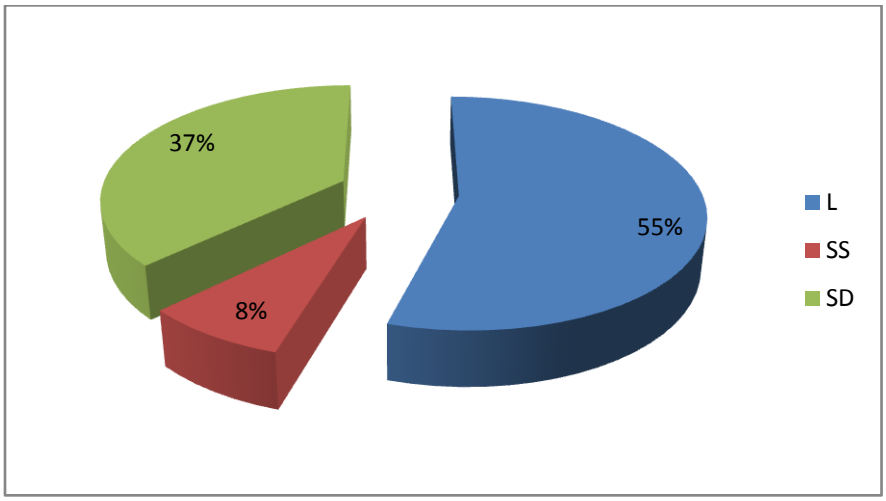

Fig 5.6: Pie chart distribution for each parameter for Cu (85%)-SiC (15%) composite

Fig. 5.6 shows the individual contribution of the input variables in statistical modeling for wear rate. In this case, applied load and the sliding distance are most significant parameters which affect the wear rate and are contributing 55% and 37%, respectively. Sliding speed has 8% contribution. Fig 5.7 shows the main effect plots for the Cu (85%)-SiC (15%) composite. It is clear from the plots that; by increasing the load and sliding distance, wear rate is increasing whereas the sliding speed has very less effect on the wear rate of the specimen.

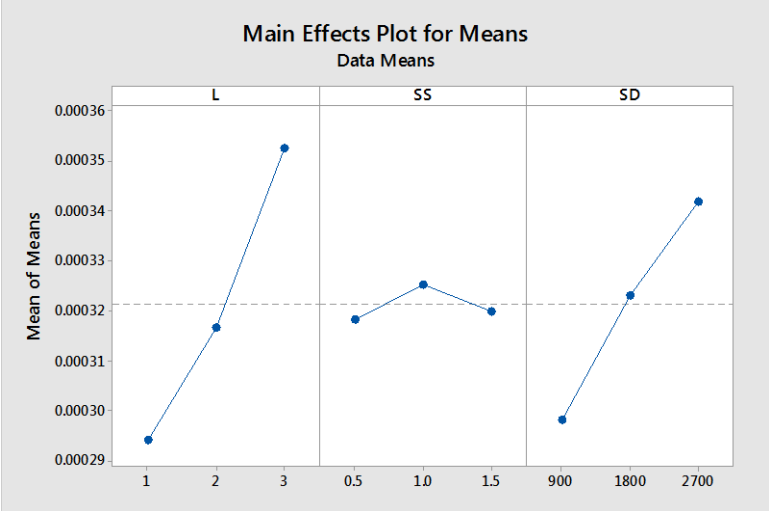

Fig 5.7: Main effect plots for Cu (85%)-SiC (15%) composite

5.9.1.4. Cu (80%) – SiC (20%) Composite:

Statistical model for the wear for Cu (80%) - SiC (20%) Composite is given below as equation (4).

Wear rate = 0.000126 + 0.000010 L + 0.000002 SS + 0.000011 SD……. (4)

Table 5.10 ANOVA Table for Composite Cu (80%) – SiC (20%)

Source	DF	Adj SS	Adj MS	F-value	P-value	R	Remarks
Regression	3	0.000000	0.000000	21.50	0.003	0.9281	Model is Adequate 21.50>3.45
L	1	0.000000	0.000000	29.47	0.003		
SS	1	0.000000	0.000000	0.68	0.446		
SD	1	0.000000	0.000000	34.35	0.002		
Error	5	0.000000	0.000000				
Total	8	0.000000					

The value of *R* is 92.81% (Table 5.10) which is a indication of strong correlation between the parameters and the output (wear rate). The F value for the model as shown in table is 21.50. The calculated F value is more than the value of $F_{0.01, 3, 5}$ which is 3.45 for the level of significance of $\alpha = 0.01$. Which prove that the model is statistically adequate for 99% confidence level.

Table 5.11: Response table for means for Composite Cu (80%) – SiC (20%)

Level	Load	Sliding speed	Sliding distance
1	0.000165	0.000171	0.000162
2	0.000175	0.000178	0.000176
3	0.000184	0.000175	0.000182
Delta	0.000039	0.000007	0.000020

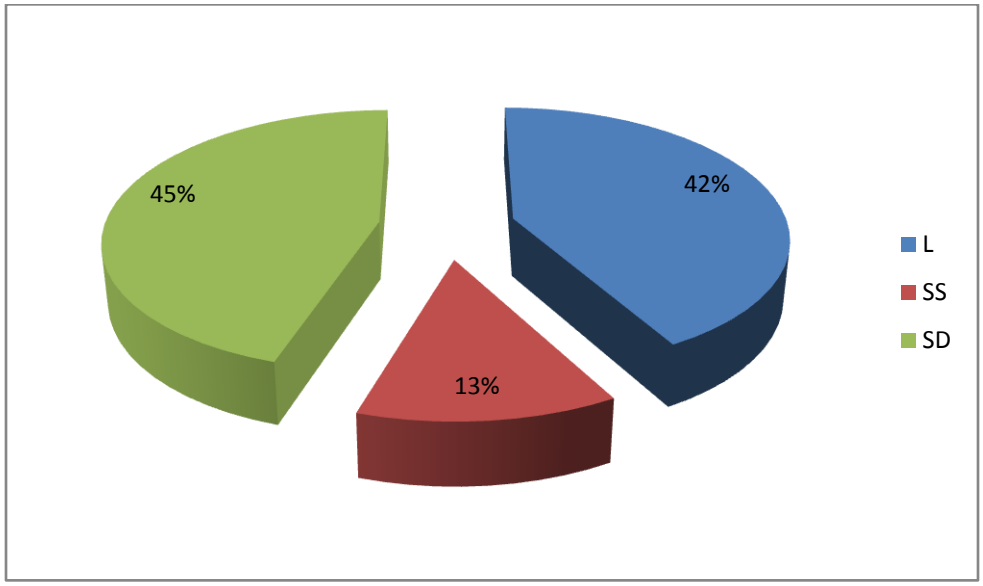

Fig 5.8: Pie chart distribution for each parameter for Cu (80%)-SiC (20%) composite

Fig. 5.8 shows the individual contribution of the input variables in statistical modeling for wear rate. Similar to the previous sample here also applied load and the sliding distance are most significant parameters. However, sliding distance is more significant than the load and is contributing 42% and 45%, respectively to wear rate. Sliding speed has 13% contribution. Fig 5.9 shows the main effect plots for the Cu (80%)-SiC (20%) composite. Wear rate is less as compared to the pure copper because of addition of SiC, which enhances the hardness of the composite. It is clear from the plots that; by increasing the load and sliding distance, wear rate is increasing significantly whereas the sliding speed has very less effect on the wear rate of the specimen.

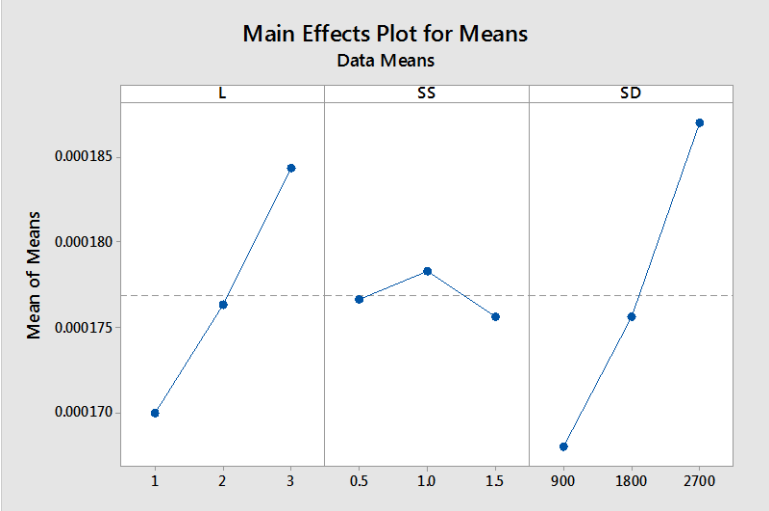

Fig 5.9: Main effects plot for Cu (80%)-SiC (20%) composite

5.9.2 Friction analysis:

For each of the combination response table for means and analysis of variance was generated and also mean effect curves were plotted to see that which parameter is more affecting the friction.

5.9.2.1 Pure Copper

A statistical model for the coefficient of friction for pure copper was developed, by correlating the input parameters namely applied load, sliding speed and the sliding distance, based on the data presented in table 5.3, and is given below as equation (5) .

$$C.o.f = 0.22111 + 0.01167\ L + 0.00020\ SS + 0.000067\ SD \ldots\ldots\ldots\ldots (5)$$

Table 5.12 ANOVA Table for Copper

Source	DF	Adj SS	Adj MS	F-value	P-value	R	Remarks
Regression	3	0.002797	0.000932	25.80	0.002	0.9393	Model is Adequate 25.80>3.45
L	1	0.000817	0.000817	22.59	0.005		
SS	1	0.000001	0.000001	0.02	0.897		
SD	1	0.001980	0.001980	54.78	0.001		
Error	5	0.000181	0.000036				
Total	8	0.002978					

Similar to the wear model, it is required to check the fitness of model of the obtained data which includes the significance test of regression model and also the lack of fit. The value of *R* is 93.93% as shown in table; which indicates that there is strong correlation between the input parameters and the output. The F value which is obtained by ANOVA is shown in the table 5.12

for the model is 25.80. The calculated F value is higher than the value of $F_{0.01, 3, 5}$ which is 3.45 for the significance level of $\alpha = 0.01$. Which prove that the model is statistically adequate for the 99% confidence level.

Table 5.13: Response table for means for Copper

Level	Load	Sliding speed	Sliding distance
1	0.2683	0.2810	0.2597
2	0.2843	0.2817	0.2867
3	0.3017	0.2777	0.2900
Delta	0.0433	0.0167	0.0303

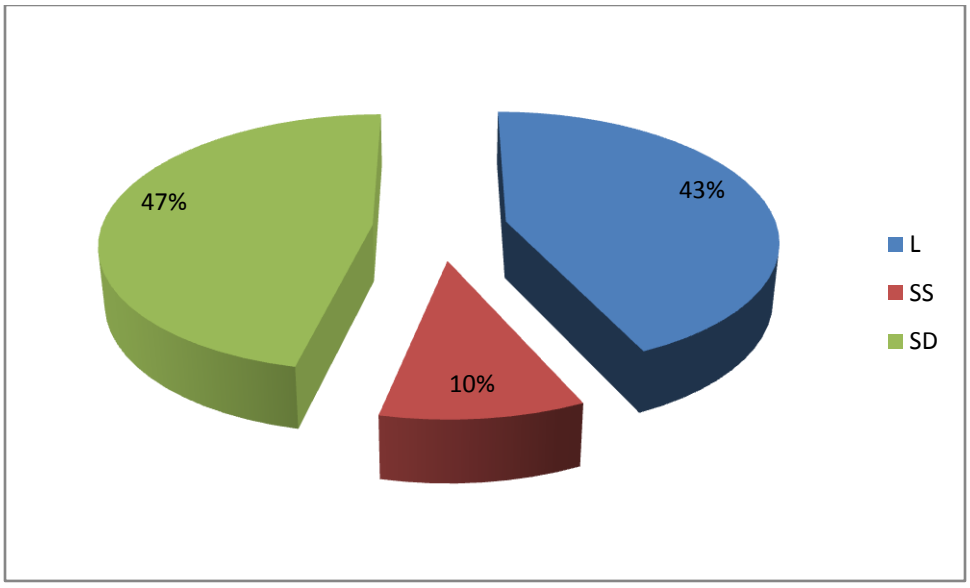

Fig 5.10: Pie chart distribution for each parameter for Copper

Fig 5.10 shows the individual contribution of the input variables in statistical modeling for wear rate. From the table and the graphs it is clear that applied load and the sliding speed are most significant parameters which affect the wear rate and are contributing 43% and 47%, respectively. Sliding distance has 10% contribution to frictional response. Fig 5.11 shows the main effect plots for pure copper. It is clear from the plots that by increasing the load there is an increase in frictional coefficient which may be due to the increased severity of the plastic deformation. As the sliding speed is increased due to frictional heating , frictional force is also increasing. Sliding distances has very less effect on the frictional coefficient.

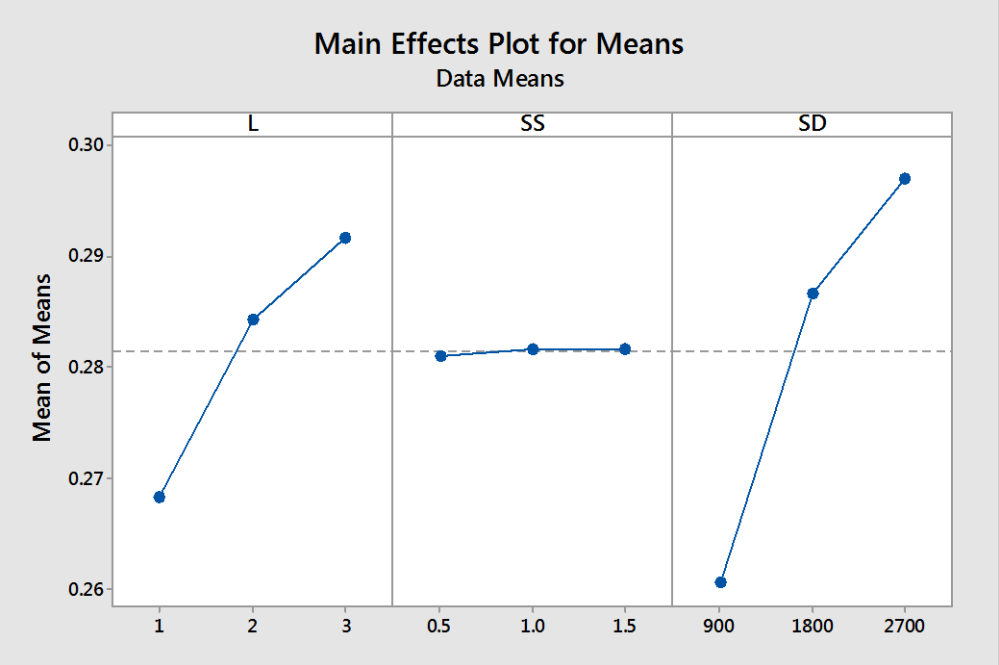

Fig 5.11: Main effects plot graphs for Copper

5.9.2.2. Cu (90%) – SiC (10%) Composite

A statistical model for the coefficient of friction for Cu (90%) – SiC (10%) Composite developed, based on the data presented in table 5.3, is given below (equation 6) .

C.o.f. = 0.1851 + 0.01100 L - 0.00333 SS + 0.000008 SD……(6)

Table 5.14 ANOVA Table for composite Cu (90%) – SiC (10%)

Source	DF	Adj SS	Adj MS	F-value	P-value	R	Remarks
Regression	3	0.001065	0.000355	56.27	0.000	0.9712	Model is Adequate 56.27>3.45
L	1	0.000726	0.000726	115.04	0.000		
SS	1	0.000017	0.000017	3.64	0.165		
SD	1	0.000323	0.000323	51.13	0.001		
Error	5	0.000032	0.000006				
Total	8	0.001097					

To check the adequacy of the model Anova is performed and is shown in table 5.14. The value of *R* from table 5.14 is 97.12% which shows that there is strong correlation between the parameters and the output. The F value which is obtained by ANOVA is shown in the table for the model is 56.27. The calculated F value as shown in table is greater than the value of $F_{0.01,\,3,\,5}$ which is 3.45

for the significance level of of α = 0.01. Which prove that the model is statistically adequate for the 99% confidence level.

Table 5.15: Response table for means for composite Cu (90%) – SiC (10%)

Level	Load	Sliding speed	Sliding distance
1	0.2137	0.2227	0.2180
2	0.2260	0.2267	0.2247
3	0.2357	0.2260	0.2327
Delta	0.0220	0.0040	0.0147

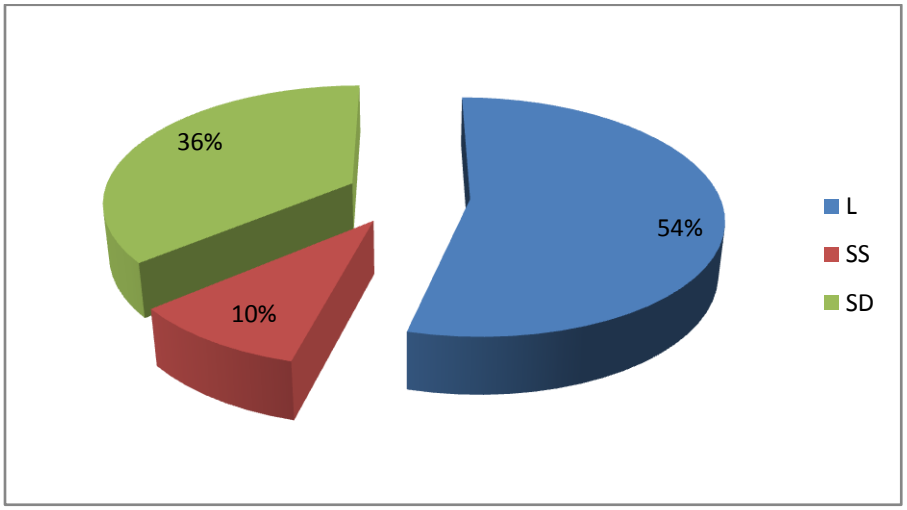

Fig 5.12: Pie chart distribution for each parameter for Cu (90%)-SiC (10%) composite

Fig 5.12 Pie chart shows the individual contribution of the input variables in statistical modeling for wear rate. From the table and the graphs it is clear that applied load and the sliding distance are most significant parameters which affects the wear rate and are contributing 54% and 36%. Sliding speed has 10% contribution also affects the wear rate. Fig 5.13 shows the main effect plots for Cu (90%)-SiC (10%) composite.

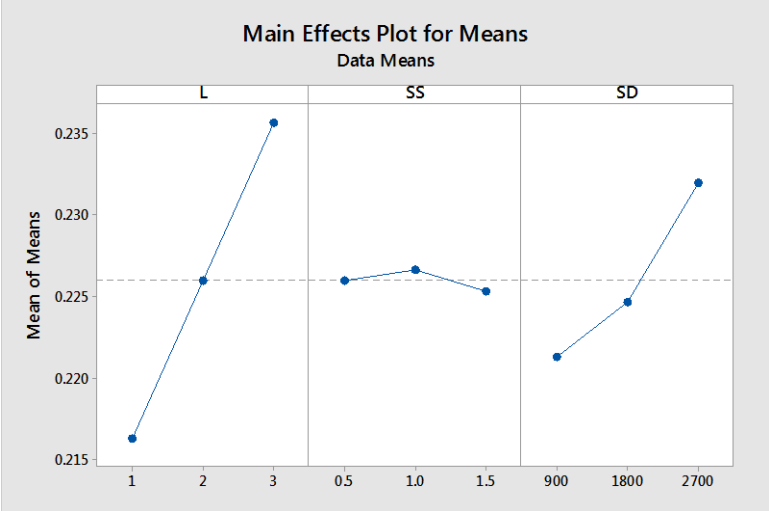

Fig 5.13: Main effects plot for Cu (90%)-SiC (10%) composite

5.9.2.3 Cu (85%) – SiC (15%) Composite

A statistical model for the coefficient of friction for Cu (85%) – SiC (15%) Composite developed, by correlating the input parameters namely applied load, sliding speed and the sliding distance, based on the data presented in table 5.3,is given below in equation (7) .

C.o.f. = 0.14989 + 0.00800 L - 0.00400 SS + 0.000006 SD……..(7)

Table 5.16 ANOVA Table for Composite Cu (85%) – SiC (15%)

Source	DF	Adj SS	Adj MS	F-value	P-value	R	Remarks
Regression	3	0.000434	0.000145	60.02	0.000	0.9730	Model is
L	1	0.000294	0.000294	121.94	0.000		Adequate
SS	1	0.000000	0.000000	0.00	1.000		60.02>3.45
SD	1	0.000140	0.000140	58.13	0.001		
Error	5	0.000012	0.000002				
Total	8	0.000446					

From the ANOVA table (table 5.16) the value of *R* is 97.30% which shows that there is strong correlation between the input parameters and the output. The F value which is obtained by ANOVA is shown in the table for the model is 60.02. The calculated F value is greater than the value of $F_{0.01,\ 3,\ 5}$ which proves that the model is statistically adequate for the 99% confidence level.

Table 5.17: Response table for means for Composite Cu (85%) – SiC (15%)

Level	Load	Sliding speed	Sliding distance
1	0.1747	0.1853	0.1770
2	0.1813	0.1820	0.1810
3	0.1617	0.1813	0.1860
Delta	0.0130	0.0040	0.0090

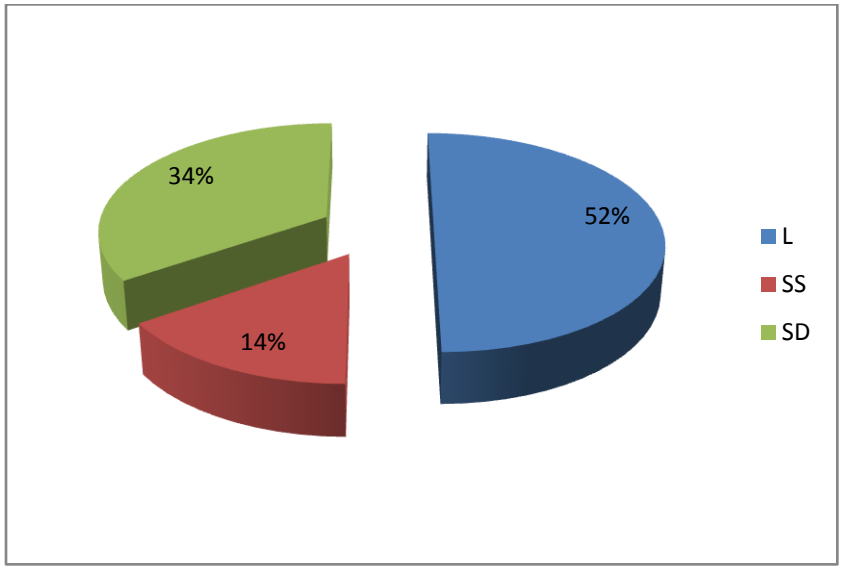

Fig 5.14: Pie chart distribution for each parameter for Cu (85%)-SiC (15%) composite

Pie chart (Fig 5.14) shows the individual contribution of the input variables in statistical modeling for wear rate. From the table and the graphs it is clear that applied load and the sliding distance are most significant parameters which affects the wear rate and are contributing 50% and 35%. Sliding speed has 15% contribution to COF.

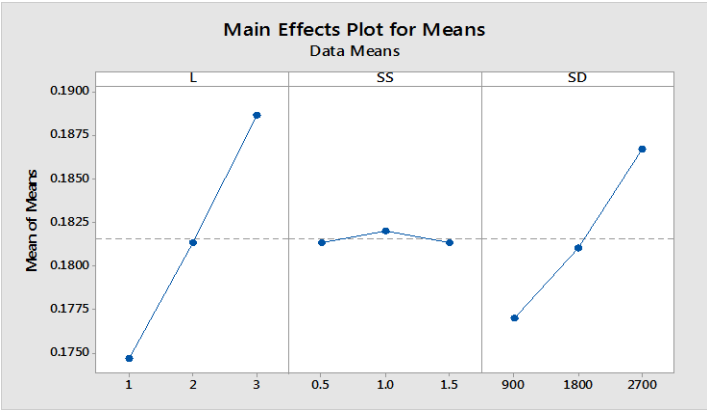

Fig 5.15: Main effect plots for Cu (85%)-SiC (15%) composite

5.9.2.4 Cu (80%) – SiC (20%) Composite

A statistical model for the coefficient of friction for Cu (80%) – SiC (20%) Composite was developed, by correlating the input parameters namely applied load, sliding speed and the sliding distance, based the data presented in table 5.3, and is given below ain equation (8) .

C.o.f. = 0.12956 + 0.006333 L + 0.00008 SS + 0.000017 SD…….(8)

Table 5.18 ANOVA Table for composite Cu (80%) – SiC (20%)

Source	DF	Adj SS	Adj MS	F-value	P-value	R	Remarks
Regression	3	0.000448	0.000149	25.57	0.002	0.9388	Model is Adequate 25.57>3.45
L	1	0.000182	0.000182	31.06	0.003		
SS	1	0.000000	0.000000	0.03	0.873		
SD	1	0.000267	0.000267	45.63	0.001		
Error	5	0.000029	0.000006				
Total	8	0.000478					

ANOVA is performed to check the adequacy and the value of *R* is 93.88% which showes that there is strong correlation between the parameters and the output (wear rate). The F value obtained by ANOVA for the model is 25.57 and the calculated F value is greater than the value of $F_{0.01, 3, 5}$ which prove that the model is statistically adequate for the 99% confidence level.

Table 5.19: Response table for means for Composite Cu (80%) – SiC (20%)

Level	Load	Sliding speed	Sliding distance
1	0.1530	0.1577	0.1514
2	0.1577	0.1597	0.1513
3	0.1367	0.1532	0.1647
Delta	0.0210	0.0065	0.0133

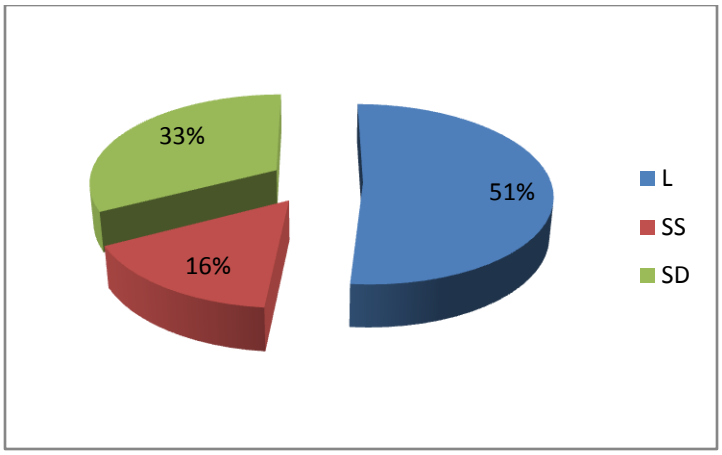

Fig 5.16: Pie chart distribution for each parameter for Cu (80%)-SiC (20%) composite

Fig 5.16 shows the individual contribution of the input variables in statistical modeling for wear rate. From the table and the graphs it is clear that applied load and the sliding distance are most significant parameters which affects the wear rate and are contributing 51% and 33%, respectively. Sliding speed has 13% contribution to the wear rate. Fig 5.17 shows the main effect plots for Cu (90%)-SiC (20%) composite. It is clear from the plots that by increasing the load and sliding distance there is a significant increase in frictional coefficient.. Sliding speed has very less effect on the frictional coefficient.

Fig 5.17: Main effect plots for Cu (80%)-SiC (20%) composite

5.10 MODEL VALIDITY

5.10.1 Wear rate

Based on the regression equation for each sample wear rate was calculated. Table 5.20 shows the wear rate for each sample.

Table 5.20: Wear rate*10^-4 (mm^3/m) for each sample based on regression equation

Sets	Cu (100%)	Cu (90%)-SiC (10%)	Cu (85%)-SiC (15%)	Cu (80%)-SiC (20%)
Set 1	11.1*10^-4	5.01*10^-4	3.91*10^-4	2.61*10^-4
Set 2	10.75*10^-4	5.301*10^-4	4.09*10^-4	2.81*10^-4
Set 3	10.73*10^-4	5.802*10^-4	4.132*10^-4	2.30*10^-4
Set 4	10.66*10^-4	7.81*10^-4	6.241*10^-4	3.24*10^-4
Set 5	16.73*10^-4	8.11*10^-4	6.31*10^-4	3.26*10^-4
Set 6	16.80*10^-4	8.512*10^-4	6.39*10^-4	3.28*10^-4
Set 7	22.11*10^-4	10.702*10^-4	8.5*10^-4	4.22*10^-4
Set 8	22.21*10^-4	11.11*10^-4	8.559*10^-4	4.25*10^-4
Set 9	22.25*10^-4	11.501*10^-4	8.65*10^-4	4.27*10^-4

From the above results it is clear that for each sample and for each set the wear rate was very near to the experimented wear rate. By using these values graphs were generated. Fig 5.18 – 5.22 shows the wear rate trend with respect to the applied load, sliding speeds and sliding distance.

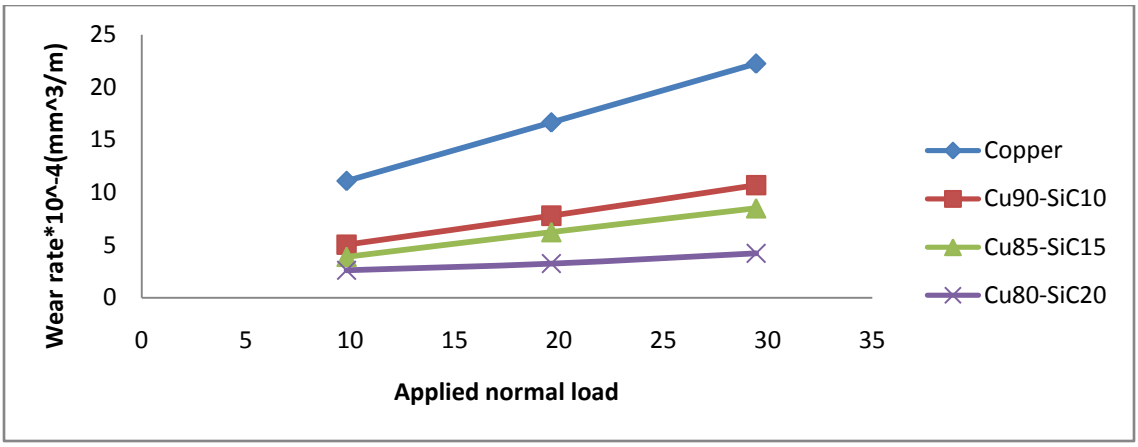

Fig 5.18: Wear rate v/s Load for sliding speed of 0.5m/sec

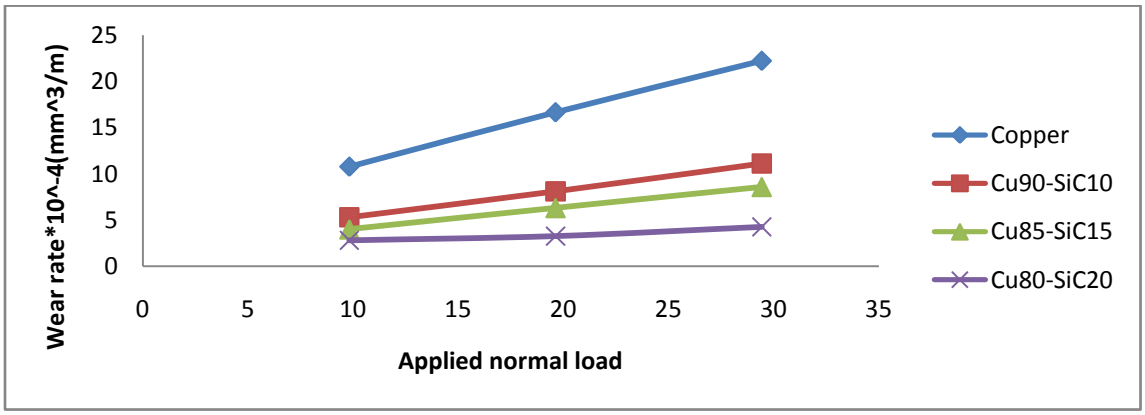

Fig 5.19: Wear rate v/s Load for sliding speed of 1.0m/sec

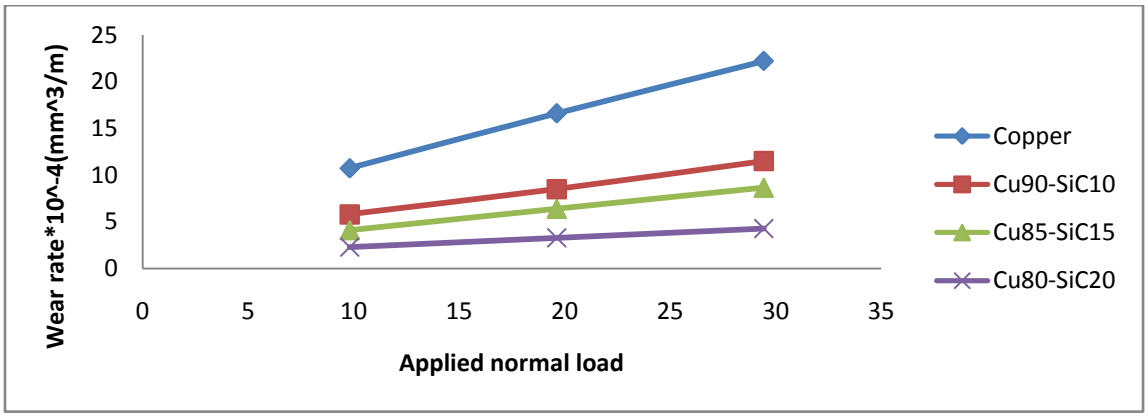

Fig 5.20: Wear rate v/s Load for sliding speed of 1.5m/sec

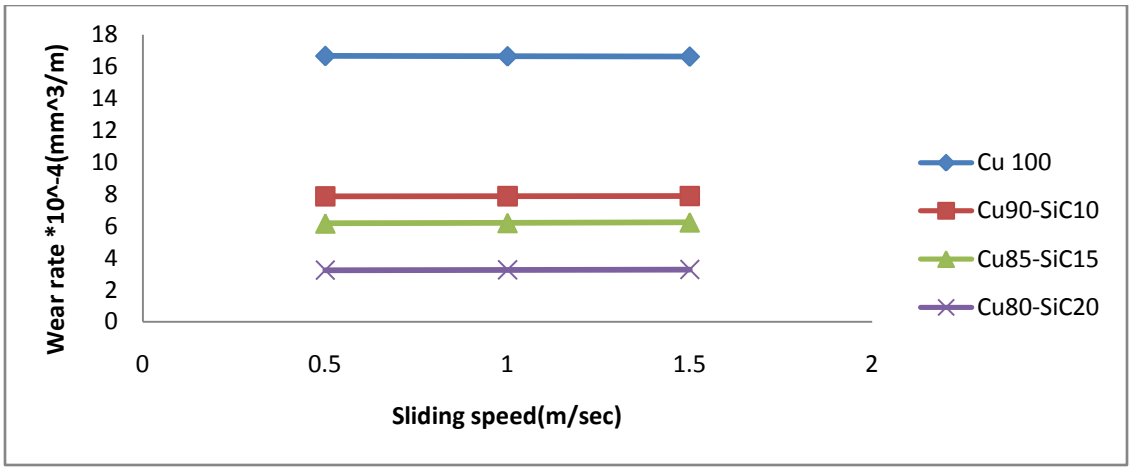

Fig 5.21: Wear rate v/s Sliding speed for the applied load of 2 kgf

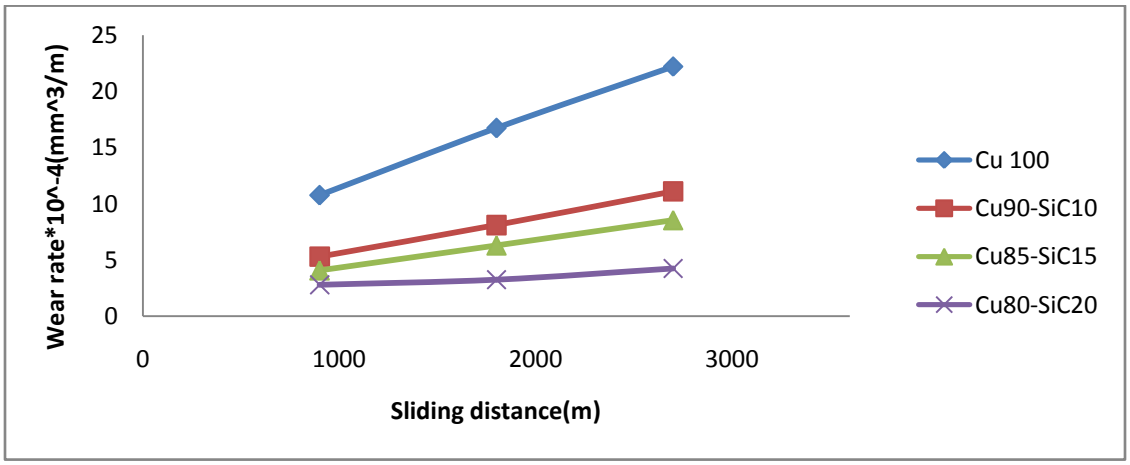

Fig 5.22 Wear rate v/s sliding distance for the sliding speed of 1 m/sec

From the table and the graph it is clear that the values of wear rate and the trends of the graphs are nearly similar to the experimented value. Also from the figure 5.22 it is clear that sliding speed has very less effect on the wear rate, and the wear rate is increasing with the sliding distance. So the applied load and the sliding distance are major factors which are affecting the wear rate.

5.10.2 Coefficient of friction

Based on the regression equation for each sample coefficient of friction was calculated. Table 5.21 shows the value of frictional coefficient for each sample. Fig 5.21 – 5.23 shows the frictional coefficient trend with respect to the applied load, sliding speeds and sliding distance.

Based on the regression equation for each sample; value of coefficient of friction was calculated. Table 5.21 shows the value of coefficient of friction for each sample.

Table 5.21: C.o.f. for each sample based on regression equation

Sets	Cu (100%)	Cu (90%)-SiC (10%)	Cu (85%)-SiC (15%)	Cu (80%)-SiC (20%)
Set 1	0.354	0.298	0.230	0.200
Set 2	0.372	0.304	0.234	0.208
Set 3	0.390	0.310	0.238	0.215
Set 4	0.486	0.413	0.314	0.269
Set 5	0.468	0.419	0.318	0.277
Set 6	0.505	0.407	0.305	0.264
Set 7	0.618	0.528	0.398	0.338
Set 8	0.582	0.512	0.385	0.325
Set 9	0.596	0.518	0.389	0.333

By using these values graphs were generated for each sliding speed.

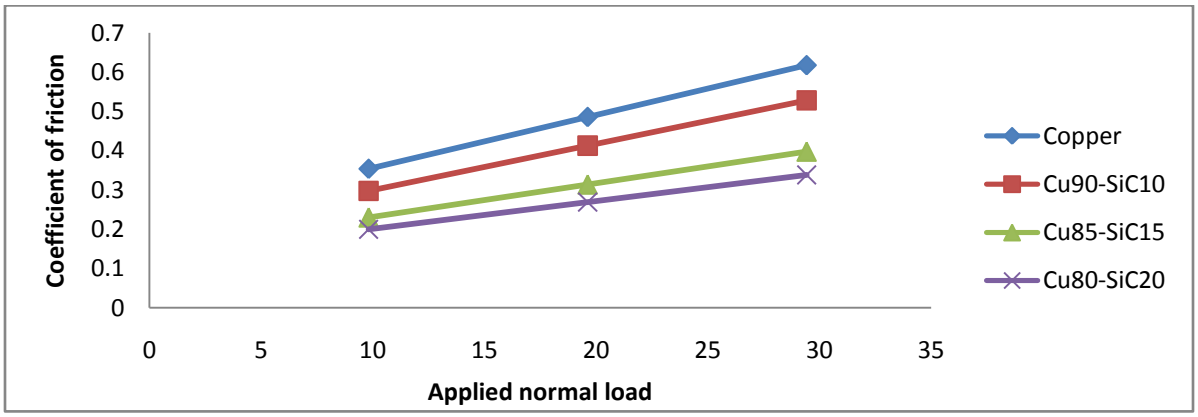

Fig 5.23: C.o.f. v/s Load for sliding speed of 0.5m/sec

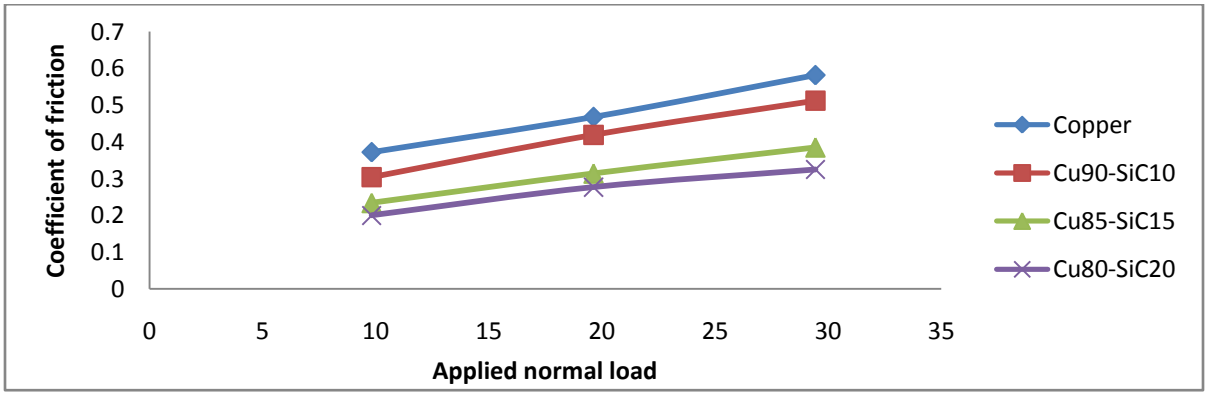

Fig 5.24: C.o.f v/s Load for sliding speed of 1.0m/sec

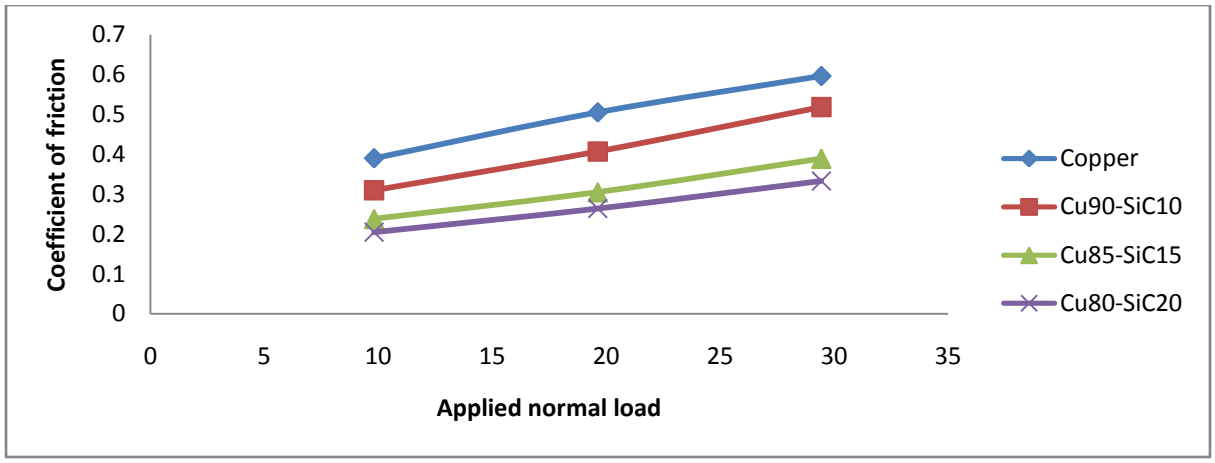

Fig 5.25: C.o.f. v/s Load for sliding speed of 1.5m/sec

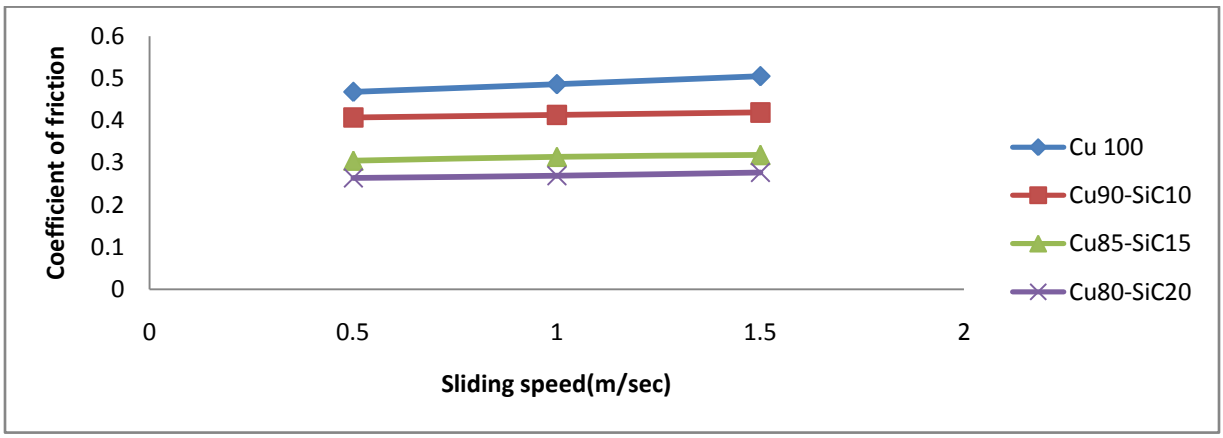

Fig 5.26 C.o.f v/s sliding speed for the sliding speed of 1 m/sec

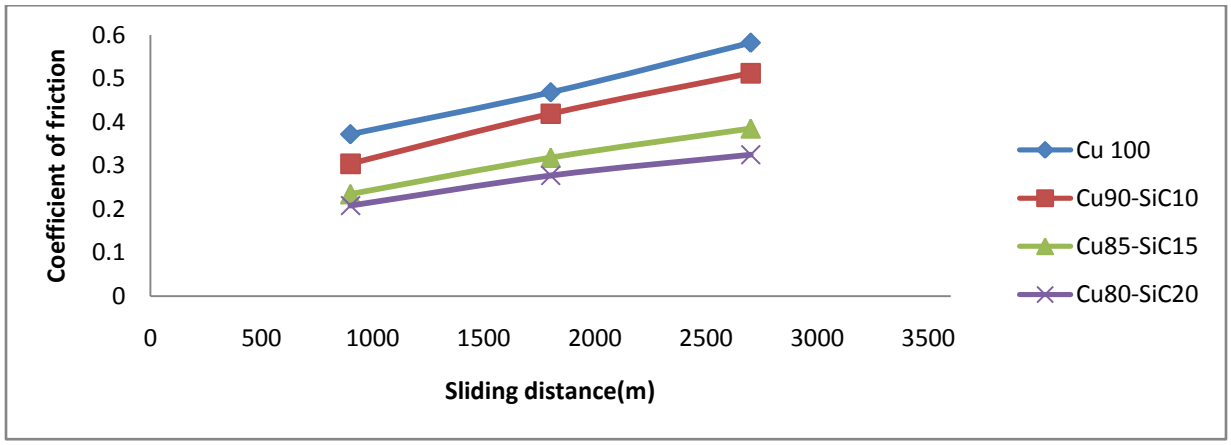

Fig 5.27 C.o.f v/s sliding distance for the applied load of 2 kgf

From the table and the graph it is clear that both the values of coefficient of friction and the trends of the graphs are nearly similar to the experimented value and the graphs and also from the figure 5.26 it is clear that sliding speed has very less effect on the frictional coefficient, and

the frictional coefficient is increasing with the sliding distance. So the applied load and the sliding distance are major factors which are affecting the coefficient of friction.

5.11 CONCLUSION

In this study, statistical model is being developed for the wear rate and the frictional coefficient by using Cu and Cu-SiC composite as work material and by correlating the input parameters, namely, sliding speed, applied load and the sliding distance. L9 orthogonal array was used to predict the behavior of the samples for different input parameters. For the model, significant parameters from the selected process parameters have been identified. The adequacy of the model has been established using ANOVA.

The results show that the statistical model is significant which is developed for wear rate and the coefficient of friction for the different compositions. It has been observed that the applied load and the sliding distance significantly affect the wear rate as well as frictional coefficient. It has been observed that wear rate and the frictional coefficient decreases with increase in volumetric fraction of SiC. Copper is showing highest wear rate and is lowest for the Cu (80%) – SiC (20%) composite due to highest fraction of SiC. Copper is having highest value of the frictional coefficient and lowest for the Cu (80%) – SiC (20%) composite due to highest fraction of SiC. The possible wear and friction mechanism are discussed in the previous chapter.

Confirmation experiments concluded that the developed model is adequate for the confidence level of 99%. The process parameters which are optimal is being identified to obtain the minimum wear rate and the less coefficient of friction.

CHAPTER 6

CONCLUSION AND SCOPE FOR FURTHER STUDY

6.1 SUMMARY OF THE PRESENT RESEARCH

In the present research, copper based composites have been successfully prepared by powder metallurgy route. SiC reinforcements were varied from 0% to 20% in the composites and were prepared for tribological studies. Characterization was performed in order to estimate the mechanical, physical and metallurgical properties of the fabricated composites. Tribological studies were carried out using pin-on-disc tribo meter to determine the wear rate and coefficient of friction. A statistical model was developed to correlate the input variables i.e. sliding speed, sliding distance and the normal load with wear rate and coefficient of friction. This model building was expended to all the compositions of the composites fabricated in this study. The adequacy of the developed model was checked by ANOVA and the most affecting parameters have been identified.

From the developed wear model, normal load was found to be most significant parameter followed by sliding distance and sliding speed. However for the composite having composition of 80% Cu and 20% SiC, sliding distance was found to be most affecting parameter followed by normal load and sliding speed. It has been observed that in general there is an increase in the wear rate with normal load, sliding distance as well as sliding speed. However, percentage contribution of each of the above parameter on the wear is different.

For the modeling of coefficient of friction, it has been observed that normal load is the most significant parameter. Sliding distance and the sliding speed have lesser significance as compared to normal load. Similar to wear, friction is also in general increased with normal load, sliding distance as well as sliding speed.

6.2 MAJOR CONCLUSIONS OF THE PRESENT WORK

- Composites of different compositions of Cu–SiC have been successfully fabricated at sintering temperature of 950^0 C by powder metallurgy technique.
- Hardness was higher for the reinforced copper composite. Increased volumetric fraction and uniform distribution of SiC in the composites leads to increase in the hardness.

- Density was lesser for the reinforced copper composite. Increased volumetric fraction of SiC in the composites leads to decrease in the density.
- Porosity was lesser for the reinforced copper composite. It is due to the fact that copper can diffuse easily to the interstices between SiC particles.
- Dry sliding wear rate and coefficient of friction was determined for different input parameters for the fabricated composites using pin-on-disc tribo meter.
    - It was found that the wear rate as well as frictional coefficient were decreased as the composition of the SiC were increased in the composite.
    - The wear resistance of the composite material is significantly improved due to the presence of hard reinforcement particles uniformly distributed in the matrix material. The reinforced particles, when adequately dispersed by way of load sharing, restricts the surface deformation of metal matrix.
    - The wear process in the composite material is either or combination of plastic deformation, smearing out of reinforcement particles which may crush to very minute particles and if reinforcement percentage is optimized it may form a mechanically mixed layer (MML) which helps in withstanding high stresses and is very effective in reducing the sliding wear.
    - The mechanism of wear observed in the composites was primarily abrasive in nature.
    - There is an increase in COF with distance and speed for all samples which provide the information on inability to generate the steady tribo layer at contact surfaces in the absence of any friction reducing agent.
- Statistical models have been developed for predicting coefficient of friction and wear rate of different compositions of Cu-SiC composites by correlating the input parameters normal load, sliding speed and the sliding distance.
    - For pure copper applied load and the sliding distance are found most significant parameters which affects the wear rate and are contributing 57% and 37%, respectively whereas sliding speed has 6% contribution. In frictional response these parameters have 43%, 47% and 10% contribution, respectively.
    - For the Cu (80%)-SiC (20%) composite, load, sliding speed and sliding distance is contributing 42%, 45% and 13% respectively, to wear rate whereas for

frictional response these parameters have 51%, 33% and 13% contribution, respectively.

6.3 FUTURE SCOPE

- Properties such as bonding strength and effective hardness can be further improved by interfacial modification using bonding agent such as Magnesium and optimizing process parameters such as sintering temperature and time.
- Friction and wear properties of fabricated composite can be further improved by reinforcing self lubricating agent such as Graphite and MoS_2.
- Size and optimal combination of the reinforced particles can be further optimized to enhance electrical and thermal conductivity of fabricated composite to make it suitable for the application such as EDM electrodes.
- Wear of EDM electrodes made of fabricated composites can be studied following the use of fabricated composite in EDM and ultrasonic assisted EDM operation.

REFERENCES:

1. K.M. Patel, P.M.Pandey, Determination of an optimum parametric combination using a surface roughness prediction model for EDM of Al2O3/SiC/TiC ceramic composite, Journal of Materials and Manufacturing Processes, 24 (2009) 675-682.
2. M.A. Mcevoy, N. Correll, Materials that couple sensing, actuation, computation and communication, Science 347 (2015) 6225.
3. G.D. Shaffer, An Archaeomagnetic Study of a Wattle and Daub Building Collapse, Journal of Field Archaeology, 12 (1993) 59-75.
4. M.N. Rahaman, Sintering of Ceramics, CRC Press, Taylor and Francis Group, Florida, U.S.A.
5. K. Kondoh, Powder Metallurgy, InTech Janeza Trdine, Rijeka, Croatia.
6. D. Kremer, J.L. Lebrun, B. Hosari, A. Moisan, Effects of Ultrasonic Vibrations on the Performances in EDM, Annals of the CIRP, 38(1) (1987) 199-202.
7. V.S.R. Murti, P.K. Philip, An analysis of the debris in ultrasonic-assisted electrical discharge machining, 117(2) (1989) 241-250.
8. T.B. Thoe, D.K. Aspinwall, N. Killey, Combined ultrasonic and electrical discharge machining of ceramic coated nickel alloy, Journal of Materials Processing Technology, 92-93 (1995) 323-328.
9. Y.C. Lin, B.H. Yan, Y.S. Chang, Machining characteristics of titanium alloy (Ti±6Al±4V) using a combination process of EDM with USM, Journal of Materials Processing Technology, 104 (2000) 171-177.
10. Z.X. Jia, J.H. Zhang, X. Ai, Ultrasonic vibration pulse electro discharge machining of holes in engineering ceramics, Journal of Materials Processing Technology, 53 (2002) 811–816.
11. Z.X. Jia, J.H. Zhang, X. Ai, Study on a new kind of combined machining Technology of Ultrasonic Machining and Electrical Discharge Machining, International Journal of Machine Tools and Manufacture, 37 (2004) 193-199.
12. A. Abdullah, M. Shabgard, Effect of ultrasonic vibration of tool on electrical discharge machining of cemented tungsten carbide (WC-Co), International Journal of Advanced Manufacturing Technology, 38 (2008) 1137–1147.

13. M. Shabgard, B. Sadizadeh, H. Kakoulvand, The Effect of Ultrasonic Vibration of Work piece in Electrical Discharge Machining of AISIH13 Tool Steel, In Proceedings of the 52nd World Academy of Science, Engineering and Technology, 40 (2010) 392–396.
14. H.M. Zaw, J.Y.H. Fuh, A.Y.C. Nee, L. Lu, Formation of a new EDM electrode material using sintering techniques, Journal of Materials Processing Technology, 89-90 (1990) 182-186.
15. N. Mohri, N. Saito, Y. Tsunekawa, Metal Surface Modification by Electrical Discharge Machining with Composite Electrode, Annals of the CIRP, 42(1) (1993) 219-222.
16. M.P. Samuel, P.K. Philip, Properties of compacted, pre-sintered and fully sintered electrodes produced by powder metallurgy for Electric Discharge Machining, Indian Journal of Engineering and Material Sciences, 3 (1995) 229-233.
17. P. Yih, J. Deborah, D. L. Chung, Powder metallurgy fabrication of metal matrix composites using coated fillers, The international journal of powder metallurgy, 31 (1996) 130-137.
18. M. P. Samuel, P. K. Philip, Power Metallurgy tool Electrodes for Electrical Discharge Machining, International Journal of Machine Tools and Manufacture, 37 (1997) 1625-1633.
19. S. Norasetthekul, P.T. Eubank, W.L. Bradley, B. Bozkurt, B. Stucker, Use of zirconium diboride-copper as an electrode in plasma applications, Journal of Materials Science, 34 (1999) 1261 – 1270.
20. N.H. Loh, S.B. Tor, K.A. Khor, Production of metal matrix composite part by powder injection molding, Journal of Material Processing Technology, 108 (2001) 398-407.
21. L Li, Y.S. Wong, J.Y.H. Fuh, L. Lu, EDM performance of TiC/Copper-based sintered electrodes, Materials and Design, 22 (2001) 669-678.
22. H.C. Tsai, B.H. Yan, F.Y. Huang, EDM performance of Cr/Cu-based composite electrodes, International Journal of Machine Tools & Manufacture, 43 (2003) 245–252.
23. J. Zhao, Y. Li, J. Zhang, C. Yu, Y. Zhang, Analysis of the wear characteristics of an EDM electrode made by selective laser sintering, Journal of Materials Processing Technology, 138 (2003) 475–478.

24. D.E. Dimla, N. Hopkinson, H. Rothe, Investigation of complex rapid EDM electrodes for rapid tooling applications, International Journal of Advance Manufacturing Technology, 23 (2006) 249–255.
25. A.K. Khanra, B.R. Sarkar, B. Bhattacharya, L.C. Pathak, M.M. Godkhindi, Performance of ZrB_2–Cu composite as an EDM electrode, Journal of Materials Processing Technology, 183 (2008) 122–126.
26. Th. Schubert, B. Trindade, T. Weibgarber, B. Kieback, Interfacial design of Cu-based composites prepared by powder metallurgy for heat sink applications, Material science and engineering, 475 (2008) 39-44.
27. S.K. Mishra, L.C. Pathak, Effect of carbon and titanium carbide on sintering behavior of zirconium diboride, Journal of Alloys and compounds, 465(1-2) (2013) 547–555.
28. M. Monzon, A.N. Benıtez, M.D. Marrero, N. Hernandez, P. Hernandez, J. Aisa, Validation of electrical discharge machining electrodes made with rapid tooling technologies, Journal of Materials Processing Technology, 196 (2013) 109–114.
29. N. Celebi, S. Chung, C. Velan, Effect of particle size distribution for Cu-SiC composite Using powder metallurgy, Procedia Materials Science 5 (2014) 2629 – 2634.
30. S.C Tjong, K.C Lau, Tribological behaviour of SiC particle-reinforced copper matrix composites Materials Letters 43, (2000) 274–280.
31. S.F Moustafaa, S.A Badry, A.M Sanadb, B Kiebackc, Friction and wear of copper–graphite composites made with Cu coated and uncoated graphite powders, International Journal of Wear 253 (2002) 699–710.
32. Y. Zhan, G. Zhang, Friction and wear behavior of copper matrix composites reinforced with SiC and graphite particles, Tribology Letters 17 (2004) 1-8.
33. K. Rajkumar, S. Aravindan, Tribological performance of microwave sintered copper–TiC–graphite hybrid composites, Tribology International 44 (2011) 347–358.
34. E. Hong, B. Kaplinb, T. Youa, M. Suha, Y. Kima, H. Choea, Tribological properties of copper alloy-based composites reinforced with tungsten carbide particles, Wear 270 (2011) 591–597.
35. S. Huang, Yi feng, K. Ding, G. Qian, H. Liu, Y. Wang, Friction and wear properties of Cu-based self-lubricating composites in air and vacuum conditions, Metallurgical Signature 25 (2012) 391-400.

36. A. K. Tiwari, T. K. Mishra, M. Choubey, R.K.Ranjan, Investigation of wear behaviour of Al -Cu powder, IOSR Journal of Engineering 2 (2012) 159-164.
37. X. Niansuo, W. Jin Study on Preparation of Copper Matrix Composites Reinforced by SiC and Graphite Particles, 160 (2012) 1333-1336.
38. Y. Reddy, T. Umale, A. Singh, Abrasive wear behaviour of copper-sic and copper-sio2 composites international journal of modern physics 22 (2013) 416–423.
39. T. Prabhu, V. Varma, Vedantam, Tribological and mechanical behavior of Cu/SiCp composites for brass 317 (2014) 201-212.
40. M. Shabani, M. Hossein Paydar, R. Zamiri, M. Goodarzi, M. Moshksara, Microstructural and sliding wear behavior of SiC-particle reinforced copper matrix composites fabricated by sintering and sinter-forging processes, JMRTEC 158, (2015).
41. T.P. Bagchi, Taguchi Methods Explained, Prentice-Hall of India, 1993.

Turnitin Originality Report

Nalin Thesis by Vineet Srivastava

From ME_Thesis_2_10words (Research)

- Processed on 22-Jun-2016 09:53 IST
- ID: 683928615
- Word Count: 16002

Similarity Index
13%
Similarity by Source

Internet Sources:
4%
Publications:
8%
Student Papers:
7%

sources:

1 3% match (student papers from 19-Jun-2016)
Submitted to Thapar University, Patiala on 2016-06-19

2 2% match (student papers from 21-Jun-2016)
Submitted to Thapar University, Patiala on 2016-06-21

3 1% match (Internet from 25-Nov-2014)
http://www.docstoc.com/docs/147907981/Tribology-of-polymer-Nanocomposites--Klaus-Friedrich

4 < 1% match (publications)
Encyclopedia of Tribology, 2013.

5 < 1% match (publications)
Srivastava, V., and P. M. Pandey, "Experimental investigation on electrical discharge machining process with ultrasonic-assisted cryogenically cooled electrode", Proceedings of the Institution of Mechanical Engineers Part B Journal of Engineering Manufacture, 2013.

6 < 1% match (student papers from 04-May-2016)
Submitted to Universiti Malaysia Perlis on 2016-05-04

7 < 1% match (Internet from 25-Jan-2015)
http://www.science.gov/topicpages/u/underwater+electrical+discharge.html